

4-17-2015 12:00 AM

## Elucidating the Role of HDAC8 in Anthrax Lethal Toxin-Induced Pyroptosis and Cytokine Gene Silencing in Macrophages

Chantelle M. Reid, *The University of Western Ontario*

Supervisor: Dr. Sung O. Kim, *The University of Western Ontario*

A thesis submitted in partial fulfillment of the requirements for the Master of Science degree in Microbiology and Immunology

© Chantelle M. Reid 2015

Follow this and additional works at: <https://ir.lib.uwo.ca/etd>

---

### Recommended Citation

Reid, Chantelle M., "Elucidating the Role of HDAC8 in Anthrax Lethal Toxin-Induced Pyroptosis and Cytokine Gene Silencing in Macrophages" (2015). *Electronic Thesis and Dissertation Repository*. 2733.  
<https://ir.lib.uwo.ca/etd/2733>

This Dissertation/Thesis is brought to you for free and open access by Scholarship@Western. It has been accepted for inclusion in Electronic Thesis and Dissertation Repository by an authorized administrator of Scholarship@Western. For more information, please contact [wlsadmin@uwo.ca](mailto:wlsadmin@uwo.ca).

ELUCIDATING THE ROLE OF HDAC8 IN ANTHRAX LETHAL TOXIN-INDUCED  
PYROPTOSIS AND CYTOKINE GENE SILENCING IN MACROPHAGES

by

CHANTELLE REID

Graduate Program in Microbiology and Immunology

A thesis submitted in partial fulfillment  
of the requirements for the degree of  
MASTER OF SCIENCE

The School of Graduate and Postdoctoral Studies  
The University of Western Ontario  
London, Ontario, Canada

© CHANTELLE REID 2015

## ABSTRACT

Anthrax is a lethal infectious disease caused by the bacterium *Bacillus anthracis*. *B. anthracis* secretes the virulence factor anthrax lethal toxin (LeTx), which causes rapid cell death known as pyroptosis and immune suppression in macrophages. Strikingly, RAW 264.7 macrophages pre-exposed to sub-lethal doses of LeTx become refractory to subsequent high cytolytic doses. The phenomenon is termed toxin-induced resistance (TIR). TIR is in part linked to the down-regulation of three mitochondrial death genes, BCL2/adenovirus E1B 19 kDa-interacting protein 3 (*BNIP3*), BNIP3-like (*BNIP3L*), and metastatic lymph node 64 (*MLN64*) protein, as well as the up-regulation of a gene-silencing epigenetic regulator, histone deacetylase (HDAC) 8. Interestingly, I found that inhibiting HDAC8 with the HDAC8-specific inhibitor PCI-34051 in RAW 264.7 TIR cells sensitized them to LeTx-induced pyroptosis. Furthermore, resistance to LeTx-induced pyroptosis is likely mediated by HDAC8-dependent H3K27Ac deacetylation in the regulatory regions of the mitochondrial death genes, *BNIP3* and *MLN64*. Although, sub-lethal doses of LeTx induced resistance to pyroptosis in RAW 264.7 macrophages, LeTx still caused immune suppression. Here, I found that RAW 264.7 LeTx-treated macrophages and RAW 264.7 macrophages over-expressing HDAC8 failed to produce pro-interleukin (IL)-1 $\beta$ , a pro-inflammatory cytokine, in response to the Gram-negative bacterial cell wall component lipopolysaccharide (LPS), whereas inhibiting HDAC8 with PCI-34051 restored IL-1 $\beta$  and tumor necrosis factor (TNF)- $\alpha$  production in response to LPS. Furthermore, chromatin immunoprecipitation (ChIP)-quantitative real-time polymerase chain reaction (qPCR) analysis revealed that inhibiting HDAC8 in the presence of LeTx increased H3K27Ac association with the genomic regions of *IL-1 $\beta$*  in response to LPS. Collectively, these results suggest that HDAC8 plays a key role in resistance to LeTx-induced pyroptosis and LeTx-induced immunosuppression, through targeting the H3K27Ac-associated regions of *BNIP3*, *MLN64* and *IL-1 $\beta$* .

## KEYWORDS

*Bacillus anthracis*, anthrax, lethal toxin, lethal toxin-induced resistance, epigenetics, histone deacetylation, histone deacetylase 8, immunosuppression.

## ABBREVIATIONS

ASC	Apoptosis speck-like protein containing a CARD
AVA	Anthrax Vaccine Adsorbed
BH	Bcl-2 homology
BMDM	Bone marrow derived macrophage
BNIP3	BCL2/adenovirus E1B 19 kDa-interacting protein 3
BNIP3L	BNIP3-like
CARD	Caspase activation and recruitment domain
ChIP	Chromatin immunoprecipitation
CMG2	Capillary morphogenesis gene 2
DMNT	DNA methyltransferase
EF	Edema factor
ERK	Extracellular signal-regulated kinase
FBS	Fetal bovine serum
GAPDH	Glyceraldehyde 3-phosphate dehydrogenase
GSH	Glutathione
H3K27Ac	Histone H3 lysine 27 acetylation
H3K27Me3	Histone H3 lysine 27 trimethylation
HAT	Histone acetyltransferase
HDAC	Histone deacetylase
IL	Interleukin
IL-1 $\beta$	Interleukin-1 beta
JNK	c-Jun Amino Terminal Kinase
LF	Lethal factor
LPS	Lipopolysaccharide
MAPK	Mitogen activated protein kinase
MEK	MAPK kinase
MEKK	MAPK kinase kinase
MLN64	Metastatic lymph node 64
NF- $\kappa$ B	Nuclear factor kappa B
NLR	Nod-like receptor

NOD	Nuclear oligomerization domain
PA	Protective antigen
PBS	Phosphate buffered saline
qPCR	Quantitative polymerase chain reaction
ROS	Reactive oxygen species
RTKs	Receptor tyrosine kinases
<i>S. typhimurium</i>	<i>Salmonella enterica</i> serovar Typhimurium
SAPK	Stress activated protein kinase
SILAC	Stable isotope labeling of amino acids in cell culture
SOS	Son of sevenless
SRM	Selected reaction monitoring
TEM8	Tumor endothelial marker 8
TIL1R	Toll-interleukin 1 receptor
TIR	Toxin-induced resistance
TLR	Toll-like receptor
TM	Transmembrane
TNF- $\alpha$	Tumor necrosis factor-alpha

## CO-AUTHORSHIP STATEMENT

I, Chantelle Reid performed experiments, analyzed data, and performed statistical analysis unless otherwise indicated in the figure legends. Dr. Soon-Duck Ha conducted experiments, analyzed data and performed statistical analysis for Figures 3.1B, 3.2B, 3.5, and 3.17. Dr. Soon-Duck Ha also prepared samples for Figure 3.18. Drs. Huadong Liu and Kyle Biggar of Dr. Shawn Li's lab (Department of Biochemistry, UWO) performed selected reaction monitoring mass spectrometry and carried out subsequent interpretation and analysis.

Please note that Figures 3.1B, 3.5, 3.12, 3.14, 3.15 and 3.16 are originally published in *The Journal of Immunology*. Ha SD, Han CY, Reid C, and Kim SO. 2014. HDAC8-Mediated Epigenetic Reprogramming Plays a Key Role in Resistance to Anthrax Lethal Toxin-Induced Pyroptosis in Macrophages. *J. Immunol.* 193:1333-43. Copyright © [2014] The American Association of Immunologists, Inc.

Link to full publication: <http://www.jimmunol.org.proxy1.lib.uwo.ca/content/193/3/1333.full>

## ACKNOWLEDGEMENTS

I would like to thank my supervisor, Dr. Sung Kim for giving me the opportunity to work in his lab, along with providing his wealth of knowledge and academic guidance. I also wish to thank my present and past lab members, Chae Young Han, Macon Coleman, Shahab Meshkibaf, and Dr. Soon-Duck Ha for their encouragement, as well as their academic and technical support throughout the duration of this project. I would especially like to thank Dr. Soon-Duck Ha for allowing me to use some of her data to compliment my thesis.

Thank you to my committee members, Dr. Rodney DeKoter and Dr. Joe Mymryk for their constructive criticism, advice, and encouragement, which were vital for the completion of this experimental and written work.

I also wish to thank my collaborators in the Dr. Shawn Li lab (Biochemistry, UWO), Drs. Huadong Liu and Kyle Biggar for there contribution to the selected reaction monitoring mass spectrometry experiments. Furthermore, I would like to thank Ali Abbas from Dr. DeKoter's lab for lending his technical advice for ChIP experiments. I would also like to acknowledge Dr. Aurigemma (NCI-FCRDC, Frederick, MD) for providing pro-IL-1 $\beta$  antibody.

Finally, I would like to thank my friends and family, especially my parents and boyfriend for their continuous encouragement, motivation, love and support. Words cannot describe how grateful I am to have you all in my life. I could not have made it through the past two years without you.

# TABLE OF CONTENTS

ABSTRACT .....	ii
ABBREVIATIONS .....	iii
CO-AUTHORSHIP STATEMENT .....	v
ACKNOWLEDGEMENTS .....	vi
TABLE OF CONTENTS .....	vii
LIST OF TABLES .....	xi
LIST OF FIGURES .....	xii
CHAPTER 1 .....	1
1 INTRODUCTION .....	1
1.1 Anthrax .....	1
1.1.1 Types of Anthrax .....	1
1.1.2 Treatment and Prevention.....	2
1.2 <i>B. anthracis</i> Virulence Factors .....	3
1.2.1 LeTx .....	3
1.3 MAPK Signaling Cascade.....	4
1.3.1 ERK1/2 .....	5
1.3.2 JNKs .....	5
1.3.3 p38 .....	6
1.4 TLR signaling.....	6
1.5 LeTx and Immune Suppression.....	7
1.6 Pyroptosis .....	11
1.6.1 NLRs and Pyroptosis.....	11
1.6.2 LeTx and Pyroptosis.....	12
1.6.3 Mitochondrial Death Genes.....	13



1.7 Cellular Adaptation .....	15
1.8 Epigenetics .....	19
1.8.1 Histone Modifications and Gene Expression .....	19
1.9 Rationale, Hypothesis, and Objectives .....	26
CHAPTER 2 .....	27
2 MATERIALS AND METHODS .....	27
2.1 Cell culture and reagents .....	27
2.1.1 Stable isotope labeling by amino acids in cell culture .....	28
2.1.2 Inhibitor treatment .....	29
2.2 Cell transfection.....	30
2.3 Measurement of cell viability .....	30
2.4 Lysate preparation and Western blot analysis .....	31
2.5 Histone purification .....	32
2.6 Digestion of histone H3 .....	32
2.7 Selected reaction monitoring mass spectrometry .....	33
2.8 Chromatin immunoprecipitation .....	34
2.9 Quantitative PCR.....	35
2.10 Enzyme-linked immunosorbent assay .....	36
2.11 Statistical analysis .....	36
CHAPTER 3 .....	39
3 RESULTS .....	39
3.1 Generating TIR macrophages.....	39
3.1.1 TIR macrophages are resistant to LeTx-induced pyroptosis.....	39
3.2 TIR is mediated in an HDAC8-dependent manner. ....	42
3.2.1 Increased HDAC8 expression is correlated with TIR. ....	42
3.2.2 Inhibiting HDAC8 expression sensitizes TIR macrophages to LeTx. ....	47

3.2.3	Knocking-down HDAC8 increases expression of the mitochondrial death genes in TIR-BMDMs. ....	50
3.3	HDAC8-dependent deacetylation at histone H3 lysine 27 (H3K27) mediates TIR. ....	53
3.3.1	H3K27Ac is reduced in TIR macrophages. ....	53
3.3.2	HDAC8-dependent H3K27 deacetylation is involved in RAW 264.7 TIR macrophages. ....	68
3.3.3	HDAC8-dependent H3K27 deacetylation is involved in the down-regulation of the mitochondrial death genes in RAW 264.7 TIR macrophages. ....	73
3.3.4	HDAC8 limits RNA polymerase II accessibility to the mitochondrial death gene promoters. ....	76
3.4	LeTx suppresses cytokine production in an HDAC8-dependent manner. ....	81
3.4.1	LeTx-treated RAW 264.7 macrophages are defective in producing IL-1 $\beta$ in an HDAC8-dependent manner in response to LPS. ....	81
3.4.2	Inhibiting HDAC8 restores the expression and production of IL-1 $\beta$ and TNF- $\alpha$ in LeTx-treated macrophages. ....	84
3.4.3	Inhibiting HDAC8 in LeTx-treated macrophages increases H3K27Ac and Pol II association in the genomic regions of <i>IL-1<math>\beta</math></i> in response to LPS. ...	91
CHAPTER 4.....		95
4	DISCUSSION.....	95
4.1	Resistance to LeTx-induced pyroptosis is HDAC8-mediated.....	95
4.2	TIR is mediated by an HDAC8-H3K27-dependent epigenetic mechanism.....	96
4.3	LeTx-induced cytokine suppression is mediated by an HDAC8-H3K27-dependent epigenetic mechanism .....	103
4.4	Future Studies .....	105
4.4.1	Examining the mechanism of LeTx-mediated HDAC8 up-regulation....	105
4.4.2	Examining LeTx-mediated H3K27 methylation .....	106
4.4.3	Examining H3K9Ac and H3K14Ac in <i>IL-1<math>\beta</math></i> and mitochondrial death gene expression .....	107

4.4.4 Examining eRNAs in regulating <i>IL-1<math>\beta</math></i> and mitochondrial death gene expression .....	108
4.5 Summary.....	109
4.6 Significance .....	112
CHAPTER 5 .....	113
5 REFERENCES .....	113
CURRICULUM VITAE .....	139

## LIST OF TABLES

Table 2.1 List of antibodies (Abs).....	29
Table 2.2 List of inhibitors .....	30
Table 2.3 List of primer sequences.....	37
Table 3.1 <i>In silico</i> digestion of histone H3 and the synthesis of standard peptides for selected reaction monitoring mass spectrometry.....	57

## LIST OF FIGURES

Figure 1.1 LeTx inhibits various cellular functions through MEK inactivation. ....	9
Figure 1.2 Key events involved in sensitivity and long-term resistance to LeTx-induced pyroptosis in macrophages. ....	17
Figure 1.3 Histone acetylation levels can mediate gene expression.....	24
Figure 3.1 Short-term TIR macrophages are resistant to LeTx-induced pyroptosis. ....	40
Figure 3.2 Short-term TIR macrophages have increased HDAC8 mRNA levels. ....	43
Figure 3.3 HDAC8 protein levels are increased in RAW 264.7 short-term TIR macrophages. ....	45
Figure 3.4 RAW 264.7 short-term TIR cells are sensitized to LeTx-induced pyroptosis when treated with the HDAC8 inhibitor PCI-34051.....	48
Figure 3.5 Short-term TIR-BMDMs knocked down in HDAC8 show increased expression levels of the three mitochondrial death genes <i>BNIP3</i> , <i>BNIP3L</i> and <i>MLN64</i> . ....	51
Figure 3.6 Stable isotope labeling of amino acids in cell culture and SRM mass spectrometry analysis. ....	55
Figure 3.7 Identification of unmodified histone H3K27 by SRM mass spectrometry.....	58
Figure 3.8 Identification of acetylated histone H3K27 by SRM mass spectrometry.....	59
Figure 3.9 Long-term TIR macrophages show decreased levels of H3K27Ac relative to wild-type macrophages by SRM mass spectrometry.....	62
Figure 3.10 RAW 264.7 short-term TIR macrophages show increased levels of unmodified H3K27 by SRM mass spectrometry. ....	64
Figure 3.11 Working model of H3K27Ac levels in RAW 264.7 short-term TIR macrophages. ....	66

Figure 3.12 HDAC8 targets H3K27Ac for deacetylation in long-term TIR macrophages....	69
Figure 3.13 Short-term TIR macrophages treated with the HDAC8-specific inhibitor PCI-34051 show decreased levels of unmodified H3K27 by SRM mass spectrometry.....	71
Figure 3.14 Long-term TIR macrophages show increased HDAC8 recruitment at the H3K27Ac-associated regulatory regions of <i>BNIP3</i> and <i>MLN64</i> . ....	74
Figure 3.15 RNA polymerase II has limited accessibility to the promoter regions of <i>BNIP3</i> , <i>BNIP3L</i> , and <i>MLN64</i> in long-term TIR.....	77
Figure 3.16 RNA polymerase II has limited accessibility to the promoter regions of <i>BNIP3</i> , <i>BNIP3L</i> , and <i>MLN64</i> in RAW 264.7 macrophages over-expressing HDAC8.....	79
Figure 3.17 LeTx-treated and over-expressing HDAC8 RAW 264.7 macrophages are defective in IL-1 $\beta$ production in response to LPS.....	82
Figure 3.18 The broad-spectrum HDAC inhibitor panobinostat (PN) restores production of IL-1 $\beta$ and TNF $\alpha$ in response to LPS in the presence of LeTx. ....	85
Figure 3.19 The HDAC8 specific inhibitor PCI-34051 restores mRNA levels of IL-1 $\beta$ and TNF $\alpha$ in response to LPS in the presence of LeTx. ....	87
Figure 3.20 The HDAC8 inhibitor PCI-34051 does not induce TNF- $\alpha$ production in RAW 264.7 macrophages in response to LPS.....	89
Figure 3.21 Inhibiting HDAC8 by PCI-34051 in LeTx-treated macrophages increases H3K27Ac and Pol II association in the genomic regions of <i>IL-1<math>\beta</math></i> in response to LPS. ....	93
Figure 4.1 The H3K27 peptide histone modifications. ....	101
Figure 4.2 Working models for HDAC8-mediated silencing of <i>BNIP3</i> , <i>MLN64</i> , and <i>IL-1<math>\beta</math></i> in response to LeTx. ....	110

## CHAPTER 1

### 1 INTRODUCTION

#### 1.1 Anthrax

Anthrax is often a fatal bacterial infection caused by the Gram-positive bacterium *Bacillus anthracis*. *B. anthracis* is primarily a soil bacterium capable of producing endospores, which are resistant to harsh environmental conditions (e.g. high heat, UV light, disinfectants etc.), and can remain dormant for decades [1,2]. When anthrax endospores are present in the host they are primarily phagocytosed by macrophages and these macrophages then migrate to the draining lymph nodes and begin to germinate to become vegetative bacteria [1,3,4]. These vegetative bacteria are then released from macrophages, allowing for dissemination throughout the host leading to bacteremia and septic shock. Furthermore, vegetative *B. anthracis* expresses virulence factors including toxins, which lead to systemic immune paralysis, shock, and eventual death of the host [3].

Throughout the world in regions including South and Central America, sub-Saharan Africa, Central and Southwestern Asia, and Southern and Eastern Europe, anthrax is found among wild and domestic animals leading to increased risk and incidence of anthrax in humans who interact with these animals [5]. Furthermore, due to the stability of the endospores and the deadly consequences of infection, anthrax has been exploited as a biological weapon on multiple occasions. Anthrax spores were used during the invasion of Manchuria in the 1940s by the Japanese army [6], in the 2001 United States postal attack [7] and to contaminate heroin supplies in the UK in 2009/2010 [8].

##### 1.1.1 Types of Anthrax

To date, the Centers for Disease Control and Prevention (CDC) recognizes four types of anthrax infections: cutaneous, gastrointestinal, injectional, and inhalational [9].

Generally, the severity of anthrax infections varies with the type of anthrax. However, all have the potential to become systemic if left untreated. Cutaneous anthrax, which occurs when spores get into the skin via lacerations, is the most common form of infection but

the least life threatening. It generally affects the skin and tissue surrounding the primary infection site and may be recognized by groups of itchy blisters or bumps, followed by the formation of a painless ulcer with black eschar [9,10]. If left untreated, death occurs in up to 20% of infected individuals [9]. Gastrointestinal anthrax is extremely rare, but nonetheless is caused by the ingestion of raw or undercooked meat from an infected animal [11]. This type of anthrax can affect the upper gastrointestinal tract, stomach, and intestines. With proper treatment about 60% of infected individuals survive. In the absence of treatment, death rates are greater than 50% [9]. In 2009, injectional anthrax was identified in Northern Europe by confirming *B. anthracis* soft tissue infections in a total of 47 patients who injected heroin contaminated with anthrax spores [8]. Although symptoms are similar to those of cutaneous anthrax, the infection generally occurs deeper under the skin or in the muscle at the drug injection site [9]. Furthermore, injectional anthrax becomes systemic more rapidly, and is extremely difficult to diagnose and treat. Lastly, inhalational anthrax occurs when an individual breathes in *B. anthracis* spores, where infection primarily begins within the lower respiratory tract and eventually progresses throughout the rest of the body [2,10]. Inhalational anthrax is the most threatening form of anthrax, such that if left untreated only about 1 in 10 individuals survive. Even with treatment, only about 50% of patients survive [9].

### 1.1.2 Treatment and Prevention

Immediate treatment is crucial for individuals with anthrax disease, as it greatly increases the chance of survival. According to the US Advisory Committee on Immunization Practices, 2 months of antimicrobial therapy with FDA-approved drugs such as ciprofloxacin, levofloxacin, and doxycycline, in addition to a 3-dose series of Anthrax Vaccine Adsorbed (AVA) at time zero, two and four weeks post-diagnosis is recommended for post-exposure prophylaxis (PEP) [12,13].

To date, the FDA has not approved AVA, but the vaccine could be made available under a declared emergency. For patients with systemic anthrax, treatment should consist of intravenous multi-antimicrobial therapy until the individual is stable, where at least one of the drugs is a protein synthesis inhibitor and another is bactericidal [13]. Furthermore, there are two antitoxins available, Raxibacumab and Anthrax Immune Globulin



Intravenous (AIGIV) [13], yet to date only Raxibacumab is FDA-approved [14,15]. Raxibacumab is a monoclonal antibody that inhibits the binding of an exotoxin protein known as protective antigen (PA) to host cell receptors, thus preventing the translocation of the effector exotoxin proteins lethal factor (LF) and edema factor (EF) into cells. AIGIV is polyclonal antiserum that may have direct effects against EF and LF [13].

## 1.2 *B. anthracis* Virulence Factors

*B. anthracis* possess two extrachromosomal plasmids, pXO1 and pXO2, which are vital for full virulence [10]. The 184.5 kilobase pair (kbp) pXO1 plasmid encodes for three genes that comprise anthrax toxin: *pag* (protective antigen, PA), *lef* (lethal factor, LF), and *cya* (edema factor, EF) [10,16]. PA combines with either EF or LF to form two exotoxins, edema toxin (EdTx) and lethal toxin (LeTx), respectively [10,16]. Furthermore, the 95 kbp pXO2 plasmid encodes three genes including, *capB*, *capC*, and *capA*, all of which are involved in the synthesis of the polyglutamic acid capsule [17]. The exotoxins, LeTx and EdTx are primarily responsible for inhibiting the host immune response against infection, whereas the polyglutamic acid capsule acts as an anti-phagocytic agent to prevent phagocytosis of vegetative bacteria [10]. Loss of either of these extrachromosomal plasmids results in attenuated virulence during infection [10].

### 1.2.1 LeTx

LeTx is the dominant virulence factor produced during anthrax infection and acts as the primary mediator of shock and death of the infected host [18-20]. LeTx is a potent inhibitor of a variety of cellular functions within host immune cells, such as differentiation, antigen presentation, phagocytosis, and cytokine production [21]. Collectively, these effects contribute significantly to systemic immune paralysis [21,22]. Furthermore, LeTx causes toxemia [23-25], manifested by vascular collapse [26], and toxic shock [27]. Interestingly, the toxic shock induced by LeTx is distinct from other bacterial-induced shock, such that it is not mediated by a cytokine storm [21].

The cellular binding component of LeTx, PA, recognizes and binds two host receptors: tumor endothelial marker 8 (TEM8), also known as anthrax toxin receptor 1 (ANTXR1) [28] and capillary morphogenesis gene 2 (CMG2), also known as anthrax toxin receptor 2

(ANTXR2) [29]. Although CMG2 is widely expressed in various tissues, TEM8 is mainly expressed in macrophages and endothelial cells [30]. Full-length PA (PA83; 83 kDa) binds to the cellular receptors through its carboxy-terminal domain and is cleaved by a furin-like protease, leaving the 63 kDa (PA63) cleaved form bound to the receptors [31]. The short PA fragment (PA20; 20 kDa) detaches from PA63, allowing for oligomerization into a heptameric or octameric ring. This processing and assembly enable the binding of LF to the PA complex [31]. Finally, the PA63-LF complexes triggers receptor-mediated endocytosis [32] and LF is translocated into the cytosol upon endosome acidification [33].

The effector component of LeTx, LF, is a zinc metalloproteinase and its enzymatic activity is crucial for its cytotoxicity [34]. LF targets and deactivates mitogen-activated protein kinase kinases (MEKs) 1 to 4, as well as 6 and 7, through N-terminal cleavage [35-37]. Consequently, the inactivation of MEKs interferes with the mitogen activated protein kinase (MAPK) signaling cascade, which controls various cell functions including proliferation, differentiation, development, immune modulation and survival [38]. The three functional domains of LF include the N-terminal domain, which binds to PA, the substrate-binding domain, which binds MEKs, and the proteolytic C-terminal domain, which cleaves target substrates [39]. In summary, LF-mediated MEK cleavage appears to play a key role in lethality through inhibiting a broad range host cell functions.

### 1.3 MAPK Signaling Cascade

The MAPK signaling cascade is a vital pathway in eukaryotes required for the activation of various transcription factors that are necessary for modulating cellular activities, such as proliferation, differentiation, and death [40]. This signaling cascade is a three-tier phosphorelay system, which is activated through various stimuli including mitogens, stress (e.g. toxins, DNA damage, ionizing radiation, and heat), pro-inflammatory cytokines, as well as G-protein coupled receptor agonists [40]. The first tier of the signaling cascade includes the MAPK kinase kinases (MEKKs). To date, there are 20 MEKKs that are differentially activated by interacting with Ras superfamily GTPases and/or protein kinase-dependent phosphorylation downstream of cell surface receptors [41]. Following activation, MEKKs phosphorylate and activate the second tier MAPK

kinases (MEKs), subsequently leading to the activation of third-tier MAPKs via dual phosphorylation of a conserved tripeptide (TxY) within the activation region by activated MEKs [40]. The literature recognizes five MAPK families, however three families including the extracellular-signal-regulated kinases (ERKs) 1 and 2, the Jun amino-terminal or the stress-activated protein kinases (JNKs/SAPKs), and the p38 group of protein kinases (p38) are of primary focus in the literature [42].

### 1.3.1 ERK1/2

ERK1 and ERK2 (ERK1/2) are related protein kinases that modulate a broad range of cellular functions including survival, differentiation, growth, and development through the Ras-Raf-MEK-ERK signaling cascade [40]. Various stimuli such as mitogens and growth factors are responsible for the activation of the ERK signal transduction pathway via the autophosphorylation of receptor tyrosine kinases (RTKs) [43]. This autophosphorylation event results in the recruitment of a guanine nucleotide exchange factor (GEF), Son of Sevenless (SOS), to convert the small GTPase Ras from the inactive state (Ras-GDP) to the active state (Ras-GTP). Ras-GTP triggers the activation of the MEKK Raf, which is a serine/threonine kinase that phosphorylates downstream MEKs including, MEK1 and MEK2 [43]. Upon activation, MEK1/2 dually phosphorylates and activates ERK1/2, thus allowing ERK to release from the multi-subunit signaling complex in the cytoplasm and enter the nucleus to initiate gene transcription [40].

### 1.3.2 JNKs

The JNK family, including the JNK1, JNK2, and JNK3 (JNK1/2/3) kinases, plays a vital role in apoptotic cell death [44], cytokine production, metabolism, and inflammation [45,46]. Initiation of the JNK signaling transduction pathway is largely mediated through environmental stressors such as heat, DNA damage, and oxidative stress, as well as inflammatory cytokines and growth factors [40]. The upstream mediators responsible for the activation of JNK signaling largely include the Rho family of GTPases, primarily Rac and CDC42 [47]. Upon activation, MEKKs phosphorylate and activate MEK4 and MEK7, which in turn triggers dual phosphorylation of JNK1/2/3 and promote JNK nuclear translocation [40].

### 1.3.3 p38

The family of p38 MAPKs consists of four splice variants p38- $\alpha$  (MAPK14), p38- $\beta$  (MAPK11), p38- $\gamma$  (MAPK 12), and p38- $\delta$  (MAPK13) [40]. Activation of the p38-signaling cascade is triggered by extracellular stimuli including UV light, heat, osmotic shock, pro-inflammatory cytokines [e.g. IL-1 and TNF- $\alpha$ ], and growth factors [e.g. macrophage-colony stimulating factor (M-CSF)] [48]. Among the p38 family, p38- $\alpha$  and p38- $\beta$  are universally expressed, whereas the expression of p38- $\gamma$  and p38- $\delta$  are tissue type-dependent [48]. The entire p38 family contains a threonine-glycine-tyrosine motif within their activation segment that is phosphorylated and activated by dual specificity kinases, MEK3 and MEK6. Like the other MEKs, MEK3/6 activation relies on phosphorylation by upstream MEKKs, such as MEKK1-4 [40]. p38 activation contributes widely to biological functions, including apoptosis, cellular differentiation, cell cycle progression, and inflammation [49,50]. In fact, its activation is essential for the production of the pro-inflammatory cytokines IL-1 $\beta$ , TNF- $\alpha$ , and IL-6 [51], all of which are produced by activated macrophages, which are at the forefront of the immune response.

## 1.4 TLR signaling

Toll-like receptors (TLRs) are pattern recognition receptors (PRRs) and are key components of innate immunity. These receptors are responsible for detecting pathogen associated molecular patterns (PAMPs) from microbes, as well as danger associated molecular patterns (DAMPs) from injured tissue [52]. The first prototypic PRR identified was TLR4, which recognizes the Gram-negative bacterial component lipopolysaccharide (LPS) [53]. To date, a total of 10 TLRs have been identified in humans and 12 in mice [52]. TLR signaling plays a crucial role during immune responses by activating various transcription factors, through MAPK-dependent or -independent pathways, which behave in combination to regulate inflammatory gene expression [54,55]. The intracellular Toll-interleukin 1 receptor (TIL1R) domain is crucial for TLR signaling transduction by acting as a docking site for TIL1R-containing cytoplasmic adaptor proteins, such as the myeloid differentiation primary response gene 88 (MyD88) [56]. With the exception of TLR3, MyD88 is the primary adaptor for all

TLRs. When TLRs are stimulated by their respective ligands, triggering TIR domain activation, this activates MyD88, which subsequently leads to IL-1 receptor-associated kinase (IRAK) 1/2/4 and TNFR-associated factor (TRAF) 6 activation. In turn, activation of IRAK and TRAF6 activates the transforming growth factor (TAK1) complex, which initiates MAPK and nuclear factor kappa B (NF- $\kappa$ B) signaling via phosphorylation [56].

## 1.5 LeTx and Immune Suppression

Immune evasion and/or immunosuppression tactics are crucial for the survival and dissemination of various pathogens. LeTx produced by *B. anthracis* is highly versatile in targeting all MEKs, with the exception of MEK5 [35-37], which leads to subversion of key immune signaling pathways necessary for innate and adaptive immune function (Fig 1.1). This immune paralysis tactic by LeTx plays a vital role in anthrax pathogenesis [57-59], as it promotes host invasion by *B. anthracis* resulting in acute bacteremia and toxemia.

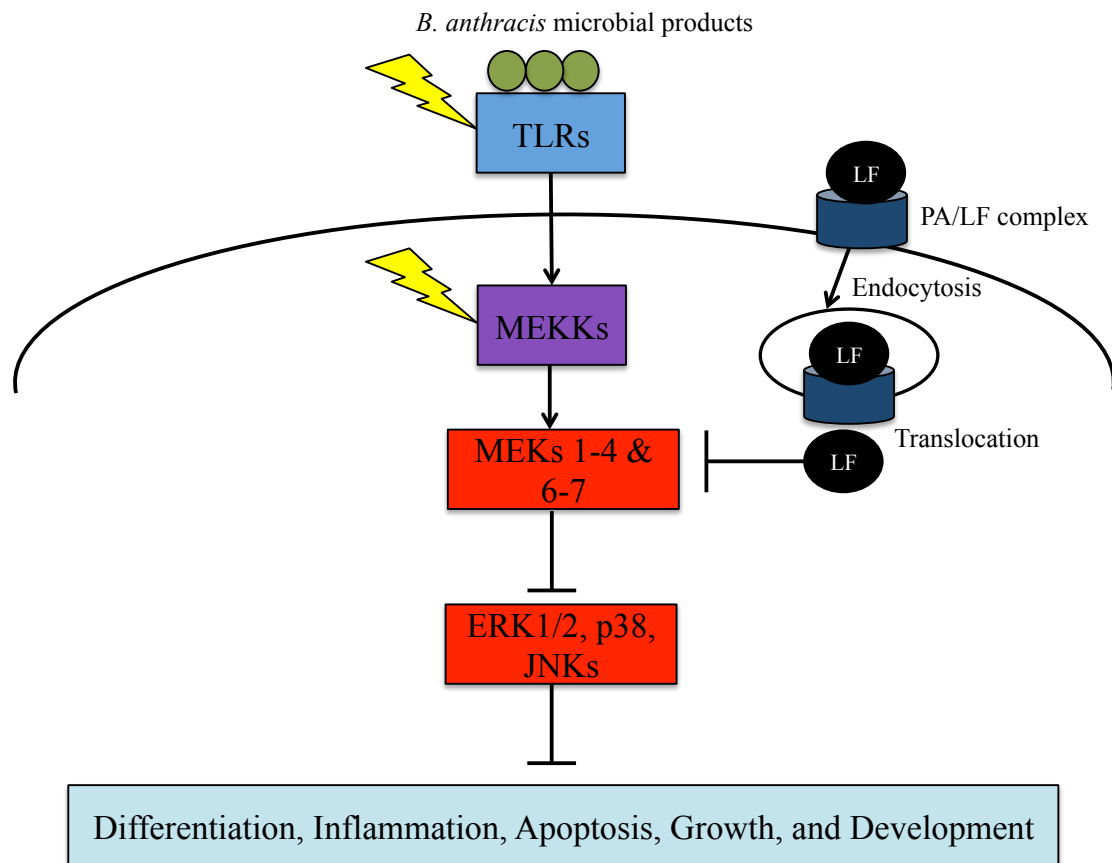
Since macrophages are the initial antigen-presenting cells (APCs) responsible for the phagocytosis and transport of *B. anthracis* to local lymph nodes where systemic infection arises [57], much attention has been placed on LeTx-mediated immune suppression in these cells. Activation of macrophages relies primarily on MAPK signaling and MAPKs including p38 and JNKs/SAPKs are coupled to TLRs [57,60]. Activation of these TLR-coupled MAPKs is crucial for the production of various pro-inflammatory cytokines, chemokines, and enzymes [e.g. inducible nitric oxide synthase (iNOS)] [50,61,62]. Not surprisingly, the cleavage and subsequent inactivation of MEKs by LeTx deters macrophage-mediated inflammation by preventing the production of inflammatory proteins such as IL-1 $\beta$ , IL-6, and TNF- $\alpha$  [63-65]. The loss of IL-1 $\beta$  production is of particular interest, as *IL-1 $\beta$ <sup>-/-</sup>* mice are more susceptible to lethality by anthrax [66]. Furthermore, LeTx also impairs antigen presentation, the production of reactive oxygen species (ROS) such as nitric oxide, and phagocytic ability in macrophages [21,22,57].

Aside from macrophages, LeTx has also been shown to suppress other innate and adaptive immune functions by targeting the MAPK signal transduction pathway in

dendritic cells (DCs), neutrophils, B-lymphocytes, and T-lymphocytes. LeTx deters immune responses in DCs by impairing cytokine production (TNF- $\alpha$  and IL-6), surface activation marker expression (CD40, CD80 and CD86), antigen presentation, phagocytosis, and bactericidal activity [21,22,67]. In neutrophils, LeTx primarily prevents chemotaxis to the site of infection, likely by impairing their actin-based motility [21,68]. Although adaptive immune cells play a much smaller role relative to macrophages and DCs in the progression of acute anthrax infection, LeTx also impairs T-cell activation, chemotaxis, and cytokine responses, as well as B-cell activation, proliferation and antibody production, particularly IgM [21,22,57,69]. Collectively, LeTx is a potent suppressor of both innate and adaptive immune functions, thus creating the ideal environment for *B. anthracis* survival and dissemination within the infected host.

**Figure 1.1 LeTx inhibits various cellular functions through MEK inactivation.**

TLRs are activated in response to infection (lightning arrow), thus activating MEKKs. However once in the cytoplasm, anthrax lethal factor (LF) cleaves and inhibits all MEKs, except for MEK5, preventing down-stream activation of MAPKs, which are essential for various cellular functions.





## 1.6 Pyroptosis

Pyroptosis is a type programmed cell death mediated by caspase-1 and is induced in response to microbial infections, such as *Salmonella*, *Legionella*, and *Shigella*, and various host factors [70]. Caspase-1 was originally recognized for its proteolytic activation of pro-inflammatory cytokines, IL-1 $\beta$  and IL-18, however more recently it is characterized as a defining feature of pyroptosis [70]. Pyroptotic cell death involves rupturing of the cell membrane, which leads to the liberation of pro-inflammatory intracellular matter [70,71]. Interestingly, nuclear integrity is maintained during pyroptosis relative to apoptotic cell death where nuclear fragmentation occurs[70]. Pyroptosis can be beneficial or detrimental to the host, either by removing intracellular niches of intracellular pathogens [72-75], or by promoting immune evasion/dissemination [76-79], respectively. The pyroptotic cell death pathway is initiated by the activation of innate immune receptors known as nuclear oligomerization domain and leucine-rich repeat receptors (NLRs) [80], which are highly expressed within the cytoplasm of innate immune cells such as macrophages.

### 1.6.1 NLRs and Pyroptosis

NLRs are a group of innate intracellular PRRs that respond to pathogenic attack, as well as tissue injury [80-83]. NLRs are composed of three core structural domains: the C-terminus, which contains a leucine-rich repeat (LRR) capable of identifying conserved ligands, the central NACHT domain that is key for NLR oligomerization and activation, and the N-terminus effector domain [82]. The N-terminus effector domain may consist of a pyrin domain (P), a caspase recruitment domain (C), or a baculovirus inhibitor of apoptosis protein repeat domain (BIR) [82]. Although cellular events such as K<sup>+</sup> efflux, the generation of ROS, and cathepsin B release from lysosomes are implicated in the activation of various NLRs[84], none of these events are sufficient to activate the receptors, and until recently NLR activation was unclear [85,86]. Current advances demonstrated that these receptors are activated by direct interaction with their ligands. For example, NLRX1 binds RNA, NOD1 and NOD2 are activated by peptidoglycan (a component of bacterial cell walls) fragments, and NLRC4 is activated by flagella [87]. Following NLR activation, they oligomerize to form the inflammasome, which consists

of NLRs, pro-caspase-1, and the adaptor protein apoptosis-associated speck-like containing a caspase activation and recruitment domain (ASC) [81-83]. Caspase-1 is expressed as an inactive 45-kDa zymogen and activated by an autocatalytic process in the inflammasome complex [70,88,89]. Furthermore, activated caspase-1 is required for the processing and release of pro-inflammatory cytokines IL-1 $\beta$  and IL-18, as well as pyroptotic cell death [70].

To date, there are 22 family members of NLRs in humans, which can be activated by numerous microbial and/or viral components [90]. For example, *Salmonella enterica* serovar Typhimurium (*S. typhimurium*) causes typhoid in humans and NLRC4 plays a vital role in resistance during *S. typhimurium* infection [91,92]. NLRC4 is activated by *Salmonella* flagellins or a type III secretion system component [93,94] in a *Salmonella* Pathogenicity Island (SPI)-I-dependent manner [95]. Furthermore, *S. typhimurium* activates NLRP3 through a SPI-II-dependent mechanism [96]. Though the activation of these NLRs by *Salmonella* is protective to the host during infection [75,92,97-99], it can also trigger septic shock [100-102]. In addition to a number of bacterial and viral infections that trigger NLR activation, LeTx production by *B. anthracis* is responsible for the activation of NLRP1 [89].

### 1.6.2 LeTx and Pyroptosis

Murine macrophages are divided into two groups based on their sensitivity to LeTx: LeTx-sensitive, and LeTx-resistant. LeTx-sensitive macrophages from Balb/cJ, C3H/HeJ, CBA/J, FVB/NJ, and SWR/J, inbred mice succumb to pyroptosis in as little as 90 minutes [21]. In contrast, LeTx-resistant macrophages from DBA/2J, AKR/J, SJL/J, A/J, and C57BL/6J inbred mice undergo slow apoptotic death, likely due to MEK inactivation [21]. Studies in these rodents led to the discovery of the LeTx sensitivity allele, defined as the NLR pyrin domain-containing protein (*NLRP1b*; also known as *NALP1b*), located on mouse chromosome 11 [103]. There have been five polymorphic *NLRP1b* alleles discovered in mice to date, including *NLRP1b1*, *NLRP1b2*, *NLRP1b3*, *NLRP1b4*, and *NLRP1b5*, which precisely associate with LeTx sensitivity [103]. Strains with LeTx-susceptible macrophages possess the *NLRP1b1* or *NLRP1b5* allele, where LeTx-resistant macrophages possess alleles 2, 3 or 4 [103]. While strains harbouring a

LeTx-sensitive *NLRP1b* allele showed increased host protection from *B. anthracis* infection through early detection of LeTx [104], another study showed that activation of NLRP1b enhances susceptibility to LeTx [105]. Strikingly, NLRP1b1-deficient mice containing NLRP1b1-expressing macrophages are also susceptible to LeTx toxemia [20], suggesting that the host is protected by *B. anthracis* through early detection of LeTx, but toxic shock remains inevitable due to NLRP1b1 activation.

The activation of NLRP1b is caused by LF-dependent cleavage of the N-terminus effector domain [106,107]. This proteolysis of NLRP1b is pertinent for inflammasome formation, particularly pro-caspase-1 recruitment [107]. The processing of pro-caspase-1 into highly active caspase-1 is accomplished through the inflammasome platform [88]. While the inductive mechanism of pyroptosis through caspase-1 is not completely understood, it is central for LeTx-induced pyroptosis [21]. Caspase-1 is also responsible for the proteolytic activation of pro-inflammatory cytokines, IL-1 $\beta$  and IL-18. During pyroptosis, caspase-1 induces plasma membrane pore formation that disrupts cellular ion gradients. This leads to increased osmotic pressure, promoting water influx, swelling of the cell and inevitable cell lysis, causing the spill of intracellular contents into the extracellular environment [71]. Unlike apoptosis, the nuclear integrity of the cell remains intact during pyroptotic cell death [70]. Aside from NLRP1b and caspase-1 activation, other cellular events including calcium influx [108], early mitochondrial dysfunction [109,110], and ROS generation [111] are essential for LeTx-induced pyroptosis. Although the precise molecular mechanisms of LeTx-induced pyroptosis remain unclear, we linked the three mitochondrial death genes BCL2/adenovirus E1B 19 kDa-interacting protein 3 (*BNIP3*), BNIP3-like (*BNIP3L*), and metastatic lymph node 64 protein (*MLN64*) to NLRP1b/caspase-1-dependent mitochondrial dysfunction [110,112].

### 1.6.3 Mitochondrial Death Genes

We and others have recognized the central role of mitochondrial impairment in LeTx-induced cell death [109,110,112]. LeTx was shown to induce mitochondrial dysfunction in murine J774.1 macrophages, manifested as a decline in mitochondrial membrane potential and succinate dehydrogenase (SDH) activity, as well as mitochondrial swelling [109]. Since proteasome activity is vital for caspase-1-mediated pyroptotic cell death [113-

116], inhibiting proteasome activity prevented LeTx-induced mitochondrial dysfunction in these macrophages [109]. Furthermore, our lab previously associated the mitochondrial death genes, *BNIP3*, *BNIP3L*, and *MLN64*, with caspase-1-mediated LeTx-induced mitochondrial dysfunction [110,112]. In LeTx-susceptible macrophages, mitochondrial dysfunction included cholesterol enrichment, a rapid increase in mitochondrial membrane potential followed by overall hypo-polarization, ROS generation, and depletion of free glutathione (GSH) [112]. The precise mechanism of BNIP3/BNIP3L in disrupting mitochondrial function is not known; however they are involved in ROS generation [110,117], whereas MLN64 is implicated in cholesterol accumulation and subsequent GSH depletion [112].

The BH (Bcl-2 homology) 3-only members of the Bcl-2 protein family contain the BNIP3 subfamily that includes BNIP3 and BNIP3L proteins [117]. BNIP3, formerly named NIP3, was the first member of the BNIP3 subfamily of proteins, and was discovered via a yeast two-hybrid screen [118]. In response to cellular stress, these proteins homodimerize within the outer mitochondrial membrane, thus initiating programmed cell death (e.g. apoptosis) or autophagy [117]. The BH3 or the C-terminal transmembrane (TM) domains are both responsible for regulating BNIP3/BNIP3L-dependent cell death [117]. These BH3-only proteins possess a BH3 interacting domain (BID), which binds through its BH3 domain and activates the pro-apoptotic factors BAX and BAK [119]. As a result, BNIP3/BNIP3L form oligomer complexes that localize to the mitochondrial membrane and consequently lead to the release of cytochrome C into the cytoplasm [119]. The C-terminal TM domain mainly plays a role in stabilizing dimer formation and targeting BNIP3/BNIP3L to the mitochondria to promote cell death activity [120]. Mutational analysis of the TM domain revealed that stable dimerization is not essential for inducing BNIP3 cell death activity [121]. However, loss of targeting BNIP3 to the mitochondria prevented mitochondrial permeability transition and ROS generation, which are key events necessary for inducing cell death [122]. The BNIP3 N-terminal domain has been shown to integrate into the mitochondrial membrane through its N-terminal TM regions [118]. The N-terminus of BNIP3 comprises a conserved cysteine residue that is oriented towards the cytosol making it susceptible to oxidation [123]. As such, under increased oxidative stress, the cysteine residue is oxidized, thus promoting

homodimerization and pro-death activity [124]. Not surprisingly, mutating the cysteine residue to alanine resulted in decreased homodimerization and cell death activity [125]. During cellular stress BNIP3 appears to function as a redox sensor and promotes cell death through cooperation of the N-terminal and C-terminal TM domain [125].

MLN64, also known as StAR-related lipid transfer domain (StARD) protein 3, belongs to a family of lipid trafficking proteins. To date, there are 15 known StARD-containing proteins in mammals, and among them MLN64 is expressed in all tissues [126,127]. The MLN64 protein is responsible for cholesterol transfer from the endolysosomal membrane to the mitochondrial membrane [128-130]. It primarily locates to the membranes of late endosomes via the N-terminal transmembrane domain termed MENTAL (MLN64 N-terminal) [128,131], whereas the C-terminal StARD signals for mitochondrial translocation [130]. During transport, the MENTAL domain seizes endolysosomal cholesterol followed by transfer of the cholesterol to the mitochondria through interaction with the StARD/translocation protein (TSPO; 18 kDa) on the outer mitochondrial membrane [132,133]. Not surprisingly, increased loads and subsequent accumulation of mitochondrial cholesterol mediated by MLN64 has been strongly linked to cell death [134-136].

## 1.7 Cellular Adaptation

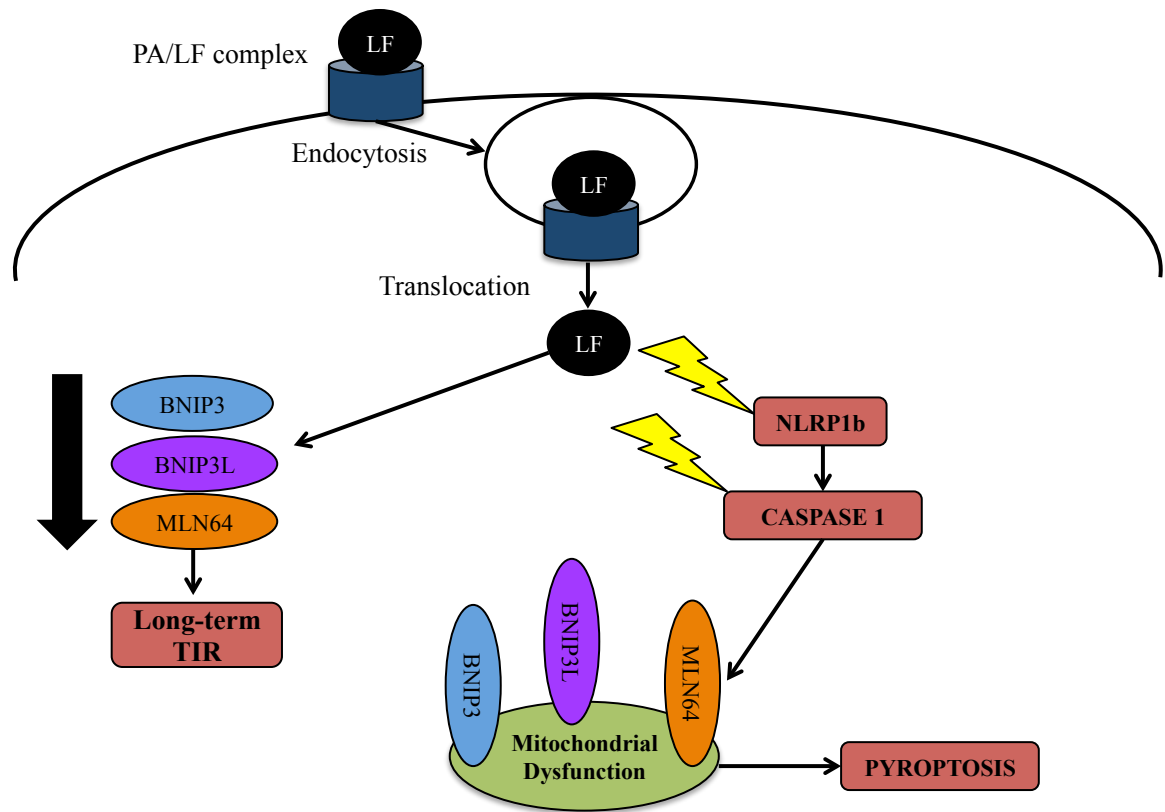
Macrophages are at the forefront of innate immunity and they encounter a variety of pathogens. Consequently, they frequently adapt to various stressors in order to preserve vigilance or moderate overwhelming inflammatory responses. For example, macrophages pre-exposed to a sub-lethal dose of endotoxins, such as lipopolysaccharides, become tolerant to subsequent challenges of the endotoxins [137,138]. Likewise, we and others showed that RAW264.7 macrophages pre-exposed to a sub-lethal dose of LeTx become refractory to subsequent high cytolytic doses of LeTx for 4-5 days [110,112,139]. This phenomenon is termed toxin-induced resistance (TIR). We further demonstrated that a small number of these TIR cells (~2 %) remain resistant for up to 5-6 weeks (long-term TIR). It was originally thought that these long-term TIR cells prevented the translocation of LF into the cytosol. However, MEK cleavage by LF was still noted, suggesting translocation into the cytosol remained unaffected [110].

Furthermore, like RAW 264.7 wild-type macrophages, long-term TIR macrophages showed typical NLRP1b and caspase-1 activation [110]. Overall, these findings suggest that there were no defects in inflammasome activation, leaving the mechanism of LeTx resistance unclear.

While inflammasome activation was normal in long-term TIR, we established key events involved in the mediation of long-term TIR (Fig. 1.2). Genome-wide transcript analysis of a single long-term TIR clone implicated two closely related pro-apoptotic genes, *BNIP3* and *BNIP3L*, in TIR [110]. Relative to wild-type, these long-term TIR macrophages down-regulate BNIP3 and BNIP3L at both mRNA and protein levels [110]. Aside from the requirement for a fully functional inflammasome, and the up-regulation of BNIP3 and BNIP3L, mitochondrial dysfunction is also an essential component to the LeTx-induced pyroptotic pathway. We demonstrated that up-regulation of MLN64 is required for mitochondrial dysfunction including, cholesterol enrichment, membrane hyperpolarization, generation of reactive oxygen species (ROS), and depletion of GSH [112]. However, long-term TIR macrophages showed decreased expression of MLN64 and therefore remained resistant to NLRP1b/caspase-1-induced mitochondrial dysfunction [112].

**Figure 1.2 Key events involved in sensitivity and long-term resistance to LeTx-induced pyroptosis in macrophages.**

High doses of anthrax lethal factor (LF) cleave and activate (lightning arrow) NLRP1b, triggering casapse-1-mediated mitochondrial dysfunction and pyroptosis via BNIP3, BNIP3L, and MLN64 expression. In contrast, sub-lethal doses of LF trigger down-regulation of BNIP3, BNIP3L, and MLN64 expression, inducing long-term TIR.





## 1.8 Epigenetics

Epigenetics was a term formulated by the scientist Conrad Waddington [140] and is a cellular mechanism that inheritably regulates gene expression or cellular phenotype without changing DNA nucleotide sequences in response to developmental and environmental signals [141]. Two of the most studied epigenetic mechanisms include DNA methylation and histone modifications. Although various types of histone modifications such as, phosphorylation, ubiquitination, SUMOylation and ADP-ribosylation have been examined, histone phosphorylation, methylation and acetylation often play a key role in transcriptional regulation [142].

### 1.8.1 Histone Modifications and Gene Expression

Histones are nuclear proteins that are responsible for the packaging and structural organization of eukaryotic DNA into fundamental chromatin units known as nucleosomes [143]. The nucleosome consists of a 147 base-pair DNA segment wrapped 1.65 times around an eight-histone protein core [144]. The histone core consists of two H2A-H2B dimers and a single H3, H4 tetramer [143]. Higher-level organization of nucleosomes is essential for the compaction of DNA in the nucleus. Epigenetic modifications of the four-histone proteins, regulates the availability of DNA for replication, repair, and transcription [145,146]. These modifications include, methylation, acetylation, SUMOylation, ADP-ribosylation, ubiquitination, and phosphorylation [143]. Most histone modifications occur at the N-terminal tails, which are rich in positively charged lysine residues [146]. The negatively charged DNA associates tightly with the positively charged lysine residues, but modifications such as acetylation neutralize these charges allowing the chromatin to "open" and promote gene transcription [147]. Various combinations of histone modifications lead to transcriptional activation or repression [148]. For example histone acetylation and deacetylation promote transcriptional activation and silencing, respectively, whereas histone methylation can induce either activation or repression. Transcriptional activation results from mono-methylation of histone H4 lysines 20 or 5, methylation of histone H3 lysines 4, 36, or 79, as well as acetylation at histone H3 lysines 9 or 14; whereas inactivation results from di- or trimethylation of histone H3 lysines 9 or 27 [146,149].

### 1.8.1.1 Histone Acetylation and Gene Expression

Two families with antagonistic functions, histone acetyltransferases (HATs) and histone deacetylases (HDACs) are responsible for modifying levels of histone acetylation, which regulates gene expression (Fig. 1.3). Histone acetylation typically plays a role in the activation of gene expression [150-152]. Acetylation at N-terminal lysine residues decreases the association with DNA, which allows transcription factors to access the promoter region of genes [147]. Acetylation of specific lysine residues also forms docking sites on modified nucleosomes for specific transcriptional regulators that contain recognition motifs such as bromodomains [153,154]. HATs are the enzymes responsible for catalyzing acetylation by transferring acetyl groups from acetyl CoA to the histone tails, thus inducing an open chromatin conformation and facilitating gene transcription [155]. The HAT family can be categorized into two classes: type A HATs, which are primarily located in the nucleus and responsible for transcriptional activation via acetylation of nucleosomal histones, and type B HATs, which are localized within the cytoplasm where they acetylate recently synthesized histones prior to chromatin assembly [156]. The majority of transcriptional regulators with acetylation activity belongs to the type A HATs and includes, CREB (cAMP response element-binding protein)-binding protein (CBP), E1a-binding protein p300 (p300), P300/CBP-associated factor (PCAF), Gcn5, and TAF<sub>II</sub>250 subunit of transcription factor IID (TFIID), to name a few [156]. To date, Hat1p is one of few type B HATs to be identified [156]. A 55-kDa polypeptide (p55) was the first discovered type A HAT from *Tetrahymena thermophile* and is analogous to Gcn5, a transcriptional co-activator from budding yeast [157]. These type A HATs preferentially target histone H3 *in vitro*, however they are also capable of acetylating histone H2B and H4 [156].

In contrast to HATs, HDACs are a family of enzymes that deacetylate histones. The removal of acetyl groups from the histone tails, leads to tight re-association between the positively charged lysine residues and negatively charged DNA; this reduces access of transcription factors to gene promoter regions, which results in transcriptional repression [150]. In addition, loss of acetylation can reduce the association of transcription factors, which specifically bind to acetylated lysine residues to promote transcription [153,154].

To date, there are a total of 18 HDACs belonging to two families: the zinc-dependent family, which includes class I, II and IV, and the nicotinamide adenine dinucleotide (NAD)-dependent family, which includes class III [150]. Class I HDACs include HDAC1, 2, 3, and 8, which are ubiquitously expressed within the nucleus, whereas class II HDACs include HDAC4, 5, 6, 7, 9, and 10, which are primarily located in the cytoplasm, however they can move back and forth between the nucleus [150]. Unlike class I HDACs, class II HDACs are not widely distributed among cell types and are likely implicated in cell differentiation [158,159]. HDACs alone do not silence gene expression, but they associate with other transcriptional repressors to form repressor complexes [160]. For example, it was reported that DNA methyltransferase (DNMT) 1 and HDACs co-operate in transcriptional repression [161,162].

#### 1.8.1.1.1 HDAC8

Unlike other class I HDACs, HDAC8, which is ~42 kDa in size, localizes in both the cytoplasm and the nucleus, thus in part making it the most atypical protein in this class [158,163-165]. *In vitro*, HDAC8 has shown deacetylase activity towards all core histones [166-168]. One specific example includes its activity towards histone H4 lysine 16 (H4K16) [164]. Despite such findings, HDAC8's activity towards specific histones *in vivo* remain unclear [164]. In contrast, HDAC8 has various non-histone substrates. For example, HDAC8 has been shown to interact with PP1 phosphatase, CBP, heat shock proteins, heat shock protein 70 binding protein, cofilin and  $\alpha$ -actin, and the human ortholog of the yeast ever-shorter telomeres 1B [163,169-171]. Nevertheless, the role of these HDAC8 interactions in cellular functions and TIR are not known. In addition to these substrates, HDAC8 has also been shown to deacetylate the C-terminal end of the transcription factor, p53 [164]. In line with these findings, a recent study demonstrated that HDAC8 suppressed p53 expression in hepatocellular carcinoma cell lines, likely through deacetylation of p53 at lysine382 [172]. Another study also demonstrated that the inv(16) fusion protein, which promotes pre-leukemic populations, inhibits acetylation of p53 by forming a complex with p53 and HDAC8 [173]. While, these data suggest a key role for HDAC8 in cancer, the role and mechanisms of HDAC8 in infection and immunity have not yet been examined.

### 1.8.1.2 LeTx and Histone Modifications

Epigenetic mechanisms controlling gene expression are exploited by a variety of bacterial products, which often act by interfering with signaling transduction pathways, as well as directly interacting in the nucleus [174]. To date, most of the histone modifications stimulated by bacterial infection include histone acetylation/deacetylation, and histone phosphorylation/dephosphorylation [174]. Strikingly, the production of LeTx by *B. anthracis* induces dynamic histone modifications in host cells suggesting a possible mechanism for toxin resistance and immunosuppression.

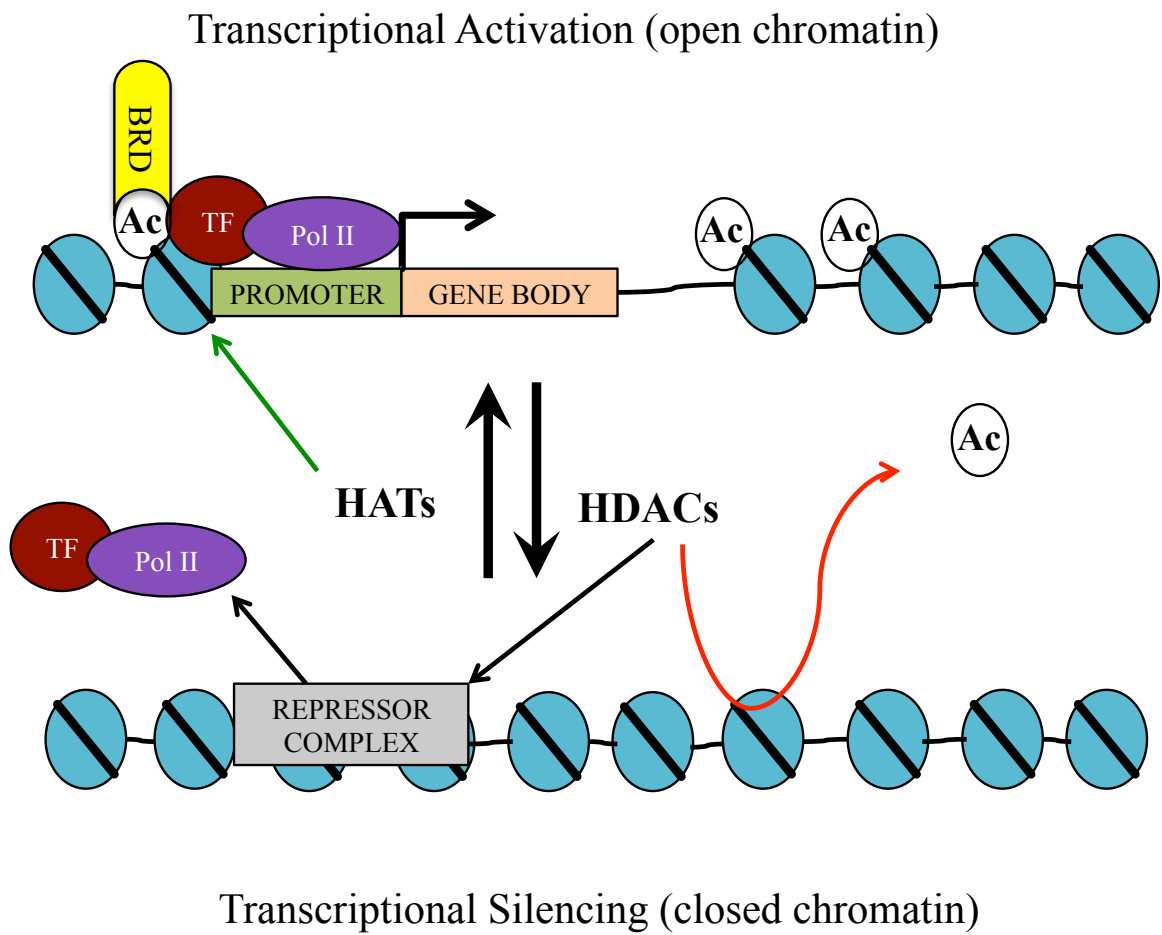
The ability of *B. anthracis* to circumvent the host immune response at least in part by LeTx-mediated MEK inhibition is remarkable. However, prior to a study conducted by Raymond *et al* [175], the mechanism that linked the MAPK signaling cascade inhibition to immune gene silencing was unclear. They showed that LeTx suppressed the expression of a neutrophil chemoattractant, IL-8 (CXCL8), in epithelial cells through blocking p38/ERK-dependent phosphorylation of histone H3 serine 10 (H3S10), which prevented recruitment of NF- $\kappa$ B to the *IL-8* and *KC* (keratinocyte chemoattractant) promoters [175]. Furthermore, decreased levels of acetylation at H3K14 (H3K14Ac) were also noted within the promoters of *KC* and *IL-8*, which is associated with a transcription-permissive state [175].

In addition to immune suppression, LeTx also induces cell death within macrophages, which are essential players in the first-line of defense against pathogens. Interestingly, a Jumonji C family histone H3 lysine 27 (H3K27) demethylase, Jmjd3, was up-regulated in LeTx resistant RAW 264.7 macrophages in response to LPS [176]. Since, Jmjd3 is known to play a vital role in the inflammatory response by contributing to macrophage differentiation, its expression may be crucial to the recovery of toxin exposed macrophages [176]. Nevertheless, this study failed to show the up-regulation of Jmjd3 in response to LeTx alone, suggesting the outcome was solely LPS-induced. As such, further study is required to examine the role of JMJD3-dependent histone demethylation in LeTx-resistance.

As previously mentioned macrophages exposed to sub-lethal doses of LeTx become refractory to subsequent cytotoxic doses, termed TIR [110,112,139]. These TIR macrophages maintain this phenotype throughout multiple cycles of cell division. This suggested the possibility of epigenetic reprogramming, which we have examined with a specific focus on histone modifications. Indeed, we showed that HDAC8 expression was positively correlated with long-term TIR [177]. Furthermore, when the H3K27 HATs, CBP and p300, were knocked-down in RAW 264.7 macrophages and mouse primary bone marrow derived macrophages (BMDMs), they mimicked the TIR phenotype [177]. Overall, this study revealed a strong correlation with histone deacetylation in maintaining long-term TIR.

**Figure 1.3 Histone acetylation levels can mediate gene expression.**

Histone acetyltransferases (HATs) acetylate histones, reducing association with DNA and inducing an open chromatin confirmation to allow for access of transcriptional machinery, and the binding of bromodomains (BRD) to acetylated histone residues, thus promoting gene transcription. In contrast, Histone deacetylases (HDACs) deacetylate histones, triggering tight association with DNA along with repressor complex formation, thus preventing access of transcriptional machinery and gene transcription.



## 1.9 Rationale, Hypothesis, and Objectives

RAW 264.7 macrophages are susceptible to LeTx-induced pyroptosis. However, RAW 264.7 long-term TIR macrophages down-regulated expression of the three mitochondrial death genes, *BNIP3*, *BNIP3L*, and *MLN64* [110,112], which conferred resistance to pyroptosis. In addition to inducing pyroptosis, LeTx also causes immune suppression in macrophages, mainly by preventing the expression of pro-inflammatory cytokine genes. Interestingly, a gene-silencing epigenetic regulator, HDAC8, was up-regulated in long-term TIR [177]. Since histone modifications are correlated to LeTx toxicity, I hypothesize that HDAC8 plays a fundamental role in the silencing of cytokine and mitochondrial death genes, leading to immune suppression and resistance to pyroptosis, respectively. Four aims were proposed to address this hypothesis:

1. Determine whether HDAC8 mediates resistance to LeTx-induced pyroptosis.
2. Identify the mechanism by which HDAC8 silences mitochondrial death gene expression.
3. Determine whether HDAC8 plays a role in LeTx immune suppression.
4. Examine the role of HDAC8 in LeTx-mediated cytokine gene silencing.



## CHAPTER 2

### 2 MATERIALS AND METHODS

#### 2.1 Cell culture and reagents

RAW 264.7 murine macrophages were cultured in DMEM containing 8% heat-inactivated fetal bovine serum [FBS (Sigma-Aldrich)], 10 mM MEM non-essential amino acid solution, 100 U/mL penicillin G sodium, 100 µg/mL streptomycin sulfate, and 1 mM sodium pyruvate. The generation of primary bone marrow-derived macrophages (BMDMs) was performed by Dr. Soon-Duck Ha. Briefly, bone marrow-derived cells (BMCs) were flushed out of the leg bones (femurs and tibia) of 129/S1/SvImj mice using a 25.5-gauge needle and 1× phosphate buffered saline (PBS). The isolated BMCs were then cultured in c-RPMI (Sigma-Aldrich), containing 10% heat-inactivated FBS (Sigma-Aldrich), 5 mM MEM non-essential amino acids solution, 1000 U/mL penicillin G sodium, 10 mg/mL streptomycin sulfate, 5 mM sodium pyruvate, and 20 ng/mL macrophage-colony stimulatory factor (M-CSF). The culture medium was replaced every 2 days and after 7 days of culture ~30 million BMDMs were generated from a single mouse. All cells were grown at 37°C in a humidified atmosphere with 5% CO<sub>2</sub>.

Long-term TIR cells were generated as previously described [110]. Briefly, RAW 264.7 macrophages were treated with a cytolytic dose of LeTx (250 ng/mL LF and 500 ng/mL PA) for 5 h and surviving cells were plated in fresh culture medium. After two weeks, surviving clones were individually picked and plated on a 96-well plate. Each clone was tested for LeTx sensitivity and resistant clones were pooled and propagated. Short-term TIR cells were generated as previously described [110]. Briefly, RAW 264.7 macrophages were treated with a sub-lethal dose of LeTx (100 ng/mL LF and 100 ng/mL PA) for 5 h and then supplemented with fresh media overnight. The next day surviving cells were pooled and plated onto new culture plates with fresh media. BMDM-TIR cells were generated by Dr. Soon-Duck Ha as previously described [177]. Briefly, BMDMs were treated with a sub-lethal dose of LeTx (100 ng/mL LF and 100 ng/mL PA) for 24 h and surviving cells were plated onto new culture dishes with fresh media.

Protective antigen (PA), lethal factor (LF) and *Escherichia coli* derived LPS were purchased from List Biological Laboratories Inc. (California USA). The following is a list of antibodies (Abs) used in this study. Ab against H3K27Ac was purchased from Active Motif (California, USA). Abs for pan H3 and actin were purchased from Bio Vision (California, USA) and Abcam Inc. (Ontario, Canada), respectively. Anti-HDAC8 and anti-HDAC3 were purchased from Epigentek. Abs against pro-IL-1 $\beta$  was received from Dr. Aurigemma (NCI-FCRDC, Frederick, MD) and anti-EGFP was purchased from Clontech Laboratories Inc. (California, USA). Abs against RNA polymerase II-phospho S5 and RNA polymerase were purchased from Abcam Inc. (Ontario, Canada) and Active Motif (California, USA), respectively. Rabbit IgG was purchased from Abcam (Ontario, Canada). Please refer to table 2.1 for more detailed information on Abs used in this study. The following is the list of chemical inhibitors used in this study: epigenetic; panobinostat (LBH-589; Selleck), mocetinostat (Selleck), PCI-34051 (Cayman Chemical), azacitidine (Sigma-Aldrich) and CAY10603 (Cayman Chemical), and non-epigenetic, AC-YVAD-CHO (Calbiochem). Predesigned small interfering RNA (siRNA) oligonucleotides directed against HDAC8 (number SI1063902) were purchased from Qiagen and siRNAs targeting mouse caspase-1 were purchased from Life Technologies (Ambion).

### 2.1.1 Stable isotope labeling by amino acids in cell culture

RAW 264.7 macrophages were cultured for 7 days in SILAC DMEM (Sigma-Aldrich; product #D9443) containing 8% dialyzed heat-inactivated FBS (Sigma Aldrich), 10 mM MEM non-essential amino acid solution, 100 U/mL penicillin G sodium, 100  $\mu$ g/mL streptomycin sulfate, 1 mM sodium pyruvate, 0.802 mM L-leucine (Sigma-Aldrich; product #L8912), 0.398 mM L-arginine (Sigma-Aldrich; product #A6969), and 0.798 mM L-lysine (Sigma-Aldrich; product #L8662). The Lys4 (4,4,5,5-D4) isotope (Cambridge Isotopes, DLM-2640) was used for TIR cells (0.798 mM). Per 500 mL of SILAC DMEM, 40 mL of heat-inactivated FBS was dialyzed using cellulose membrane dialysis tubing with a molecular weight cut-off of 12 kDa (Sigma-Aldrich; product #D9277) in 4L of buffer (0.15M NaCl). The dialysis buffer was changed every 30 minutes for the first 3 hours and then left for an additional 9 hours. The dialyzed heat-

inactivated FBS was then sterile-filtered using vacuum filtration (VWR; catalog # 29552-016) and added to SILAC DMEM. RAW 264.7 Short-term TIR cells were generated as described in section 2.1, however cells were labeled in respective SILAC DMEM for 5 days prior to the administration of LeTx.

### 2.1.2 Inhibitor treatment

For treatments with chemical inhibitors, stock solutions of panobinostat as a histone deacetylase inhibitor (HDACi), mocetinostat as an HDACi for HDACs 1, 2, 3 and 11, PCI-34051 as a selective HDAC8 inhibitor, CAY10603 as a selective HDAC6 inhibitor, azacitidine as a DNA methyltransferase inhibitor (DNMTi), and AC-YVAD-CHO as a caspase-1-inhibitor were dissolved in DMSO. The macrophages were incubated with respective inhibitors at the indicated concentration and time as described in Figure legends. Please see table 2.2 for more information on inhibitors used in this study.

**Table 2.1 List of antibodies (Abs)**

Ab	Company	Product Number	Host (Isotype)	Clonality	Working Dilution	Amount/ChIP
Actin	Abcam	ab3280	Mouse (IgG1)	monoclonal	1:500	
eGFP	Clontech	632380	Mouse (IgG2a)	monoclonal	1:1000	
H3	Bio Vision	3623	Rabbit	polyclonal	1:1000	
H3K27Ac	Active Motif	39135	Rabbit (serum)	polyclonal	1:5000	3 $\mu$ L
HDAC3	Epigentek	A-4003	Mouse (IgG)	monoclonal		6 $\mu$ g
HDAC8	Epigentek	A-4008	Mouse (IgG)	monoclonal	1:500	6 $\mu$ g
IgG	Abcam	ab46540	Rabbit (IgG)	polyclonal		1/4/6 $\mu$ g
Pro-IL-1 $\beta$	Gift from Dr. Aurigemma				1:1000	
Pol II	Active Motif	39097	Mouse (IgG)	monoclonal		1 $\mu$ g
Pol II phospho S5	Abcam	ab5131	Rabbit (IgG)	polyclonal		4 $\mu$ g

**Table 2.2 List of inhibitors**

<b>Inhibitor</b>	<b>Company</b>	<b>Product Number</b>	<b>Stock Concentration</b>	<b>Storage Conditions</b>
AC-YVAD-CHO	Calbiochem	400010	50 mM (DMSO)	-20°C
Azacytidine	Sigma-Aldrich	A2385	20 mM (DMSO)	-20°C
CAY10603	Cayman Chemical	13146	2 mM (DMSO)	-20°C
Mocetinostat	Selleck	S1122	50 mM (DMSO)	-20°C
Panobinostat	Selleck	S1030	50 mM (DMSO)	-20°C
PCI-34051	Cayman Chemical	10444	5 mM (DMSO)	-20°C

## 2.2 Cell transfection

Transfection of RAW 264.7 macrophages and primary mouse BMDMs with siRNAs and the pEGFP-HDAC8 plasmid was performed using the Lipofectamine RNAi Max kit and Lipofectamine 2000 reagent (Invitrogen™), respectively, according to the manufacturer's instructions.  $5.0 \times 10^5$  RAW 264.7 macrophages or  $2.5 \times 10^5$  BMDMs were seeded on 6-well plates 24 hours prior to transfection. 100 pmol for RAW264.7 cells or 150 pmol for BMDMs of siRNAs in RNAi Max reagent were used for transfection for a total of 40 hours, unless otherwise indicated in the figure legends. Total RNAs were collected from  $2 \times 10^6$  cells and mRNA expression levels were analyzed by quantitative polymerase chain reaction (qPCR). Primers used for qPCR are listed in Table 2.3. Control pEGFP or pEGFP-HDAC8 plasmids were previously generated by Dr. Soon-Duck Ha. Briefly, Full-length mouse HDAC8 cDNA (NM 027382) was amplified from a cDNA library by PCR using primers (forward; 5'-TTGCGAATCTGATGGAGATGCCAGAGGAACCC-3', reverse; 5'-TTGCGGATCCCGGACCACATGCTTCAGATTCCC-3') and cloned into the pEGFP-N1 vector using *EcoR* I and *Bam*H I restriction enzymes. Dr. Soon-Duck Ha then stably transfected RAW264.7 cells with 4 µg of pEGFP or 4 µg of pEGFP-HDAC8 using Lipofectamine 2000 (Invitrogen) as described by the manufacturer's protocol. Stably transfected cells were selected in the presence of G418 (500 µg/ml) antibiotics for 1 week and surviving cells were pooled and further propagated under G418 selection for an additional week.

## 2.3 Measurement of cell viability

$1.5 \times 10^5$  RAW 264.7 macrophages or  $0.75 \times 10^5$  primary BMDMs were cultured in the

presence or absence of LeTx in a 96-well plate for 5 hours, and 3-(4,5-dimethylthiazol-2-yl)-2,5-diphenyltetrazolium bromide (MTT) was added at a final concentration of 1 mg/mL. After incubating at 37 °C for an additional 3 hours, culture medium was carefully aspirated, and 100  $\mu$ L of dimethyl sulfoxide (DMSO) was added to dissolve the crystals. Optical densities of the wells were analyzed using an automatic ELISA plate reader (Bio-Rad) at a wavelength of 570 nm. The percentage of cell survival was estimated based on a standard curve generated from a known number of cells and their respective optical density (cell number versus optical density at 570 nm).

## 2.4 Lysate preparation and Western blot analysis

After cells were cultured for the indicated times in the presence or absence of LeTx, inhibitors or siRNAs,  $3 \times 10^6$  cells were collected and lysed in 150  $\mu$ L of ice-cold cell lysis buffer (20 mM MOPS, 2 mM EGTA, 5 mM EDTA, 1 mM  $\text{Na}_3\text{VO}_4$ , 40 mM  $\beta$ -glycerophosphate, 30 mM sodium fluoride, and 20 mM sodium pyrophosphate, pH 7.2) containing 1% Triton X-100, and 1/8 of a cOmplete EDTA-free protease inhibitor cocktail tablet (Roche Applied Science; product #11873580001). Cell lysates were incubated on ice for 10 minutes and then centrifuged at  $16,100 \times g$  for 10 min at 4°C. These extracts were run on 12.5% SDS gels, followed by transfer onto 0.2  $\mu$ M nitrocellulose membranes (Bio-Rad). Membranes were subsequently blocked at room temperature (RT) for 1 hour with 5% (w/v) skim milk. Various H3, HDAC8, IL-1 $\beta$ , EGFP and actin Abs were used at dilutions ranging from 1:500-1:5000 (see Table 2.1 for working dilutions) and incubated overnight at room temperature. After washing 3 times for 10 minutes at RT with TTBS buffer [Tris-buffered saline (50 mM Tris, 150 mM NaCl, pH 7.6) containing 0.05% Tween 20], the secondary antibody was applied at a 1:5000 dilution and incubated for 60 min at RT. The membranes were then washed 3 times for 10 minutes with TTBS and developed using the Enhanced Chemiluminescent Detection reagent (Thermo scientific). The NIH image J program was used to analyze band intensity as indicated in the Figure legends.

## 2.5 Histone purification

SILAC treated samples were combined in a 1:1 ratio ( $1.5 \times 10^7$  cells per sample) and histones were acid extracted with 150  $\mu\text{L}$  of 0.25 M HCl overnight with rotation at 4°C. Samples were then centrifuged at 20,800  $\times g$  for 30 min and supernatants containing the histones were collected. Supernatants were neutralized with 15  $\mu\text{L}$  of 2.5 M NaOH. The extracted histones (35  $\mu\text{L}$ ) were separated on 12.5 % SDS gels at a voltage of 110V for 1.5 hours. The gel was then stained with Brilliant Blue-R concentrate electrophoresis reagent (Sigma-Aldrich). Briefly, Brilliant Blue-R solution was added to a volume just enough to cover the gel and incubated with shaking for 2 hours. The gel was then destained in destaining solution (45:10:45; methanol: acetic acid: ddH<sub>2</sub>O) overnight, and for the first 3 hours the destaining solution was changed every 30 minutes. Gels were then stored at 4°C in 5% acetic acid.

## 2.6 Digestion of histone H3

In-gel digestion of histone H3 (~17 kDa) was conducted using the Endoproteinase Arg-C (Roche, Cat No. 11370529001). Digestion was carried out over four phases and all incubations are at RT, unless stated otherwise. For the wash phase, two histone H3 gel bands cut into cubes were incubated in 200  $\mu\text{L}$  of ddH<sub>2</sub>O for 15 minutes, followed by incubation with 100  $\mu\text{L}$  of 50/50 acetonitrile (ACN)/ddH<sub>2</sub>O for 20 minutes (repeat 3 $\times$ ), incubation with 100  $\mu\text{L}$  ACN for 5 minutes, and incubation with 100  $\mu\text{L}$  of 100 mM NH<sub>4</sub>HCO<sub>3</sub> for 5 minutes plus the addition of 100  $\mu\text{L}$  ACN to make a 1:1 ratio for 15 minutes. The gel pieces were then dried in a speed vacuum for ~2 hours. For the reduction and alkylation phase, gel pieces were incubated in a water bath at 56°C for 1 hour with 100  $\mu\text{L}$  of 10 mM Dithiothreitol (DTT)/100 mM NH<sub>4</sub>HCO<sub>3</sub> and the solution was discarded. Next, the gel pieces were incubated in the dark for 45 minutes in 100  $\mu\text{L}$  of 5 mM iodoacetamide/100 mM NH<sub>4</sub>HCO<sub>3</sub>. The samples were then washed with 100  $\mu\text{L}$  of 100 mM NH<sub>4</sub>HCO<sub>3</sub> for 5 minutes, followed by incubation with 100  $\mu\text{L}$  50/50 ACN/ddH<sub>2</sub>O for 15 minutes, incubation with 100  $\mu\text{L}$  of ACN for 5 minutes, and incubation with 100  $\mu\text{L}$  of 100 mM NH<sub>4</sub>HCO<sub>3</sub> for 5 minutes plus the addition of 100  $\mu\text{L}$  of ACN to make a 1:1 ratio for 15 minutes. Again, gel pieces were dried in a speed vacuum. For the digestion phase, the gel pieces were dissolved in 100  $\mu\text{L}$  digestion

buffer (100 mM Tris/HCl, 10 mM CaCl<sub>2</sub>, pH 7.6), 10  $\mu$ L of activation solution (50 mM DTT, 5 mM EDTA), and 5  $\mu$ L of endoproteinase Arg-C (50 mM Tris/HCl buffer, 10 mM CaCl<sub>2</sub>, 5 mM EDTA, pH 8.0), creating the digestion mixture (90 mM Tris/HCl buffer, 8.5 mM CaCl<sub>2</sub>, 5mM DTT, 0.5 mM EDTA, pH 7.6). Digestion was carried out at 37 °C for 18 hrs. Following digestion, the supernatant was set aside (tube B) and the extraction of the histone H3 peptides phase was performed as follows. 30  $\mu$ L of 25 mM NH<sub>4</sub>HCO<sub>3</sub> was added to the gel pieces (tube A) and incubated for 15 minutes, with sonication 2 $\times$  for 3 minutes in an ice-filled sonication water bath. Next, 30  $\mu$ L of ACN was added to tube A to make a 1:1 solution of ACN: NH<sub>4</sub>HCO<sub>3</sub> and incubated for 15 minutes. The Supernatant from tube A was collected and combined with the supernatant in tube B. The gel pieces in tube A were then incubated with 30  $\mu$ L of 5% formic acid for 15 minutes, plus the same amount of ACN for an additional 15 minutes to make a 1:1 ratio of formic acid:ACN, and then supernatants were collected and combined with tube B. This step was then repeated one more time. The extracted peptide solution in tube B was then dried in a speed vacuum for 4 hours. At this stage samples were given to either Drs. Huadong Liu or Kyle Biggar in the Dr. S. Li Lab (Biochemistry, UWO) for selected reaction monitoring mass spectrometry analysis.

## 2.7 Selected reaction monitoring mass spectrometry

The extracted histone H3 peptide was resuspended in 30  $\mu$ L of buffer containing 95% ddH<sub>2</sub>O, 5% ACN and 0.1% formic acid. 3  $\mu$ L was injected into the LC-Mass Spectrometer. The peptides were analyzed by positive ESI-LC-MS/MS on a triple quadrupole (Q3 linear ion trap) mass spectrometer (QTRAP 4000, Applied Biosystems). A nanoAcquity UPLC system (Waters) equipped with a C18 analytical column (1.7  $\mu$ m, BEH130, 75  $\mu$ m  $\times$  200 mm and/or 75  $\mu$ m  $\times$  250 mm) was used to separate the peptides at the flow rate of 300 nL/min and operating pressure of 7000 psi (at 95/5 ddH<sub>2</sub>O:ACN). Eluted peptides were directly electrosprayed (Nanosource, ESI voltage +2000 V) into the QTRAP instrument. Peptides were eluted using a 62 min gradient with solvents A (ddH<sub>2</sub>O, 0.1% formic acid) and B (ACN, 0.1% formic acid) for 41 min from 5% B to 50% B, 6 min 90% B, and 10 min 5% B. The *in silico* protease digest patterns and the corresponding SRM transitions were compiled with the Skyline software. Transitions that are larger

than the precursor ion were selected on the basis of Skyline predictions and the specific b/y ions that allow unambiguous identification of the methylated lysine sites were included.

## 2.8 Chromatin immunoprecipitation

ChIP analysis was conducted as previously described [178], using H3K27Ac (Active Motif, California), HDAC3 (Epigentek, NY), HDAC8 (Epigentek, NY), RNA polymerase II-phospho S5 (Abcam, Ontario, Canada), and RNA polymerase II (Active Motif, California) antibodies.  $1.5 \times 10^7$  RAW 264.7 macrophages in 8% DMEM medium were cross-linked by adding formaldehyde (37% stock) to a 1% final concentration for 10 minutes at RT. Adding glycine to a final concentration of 125mM stopped cross-linking. Cells were then lysed in 160 $\mu$ L lysis buffer (50 mM Tris [pH 8.1], 5 mM EDTA and 1% sodium dodecyl sulfate [SDS]) containing Halt<sup>TM</sup> protease inhibitor mixture (Thermo Scientific). Chromatin solutions were sheared by sonication at high speed (Bioruptor UCD-200 ultrasound sonicator, Diagenode) for 20 min resulting in DNA fragments between 200-750 bp. Chromatin solutions were then centrifuged at 16,100  $\times$ g for 15 minutes and supernatants were collected. The sonicated chromatin was diluted 10 $\times$  in dilution buffer (50 mM Tris [pH 8.1], 0.5% Triton X-100, 0.1 M NaCl, and 2 mM EDTA) and 50  $\mu$ L was set-aside for INPUT. After preclearing 50  $\mu$ L of Protein G-conjugated Dynabeads (Invitrogen) for 1 h at 4°C, the protein G-conjugated Dynabeads were incubated with respective antibodies (see Table 2.1 for amounts used) diluted in 200  $\mu$ L of PBST [PBS-tween 20 buffer (Tween 20: 0.1%)] for 30 minutes at RT. The remaining sonicated chromatin was then immunoprecipitated overnight at 4 °C with the antibody-conjugated Dynabeads. The immunoprecipitates were washed 5 times for 10 minutes each at 4°C as follows: once with 1mL of Wash Buffer I (0.1% SDS, 1% TritonX-100, 2mM EDTA, 20 mM Tris [pH 8.1], 150 mM NaCl), once with 1 mL of Wash Buffer II (0.1% SDS, 1% TritonX-100, 2mM EDTA, 20 mM Tris [pH 8.1], 500 mM NaCl), once with 1mL of Wash Buffer III (0.25M LiCl, 1% NP-40, 1% Deoxycholate, 1mM EDTA, 20mM Tris [pH 8.0]), and twice with 1mL of TE Buffer (10mM Tris [pH 8.0], 1mM EDTA). Bound and INPUT chromatin were eluted with 300  $\mu$ L of Elution Buffer (10 mM Tris [pH 8.1], 5 mM EDTA, 300mM NaCl, and 0.5% SDS)



and then heated overnight at 65 °C to reverse cross-linking. DNA fragments were then purified using QIAquick Spin columns (Qiagen) in 50 µL of DPEC water according to the manufacturer's instructions. 1 µL of purified DNA was then used in each ChIP-qPCR analysis. For HDAC3 and HDAC8 ChIP assays, primers were designed to target genomic sites known to be associated with H3K27Ac based on the ENCODE data base (<http://encodeproject.org/ENCODE/>): *BNIP3* (amplifying ~1 kb upstream of exon 1) and *MLN64* (amplifying ~1 kb upstream of exon 1). For Pol II-phospho S5 ChIP assays, primers were designed to target the promoter regions of *BNIP3*, *BNIP3L*, *MLN64*, *HDAC8*, and *GAPDH* encompassing the transcription start sites [TSS (amplifying ~150 bps upstream of the TSS)], based on the Transcriptional Regulatory Element Database (<http://rulai.cshl.edu/cgi-bin/TRED/tred.cgi?process=home>). For *IL-1β* H3K27Ac and RNA Pol II ChIP, primers were randomly designed to amplify regions across the entire gene and cover both Pol II- and H3K27Ac-associated sites based on ENCODE. Data are presented as percentage of the precipitated target sequence as compared to input DNA (% Input Method). Rabbit IgG (Abcam) was used as a background control. Sequences of ChIP-specific primers are listed in Table 2.3.

## 2.9 Quantitative PCR

Briefly, total cellular RNA was isolated from  $2 \times 10^6$  million cells using 500 µL of TRIzol (Invitrogen) according to the manufacturer's instructions. cDNA was synthesized from 1 µg of total RNA using oligo (dT) primers and Moloney murine leukemia virus (M-MuLV) reverse transcriptase (New England Biotechnology). The amplification mixture (20 µL) contained 100 ng of cDNA, 500 nM of each specific primer set, and 10 µL of Power SYBR Green PCR Master Mix (Applied Biosystems). mRNA expression levels were determined by subjecting the amplification mixtures to qPCR analyses. The data were normalized by expression of the GAPDH housekeeping gene using the delta-delta-CT method. 1 µL of purified DNAs from Pol II-phospho S5 ChIP were subjected to qPCR using Power SYBR Green PCR Master Mix for *MLN64*, *GAPDH*, and *HDAC8* or TaqMan qPCR analysis for *BNIP3* and *BNIP3L*, using the ZEN quencher system (Integrated DNA Technologies) containing the qPCR mixture (50 U/ml Taq DNA polymerase, 1 X ThermoPol reaction buffer, 200 mM 2'-deoxynucleoside 5'-

triphosphates, 900 nM forward and reverse primers, and 250 nM double-quenched probe). ChIP data are presented as percentage of the precipitated target sequence as compared to input DNA (% Input Method). All qPCR analyses were performed with a Rotor-Gene RG3000 quantitative multiplex PCR instrument (Montreal Biotech). The PCR conditions for SYBR green qPCR were as follows: 95°C for 10 min, then 40 cycles at 95°C for 15 sec, 58°C for 30 sec, 72°C for 25 sec, and 83°C for 15sec. The PCR conditions for TaqMan qPCR were as follows: 95°C for 10 min, then 50 cycles at 95°C for 15 sec, and 53°C for 45 sec. Following qPCR analyses the samples were run on a 2% Agarose gel to confirm amplicon sizes for each specific primer set.

## 2.10 Enzyme-linked immunosorbent assay

RAW 264.7 macrophages ( $1 \times 10^6$  cells/1 mL of media) were cultured in the presence or absence of various epigenetic inhibitors, LeTx, and LPS (100 ng/mL) for various times as indicated in the Figure legends. The media was then collected and spun  $16,100 \times g$  for 5 minutes at 4°C and supernatants were saved for ELISA. The concentrations (pg/mL) of mouse IL-1 $\beta$  and TNF- $\alpha$  were measured using Ready-SET-Go! ELISA kits (eBioscience) from cell culture supernatants as described by the manufacturer's protocol.

## 2.11 Statistical analysis

Data is expressed as the mean  $\pm$  standard error (SE). The GraphPad Prism 4.0 software was used to determine statistical significance using the statistical test as indicated in the figure legend. Statistical significance was defined as \*  $P < 0.05$ , \*\*  $P < 0.01$ , and \*\*\*  $P < 0.001$ .

**Table 2.3 List of primer sequences**

Analysis	Gene	Primer Sequence (5'→3')	Amplicon size (bp)
qPCR	<i>BNIP3</i>	F: GCTCCCAGACACCACAAGAT R: TGAGAGTAGCTGTGCGCTTC	222
	<i>BNIP3L</i>	F: CCTCGTCTTCCATCCACAAT R: GTCCCTGCTGGTATGCATCT	161
	<i>MLN64</i>	F: CAGGCAGTCACCGTCTTGTT R: TGCGGTGGTGGATCAGATCT	213
	<i>TNF-α</i>	F: CATTTGGGAAGTCTCTCATCC R: CTGGAAATAGCTCCCAGAA	298
	<i>IL-1β</i>	F: GTGGACCTTCCAGGATGAGG R: GCTTGGGATCCCACTCTCC	374
	<i>HDAC8</i>	F: ACGGGAAGTGTAAGTAGCCA R: TCCACGTAGAGAATACGGTCAAA	145
	<i>GAPDH</i>	F: GCATTGTGGAAGGGCTCATG R: TTGCTGTTGAAGTCGCAGGAG	361
HDAC3 and HDAC8 ChIP	<i>BNIP3</i>	F: AATCTGTCCCTCAACGGCTG R: GTTGGTAGATGCACCAGGCT	100
	<i>MLN64</i>	F: CCTTCCGCTCTGAGGAGTTG R: GACCGAACCAGACGGACA	184
	<i>GAPDH</i>	F: GTTCAGACCCATCCCGTAATC R: CAAAGGTATGCACCTCACAAC	145
Pol II-phospho S5 ChIP	<i>BNIP3</i>	F: CCCTTGTCCTCAGTCCA R: GAACCAACTGCGACAGG Probe: 56-FAM/TGTCGCCTG/ZEN/GCCTCAGAACT/3IABkFQ/	104
	<i>BNIP3L</i>	F: AGCTGCCTGTGTTGTCATC R: ACACAACAAGTCGAGTTCCC Probe: 56-FAM/TGACGTCAC/ZEN/GAAGGGAGG GACT/3IABkFQ/	104
	<i>MLN64</i>	F: AATTGTCCTGAGACTCCTCTTTC R: CAAGATCCTGACCCTAAGATAACC	101
	<i>HDAC8</i>	F: TTGACCGTGCTACTTGTGCC R: TGGTCCCTCGTCCAACACTACA	153
	<i>GAPDH</i>	F: GTTCAGACCCATCCCGTAATC R: CAAAGGTATGCACCTCACAAC	145
H3K27Ac and Pol II ChIP	<i>IL-1β</i> (1)	F: ATGGTTCAGGGTCTCAGTTGC R: CCCTGTGAAGGCAGAACAGA	151
	<i>IL-1β</i> (2)	F: TGCGBAACAAAGGTAGGCAC R: AGAAGCCCCTGCTAACACAG	151
	<i>IL-1β</i> (3)	F: GAAGCTTGGCTGGAGAGGAT R: TTCACAGCTCTTCACTTCTGC	125

Analysis	Gene	Primer Sequence (5'→3')	Product size (bps)
H3K27Ac and Pol II ChIP	<i>IL-1<math>\beta</math></i> (4)	F: AGTGACAGCACCTAAGTCCCT R: AGTGGGTACTGGAGAGTGGTC	184
	<i>IL-1<math>\beta</math></i> (5)	F: GTCAGTGTGTGGGTTGCCTTA R: TGGCTCCTAACCTGTGGAGG	146
	<i>IL-1<math>\beta</math></i> (6)	F: CAGGCAGTGAGCACATCAAG R: GTGTCTGGTTGCCATGTACC	158
	<i>IL-1<math>\beta</math></i> (7)	F: CAGGGTGGGCTCAAGCATT R: GGATCGGCCTACTGACCTTG	148
	<i>IL-1<math>\beta</math></i> (8)	F: TTGGCCGAGGACTAAGGAGT R: ACCTCACAAGCAGAGCACAA	200

## CHAPTER 3

### 3 RESULTS

#### 3.1 Generating TIR macrophages.

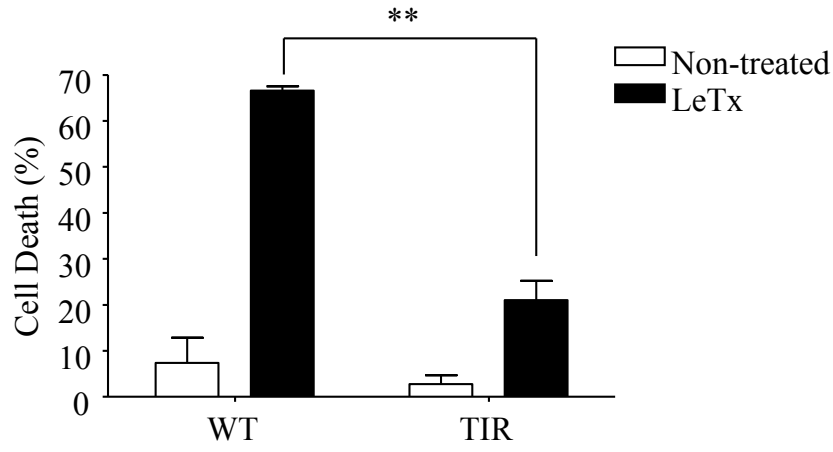
##### 3.1.1 TIR macrophages are resistant to LeTx-induced pyroptosis.

As shown previously in our lab, RAW 264.7 macrophages exposed to a sub-lethal dose of LeTx become resistant to subsequent lethal challenges for up to 4 days, a process termed toxin-induced resistance (TIR) [110,112]. Furthermore, a small fraction (~2%) of these TIR macrophages retained resistance for up to 6 weeks, which was termed long-term TIR [110,112]. Similar to our previous reports, RAW 264.7 macrophages exposed to LeTx for 5 hours caused ~65 % cell death in wild-type cells, but only ~20% cell death in short-term TIR cells (Fig. 3.1A). Additionally, BMDMs pre-exposed to a sub-lethal dose of LeTx became resistant after 24 hours. Wild-type BMDMs showed ~80% cell death, whereas short-term TIR-BMDMs showed less than 25% cell death after a 5 hour LeTx exposure (Fig. 3.1B). To determine whether these RAW 264.7 macrophages were undergoing pyroptosis, as previously shown in the literature [110,112,177], cells were pre-treated with the caspase-1 inhibitor AC-YVAD-CHO (20  $\mu$ M) followed by LeTx challenge. MTT assays revealed that LeTx-induced cell death was significantly reduced (~40%) in wild-type cells treated with the caspase-1 inhibitor (Fig. 3.1C), suggesting that they were in fact undergoing pyroptosis. The protection against LeTx was not 100% in these macrophages, likely because caspase-1 may only be partially inhibited at 20  $\mu$ M, which has been reported as the optimal concentration without causing macrophage toxicity [179].

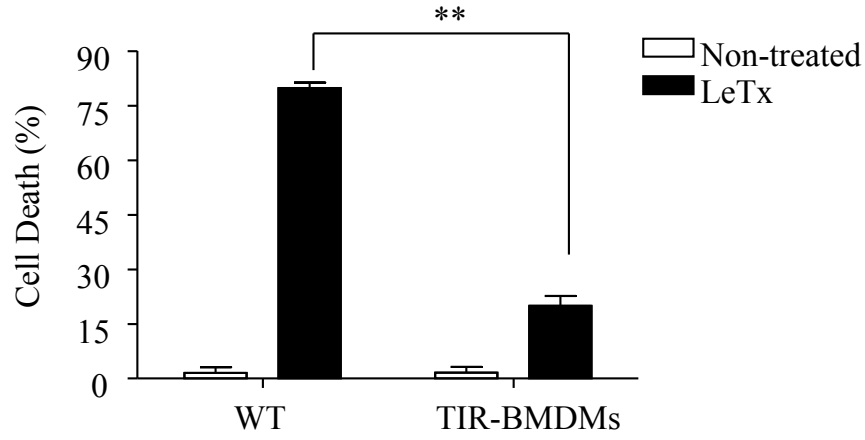
**Figure 3.1 Short-term TIR macrophages are resistant to LeTx-induced pyroptosis.**

(A) RAW 264.7 wild-type macrophages (WT) and RAW 264.7 TIR macrophages and (B) wild-type (WT) BMDMs and TIR-BMDMs were treated with or without a lethal dose of LeTx (PA: 500 ng/mL, LF: 250 ng/mL) for 5 hours and cell death was quantified by MTT assays. (C) RAW 264.7 wild-type cells (WT) were treated in the presence or absence of the caspase-1 inhibitor (20  $\mu$ M) for 12 hours and then treated with or without a lethal dose of LeTx (PA: 500 ng/mL, LF: 250 ng/mL) for 5 hours. Cell death was measured by an MTT assay. Data are expressed as means  $\pm$  SE ( $n \geq 3$ ), \*\*  $P \leq 0.01$ , \*\*\* $P \leq 0.001$  (Student's T-test). **Part B solely performed by Dr. Soon-Duck Ha.**

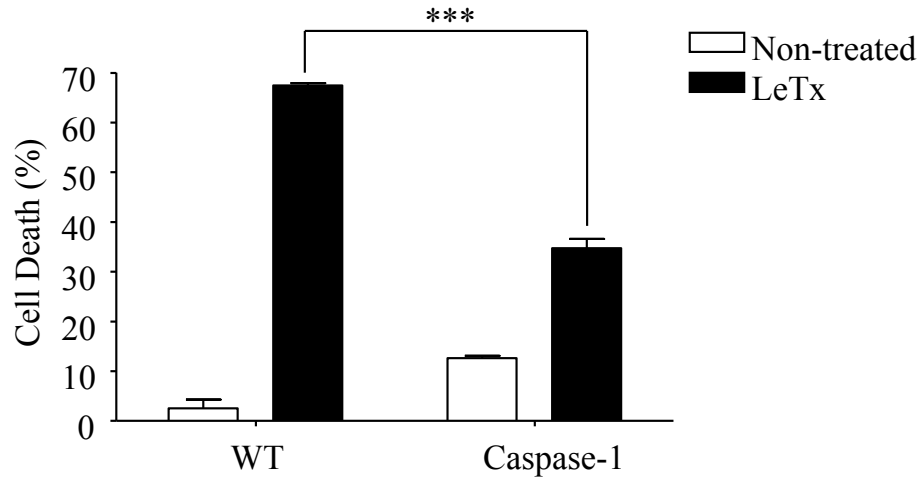
A)



B)



C)



## 3.2 TIR is mediated in an HDAC8-dependent manner.

### 3.2.1 Increased HDAC8 expression is correlated with TIR.

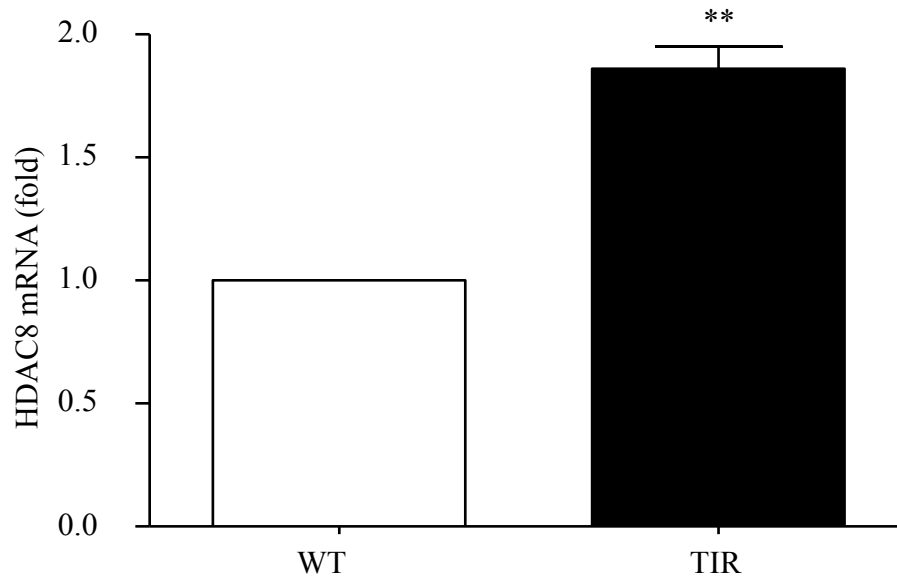
Due to the non-permanent, but inheritable characteristics of TIR, our lab investigated epigenetic players, including HDACs and DNMTs to examine their potential role in maintaining the TIR phenotype. In fact, long-term TIR was found to be positively correlated with HDAC8 mRNA expression, but not with other HDACs, including HDAC 1, 2, and 5 [177]. Although long-term TIR occurs in *in vitro* settings, it is more likely that macrophages experience short-lived resistance to LeTx *in vivo*, as anthrax is an acute infection, thus LeTx exposure is likely not sufficient to promote long-term resistance. As such, HDAC8 mRNA levels were measured by qPCR in short-term TIR macrophages and TIR-BMDMs. Like long-term TIR, short-term TIR RAW 264.7 macrophages (Fig. 3.2A) and short-term TIR-BMDMs (Fig 3.2B) showed ~2-fold and ~2.5-fold increase, respectively, in HDAC8 mRNA levels relative to wild-type macrophages. Although short-term TIR macrophages showed increased expression of HDAC8 at the transcriptional level, this does not always correlate with increased protein production. Therefore, HDAC8 protein expression was measured in short-term RAW 264.7 TIR cells by Western blot. As shown in Figure 3.3, short-term TIR macrophages showed a greater than 3-fold increase in HDAC8 protein expression relative to wild-type macrophages. Overall, these results suggest that HDAC8 may play a role in maintaining the TIR phenotype in both RAW 264.7 macrophages and BMDMs.



**Figure 3.2 Short-term TIR macrophages have increased HDAC8 mRNA levels.**

(A) mRNAs from RAW 264.7 wild-type (WT) and TIR macrophages and (B) mRNAs from wild-type (WT) BMDMs and TIR-BMDMs were prepared and analyzed for HDAC8 expression using qPCR. GAPDH was used as a reference gene for calculating all mRNA expression. Data are expressed as means  $\pm$  SE ( $n \geq 3$ ), \*\*  $P \leq 0.01$  (Student's T-test). **Part B solely performed by Dr. Soon-Duck Ha.**

**A)**



**B)**

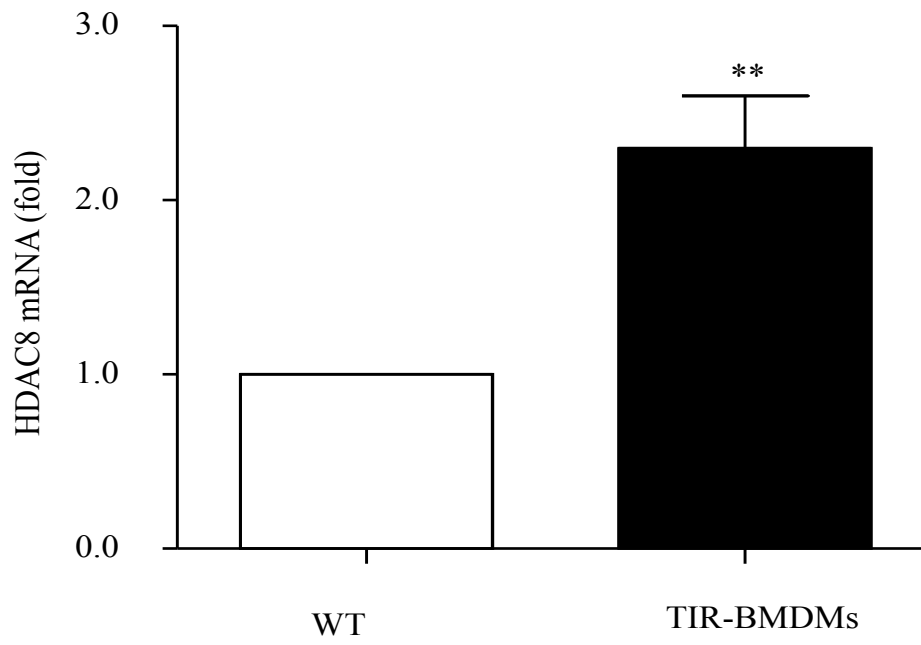
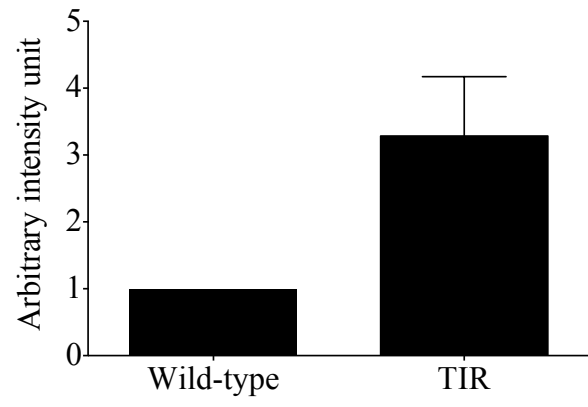
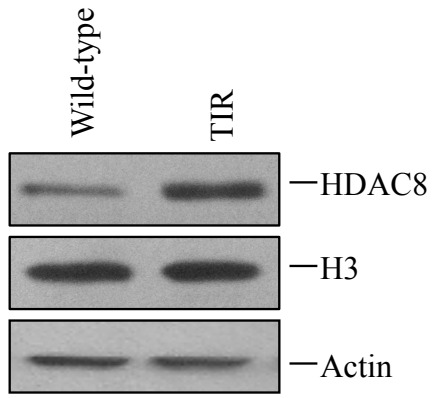


**Figure 3.3 HDAC8 protein levels are increased in RAW 264.7 short-term TIR macrophages.**

Total cell lysates were prepared from RAW 264.7 wild-type and short-term TIR macrophages and HDAC8 protein expression was measured by Western blot (left panel). Band intensities of HDAC8 were analyzed using the NIH image J program (right panel). Intensities of HDAC8 bands in short-term TIR cells were expressed as fold of change relative to those of wild-type cells. Histone H3 and actin were used for loading controls. Data are representative images of three independent experiments. Data are expressed as means  $\pm$  SE (n=3).

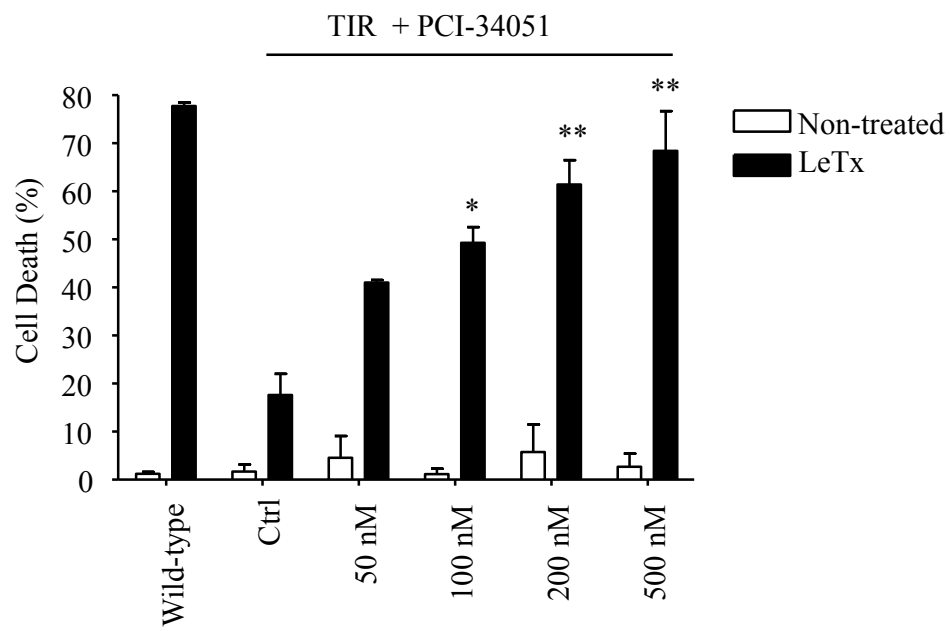
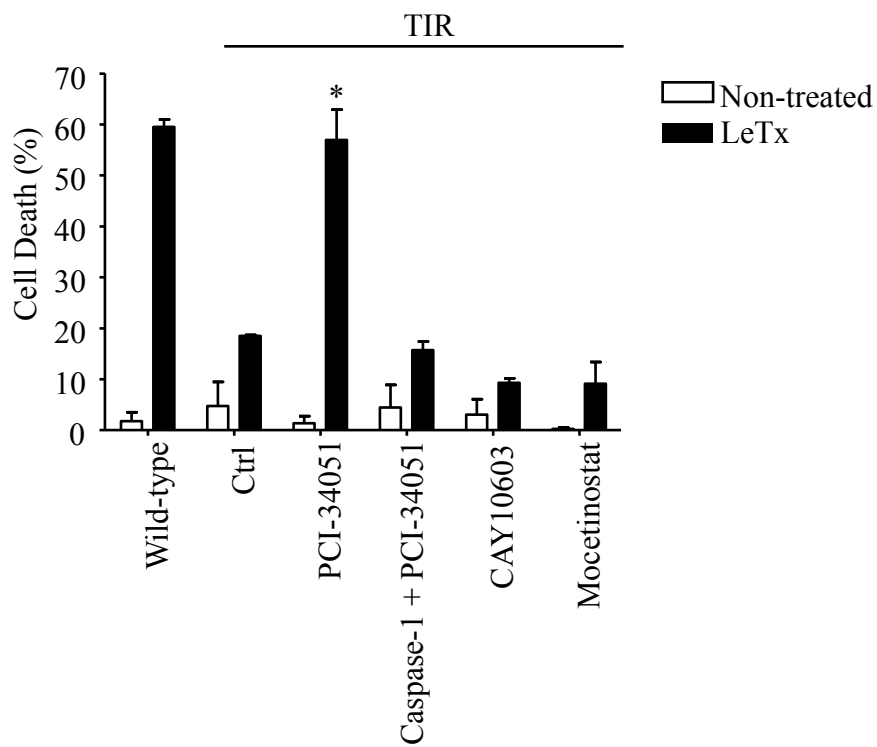


### 3.2.2 Inhibiting HDAC8 expression sensitizes TIR macrophages to LeTx.

Our previous work demonstrated that treating long-term TIR macrophages with the broad-spectrum HDAC inhibitor panobinostat or specifically knocking down HDAC8 by siRNAs sensitized these cells to LeTx-induced pyroptosis [177]. To further determine if HDAC8 was implicated in resistance to LeTx, short-term TIR macrophages were treated overnight in the presence or absence of varying doses of the HDAC8-specific inhibitor PCI-34051, and then exposed to a lethal dose of LeTx for 5 hours. As expected, short-term TIR cells treated with PCI-34051 were sensitized to LeTx in a dose-dependent manner (Fig. 3.4A). Additionally, short-term TIR cells were not sensitized to LeTx when treated overnight with other HDAC inhibitors, including the HDAC6 inhibitor CAY10603 (20 pM), or the HDAC1, 2, 3 and 11 inhibitor Mocetinostat (50 nM) (Fig. 3.4B). Furthermore, when PCI-34051 (100 nM) and the caspase-1 inhibitor AC-YVAD-CHO (20  $\mu$ M) were used in combination, short-term TIR macrophages were no longer sensitized by LeTx (Fig. 3.4B) and exhibited cell death levels similar to those of the control cells (< 20%). Inhibitor concentrations for mocetinostat, CAY10603 and PCI-34051 were chosen based on dose studies previously conducted in our lab [177]. Furthermore, the concentration for the caspase-1 inhibitor (AC-YVAD-CHO) was chosen based on that reported in the literature [179].

**Figure 3.4 RAW 264.7 short-term TIR cells are sensitized to LeTx-induced pyroptosis when treated with the HDAC8 inhibitor PCI-34051.**

(A) Short-term TIR cells were treated with various concentrations of the HDAC8-specific inhibitor PCI-34051 for 24 h. Wild-type and PCI-34051-treated cells were exposed or not exposed to a lethal dose of LeTx (PA: 500 ng/mL, LF: 250 ng/mL) for 5 h, and cell death was then measured by MTT assays. (B) TIR cells were treated with 3 different HDAC inhibitors, the HDAC8 inhibitor PCI-34051 (100 nM)  $\pm$  the caspase-1 inhibitor I (20  $\mu$ M), the HDAC6 inhibitor CAY10603 (20 pM), or the HDAC 1,2, 3 and 11 inhibitor mocetinostat (50 nM) for 24 hours. Wild-type, TIR (Ctrl) and inhibitor-treated TIR cells were exposed or not exposed to a lethal dose of LeTx (PA: 500 ng/mL, LF: 250 ng/mL) for 5 h, and cell death was measured by MTT assays. Data are expressed as means  $\pm$  SE (n=3), \*  $P < 0.05$  and \*\*  $P < 0.01$  relative to LeTx-treated TIR control (One-way Anova, Tukey's post-test).

**A)****B)**

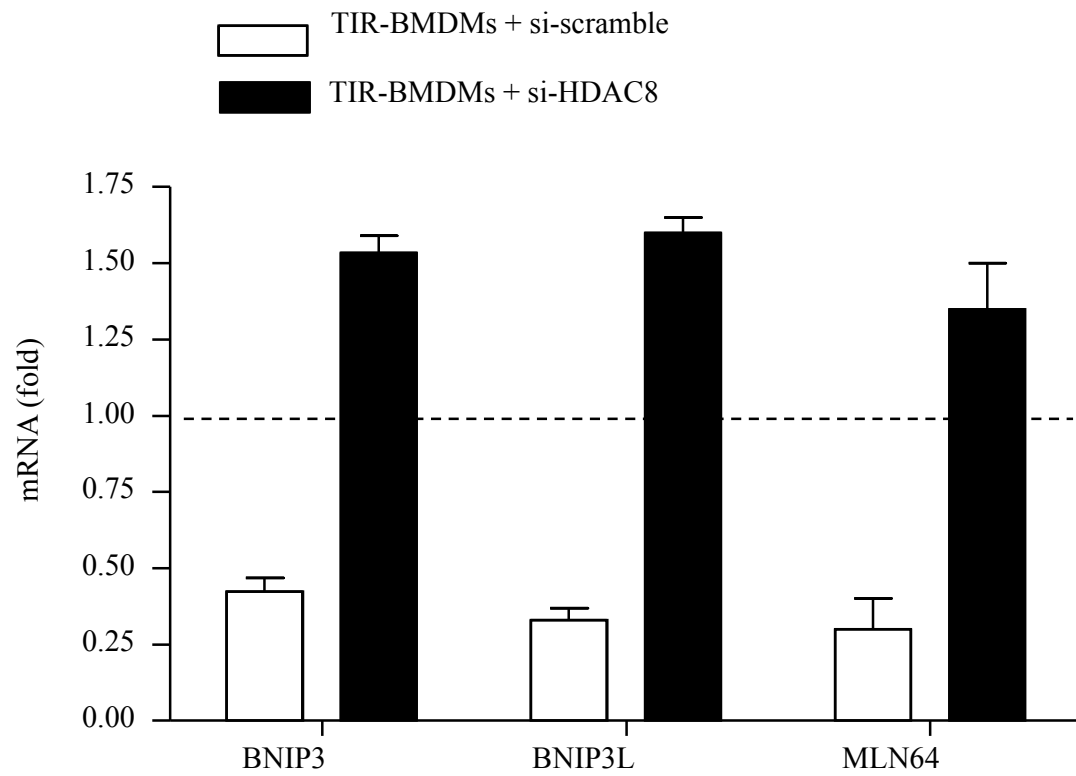
### 3.2.3 Knocking-down HDAC8 increases expression of the mitochondrial death genes in TIR-BMDMs.

To date, our lab has shown three mitochondrial death genes to be correlated with LeTx-induced pyroptosis: *BNIP3*, *BNIP3L*, and *MLN64*, and of these genes all three are significantly down-regulated in TIR cells [110,112,177]. Since HDAC8 was shown to be up-regulated in long-term TIR [177], and HDACs are known to contribute to gene silencing, we investigated whether its expression influenced suppression of the three mitochondrial death genes in TIR. As such, when HDAC8 was knocked-down in long-term TIR cells via siRNAs, *BNIP3*, *BNIP3L*, and *MLN64* mRNA levels were significantly increased relative to the control [177]. To test this hypothesis in a more physiologically relevant setting, HDAC8 was knocked-down in short-term TIR-BMDMs and mRNA levels of *BNIP3*, *BNIP3L*, and *MLN64* were measured by qPCR. As expected, short-term TIR-BMDM controls (si-scramble) showed a greater than 2-fold reduction in mRNA levels of all three mitochondrial death genes relative to wild-type BMDMs and when treated with HDAC8 siRNAs, the mRNA levels of the mitochondrial death genes increased to levels even greater than wild-type BMDMs (Fig. 3.5). Collectively, the data presented in figures 3.4 and 3.5 suggest that increased HDAC8 levels suppress the expression of the three mitochondrial death genes leading to resistance to LeTx-induced pyroptic cell death.



**Figure 3.5 Short-term TIR-BMDMs knocked down in HDAC8 show increased expression levels of the three mitochondrial death genes *BNIP3*, *BNIP3L* and *MLN64*.**

Short-term TIR-BMDMs were transfected with scrambled siRNA (si-scramble) or siRNA targeting HDAC8 (si-HDAC8) for 24 hours. The expression of BNIP3, BNIP3L, and MLN64 was analyzed by qPCR, and levels of mRNAs were expressed as fold of change relative to those of wild-type BMDMs transfected with scrambled siRNA for 24 hours (dotted line). GAPDH was used as a reference gene for calculating all mRNA expression. Data are expressed as means  $\pm$  SE (n = 3). **Experiment solely performed by Dr. Soon-Duck Ha.**



### 3.3 HDAC8-dependent deacetylation at histone H3 lysine 27 (H3K27) mediates TIR.

#### 3.3.1 H3K27Ac is reduced in TIR macrophages.

Histones may undergo various modifications that influence the expression of genes, such as histone acetylation, which is generally a marker of gene activation [151,152,180]. Since HDAC8 expression was increased in long-term TIR macrophages, we examined whether histone acetylation was decreased in these cells using Western blots. Our lab previously showed that overall levels of histone H4 acetylation remained unchanged between wild-type and long-term TIR cells, whereas overall levels of histone H3 acetylation were significantly lower in long-term TIR cells compared to wild-type cells [177]. Further examination at specific H3 lysine residues revealed decreased acetylation levels in long-term TIR cells at H3K9, H3K14, and H3K27, but of these three sites, H3K27Ac was most significantly down-regulated in long-term TIR [177].

To further confirm and quantify the down-regulation of H3K27Ac in long-term TIR, selected reaction monitor mass spectrometry (SRM-MS) was performed in collaboration with Dr. Huadong Liu, Dr. Kyle Biggar, and Dr. Shawn Li in the Department of Biochemistry, UWO, who previously used this technique to systematically map protein lysine methylation events [181]. SRM-MS allows for the direct quantification of histone modifications between two samples using stable isotope labeling of amino acids in cell culture (SILAC). To quantify H3K27Ac levels, wild-type and long-term TIR macrophages were cultured with light lysine (4,4,5,5-H4) or heavy lysine (4,4,5,5-D4), respectively, for one week to ensure maximal lysine labeling. The same number of cells cultured with light or heavy lysine-containing media were pooled and then processed to extract histone H3 (Fig. 3.6). Following in-gel digestion of histone H3 by the Arg-C endopeptidase, the quantity of H3K27Ac was analyzed by interrogating the H3K27 peptide sequence as described in Method and Materials. *In silico* digestion of histone H3 and the synthesis of standard peptides (Table 3.1) for the generation of the standard unmodified peptide chromatograph (Fig. 3.7B) and the standard H3K27Ac peptide chromatograph (Fig. 3.8B) were used to confirm the detection of the unmodified (Fig 3.7C) and acetylated H3K27 peptide (Fig 3.8C) from RAW 264.7 wild-type

macrophages. Figure 3.7A and 3.8A are the transitions used for the detection of H3K27 and H3K27Ac, respectively. For SILAC treated samples, the transitions indicated in figure 3.9A were used for H3K27Ac peptide confirmation. Although the same transitions were used for both light and heavy labeled samples, the peak intensity (peak height) of the long-term TIR sample was differentiated from the wild-type peak intensity based on a +12 Da mass shift ( $m/z$ ) in the SRM mass spectrometry spectrum. This +12 Da  $m/z$  is due to the fact that the long-term TIR sample contains four deuterium atoms (4,4,5,5-D4) at the three H3K27 peptide lysine residues, whereas the wild-type sample contains four hydrogen atoms (4,4,5,5-H4) at these lysine residues. As such, based on H3K27Ac peak intensities of the wild-type (light lysine) and long-term TIR (heavy lysine) samples, H3K27Ac was significantly lower (~ 70%) in long-term TIR relative to wild-type macrophages (Fig 3.9B and Fig. 3.9C).

To further examine the correlation of H3K27Ac levels in resistance, wild-type and short-term TIR macrophages were labeled with light and heavy lysine respectively and subjected to SRM mass spectrometry analysis. H3K27 can undergo two mutually exclusive covalent modifications, such that at a single time it can only be methylated, acetylated, or unmodified [182]. Therefore, given that H3K27Ac levels were significantly lower in long-term TIR (Fig. 3.9) and unmodified H3K27 levels were ~2.5 fold greater in TIR macrophages compared to wild-type macrophages (Fig. 3.10A), I suspected that unmodified H3K27 levels increased due to a decrease in H3K27Ac levels. While H3K27 can also be tri-methylated, since mitochondrial death gene silencing is involved in TIR and H3K27 tri-methylation (H3K27Me3) is a general marker for gene suppression [183], it seems most likely for H3K27Me3 levels to increase and H3K27Ac levels to decrease in short-term TIR. To confirm equal loading of wild-type (light) versus short-term TIR (heavy), a peptide from histone H3 [E(73)IAQDFKTDLR(83)] was used as a control. Quantifying unmodified H3K79 from the control peptide confirmed that wild-type and short-term TIR samples were in fact loaded in a 1:1 ratio (Fig. 3.10B). Based on the mutual exclusiveness of modifications at H3K27, figure 3.11 demonstrates a working model of H3K27Ac levels in short-term TIR. Further optimization is required to specifically quantify H3K27Ac in short-term TIR by SRM mass spectrometry.

**Figure 3.6 Stable isotope labeling of amino acids in cell culture and SRM mass spectrometry analysis.**

RAW 264.7 wild-type macrophages and long-term TIR macrophages were labeled with light lysine (4,4,5,5-H<sub>4</sub> L-Lysine; Lys-0) or heavy lysine (4,4,5,5-D<sub>4</sub> L-Lysine; Lys-4), respectively, for 7 days and pooled in a 1:1 ratio. The histones were acid extracted overnight and run on a SDS gel for Brilliant Blue-R staining. Histone H3 (17 kDa) was in-gel digested using the Arg-C endopeptidase and subjected to SRM mass spectrometry for the unmodified and acetylated H3K27 peptide. The H3K27 peptide for the heavy-labeled long-term TIR shows a mass shift by +12 Da relative to the light-labeled sample and peak intensities (peak height) from the mass spectrum are used to quantify the relative amount of H3K27/H3K27Ac peptides relative to the control (wild-type macrophages).

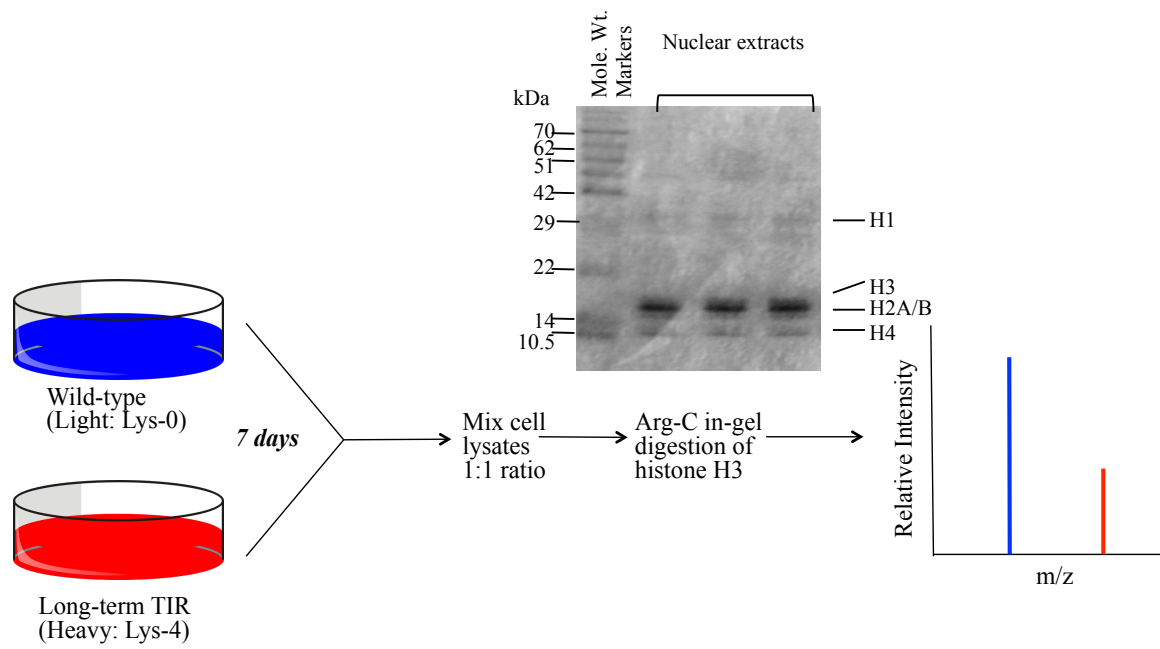


**Table 3.1** *In silico* digestion of histone H3 and the synthesis of standard peptides for SRM mass spectrometry.

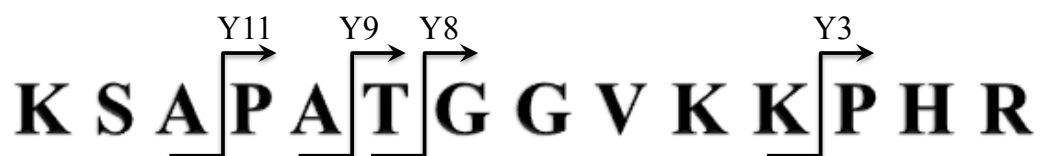
Peptides	Modification	Sequences
1	None	NH <sub>2</sub> -KSAPATGGVKKPHR-COOH
2	H3K27Ac	NH <sub>2</sub> -K(Ac)SAPATGGVKKPHR-COOH
3	H3K36Ac	NH <sub>2</sub> -KSAPATGGVK(Ac)KPHR-COOH
4	H3K37Ac	NH <sub>2</sub> -KSAPATGGVKK(Ac)PHR-COOH

**Figure 3.7 Identification of unmodified histone H3K27 by SRM mass spectrometry.**

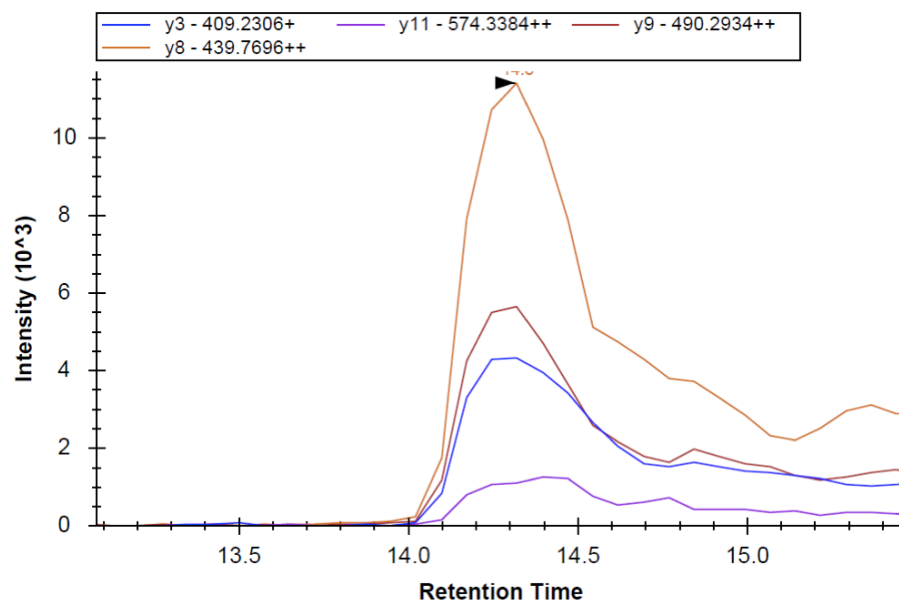
(A) Transitions used in the experiment. (B) *In-silico* Arg-C digestion of histone H3 and standard peptides were synthesized and extracted ion chromatographs (XICs) show that the SRM transitions detected the unmodified H3K27 peptides from standard samples and from (C) Arg-C digested histone H3 prepared from RAW264.7 wild-type macrophages.



A)



B)



C)

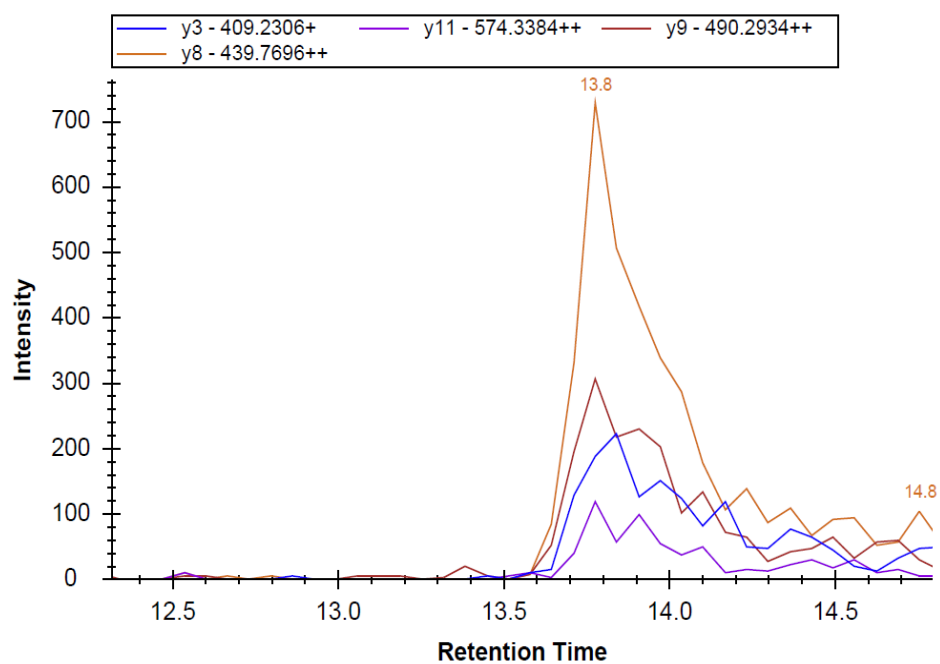
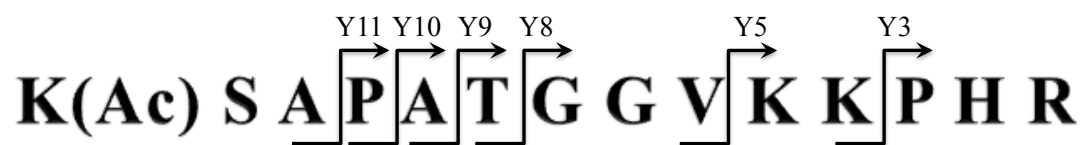


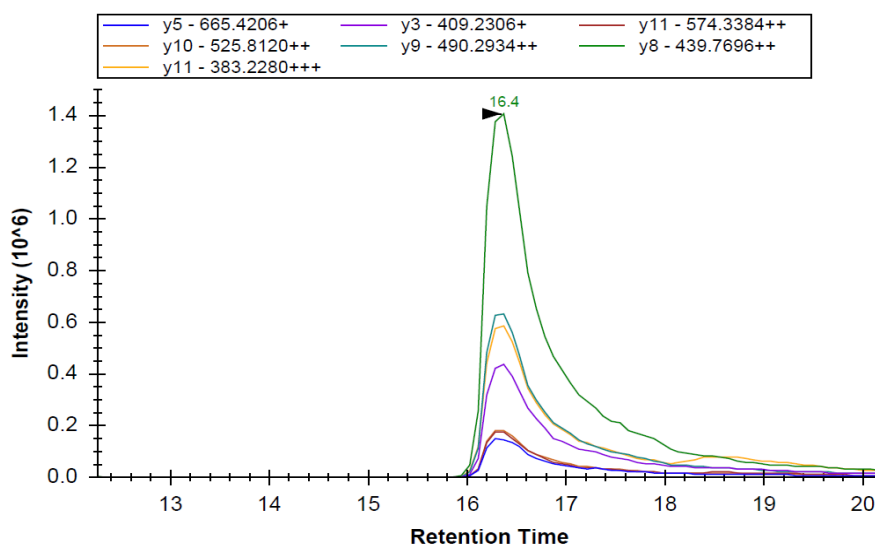
**Figure 3.8 Identification of acetylated histone H3K27 by SRM mass spectrometry.**

(A) Transitions used in the experiment. (B) *In-silico* Arg-C digestion of histone H3 and standard peptides were synthesized and extracted ion chromatographs (XICs) show that the SRM transitions detected the acetylated H3K27 peptides from standard samples and from (C) Arg-C digested histone H3 prepared from RAW264.7 wild-type macrophages.

A)



B)



C)

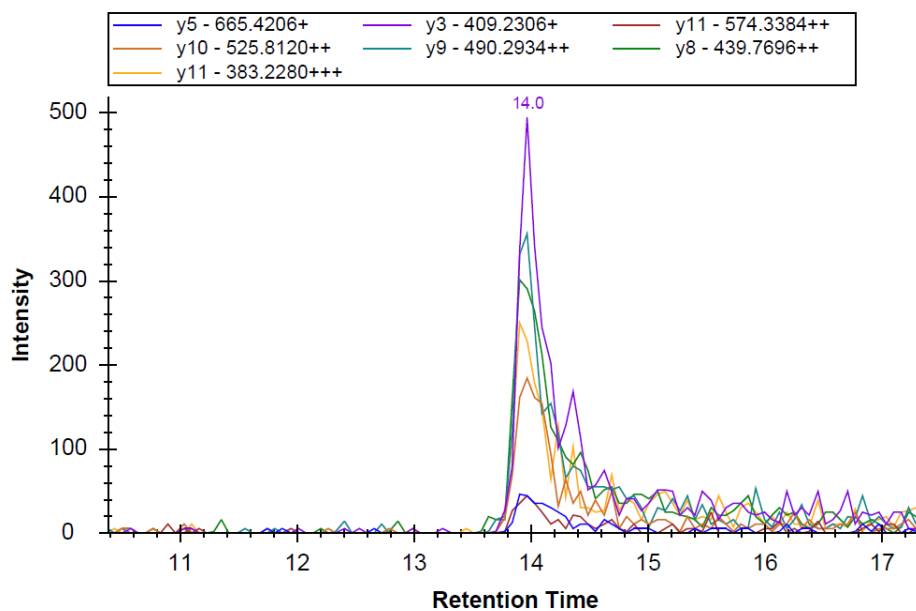
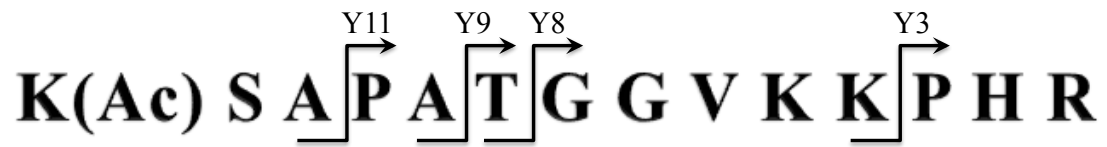


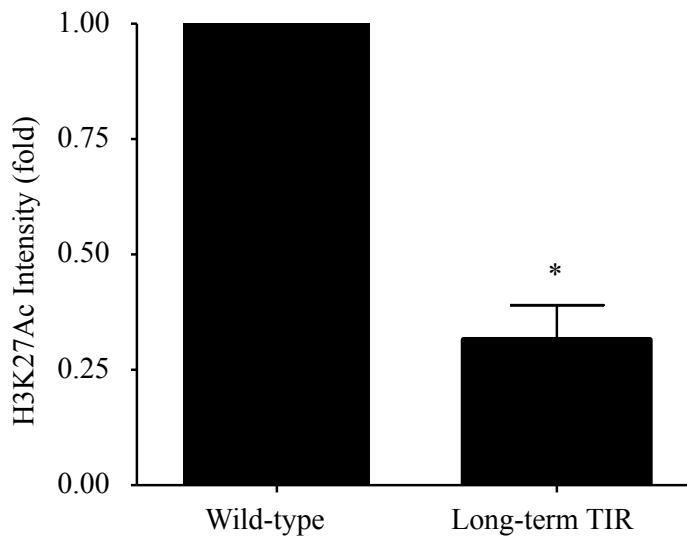
**Figure 3.9 Long-term TIR macrophages show decreased levels of H3K27Ac relative to wild-type macrophages by SRM mass spectrometry.**

RAW 264.7 wild-type and long-term TIR macrophages were cultured in light (4,4,5,5-H<sub>4</sub> L-Lysine) or heavy (4,4,5,5-D<sub>4</sub> L-Lysine) lysine-containing media, respectively, for 7 days and then pooled in a 1:1 ratio. Histone H3 was then in-gel digested using the Arg-C endoproteinase. The liquid chromatography-coupled triple quadrupole mass spectrometer with Q3 as a linear ion trap was used to quantify H3K27Ac by interrogating the SAPATGGVKKPHR<sup>40</sup> peptide from digested histone H3. The Skyline software was used for the following data acquisition, (A) transitions used in the experiment, B) a bar graph of the relative intensity of H3K27Ac between light (wild-type) and heavy (long-term TIR) medium and C) the relative expression of H3K27Ac (samples were first normalized to the peak height of the respective H3K27 peptide, then presented relative to the wild-type peptide). For panel B data are expressed as means  $\pm$  SE (n=3), \* P< 0.05; (Student's T-test) and panel C is a representative figure.

A)



B)



C)

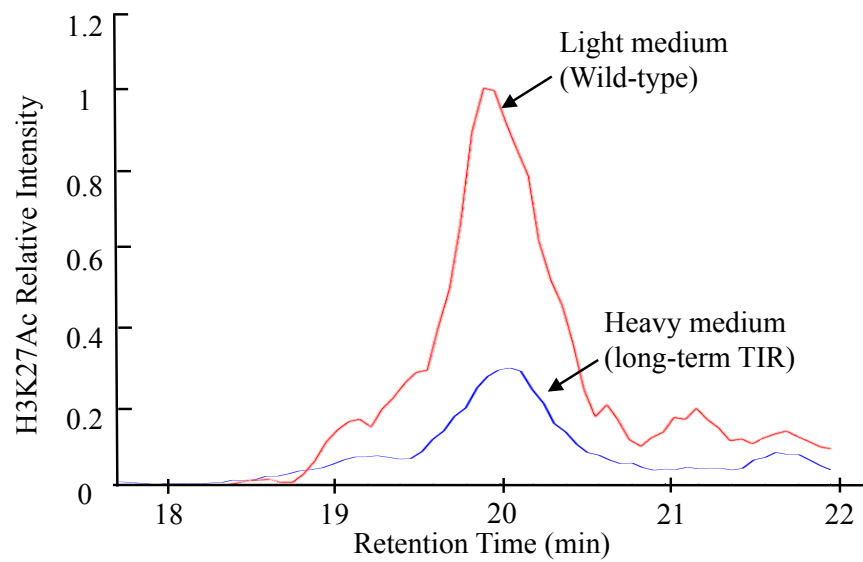
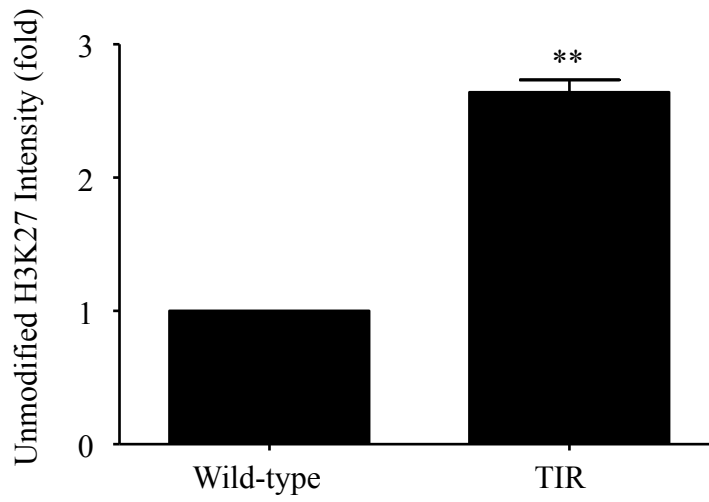
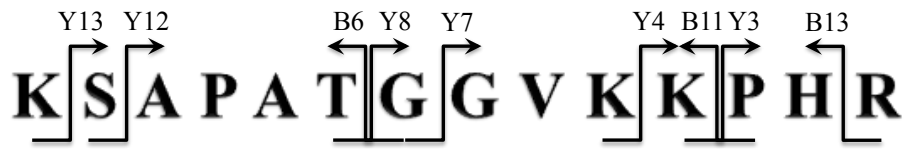


**Figure 3.10 RAW 264.7 short-term TIR macrophages show increased levels of unmodified H3K27 by SRM mass spectrometry.**

RAW 264.7 wild-type and short-term TIR macrophages were cultured in light (4,4,5,5-H4 L-Lysine) or heavy (4,4,5,5-D4 L-Lysine) lysine-containing media, respectively, for 7 days and then pooled in a 1:1 ratio. Histone H3 was then in-gel digested using the Arg-C endoproteinase. The liquid chromatography-coupled triple quadrupole mass spectrometer with Q3 as a linear ion trap was used to quantify (A) H3K27 and (B) H3K79 by interrogating the K<sup>27</sup> SAPATGGVKKPHR<sup>40</sup> peptide and the E<sup>73</sup>IAQDFKTDLR<sup>83</sup> peptide, respectively, from digested histone H3. The Skyline software was used for the following data acquisition. (A) Transitions used for H3K27 (upper panel) and the intensity of H3K27 (lower panel) in wild-type and TIR macrophages (H3K27 peak heights were normalized to wild-type). (B) Transition used for H3K79 (upper panel) and the intensity of H3K79 (lower panel) in wild-type and TIR macrophages (H3K79 peak heights were normalized to wild-type). Data are expressed as means  $\pm$  SE (n=2), \* P< 0.05; (Student's t-test).

A)



B)

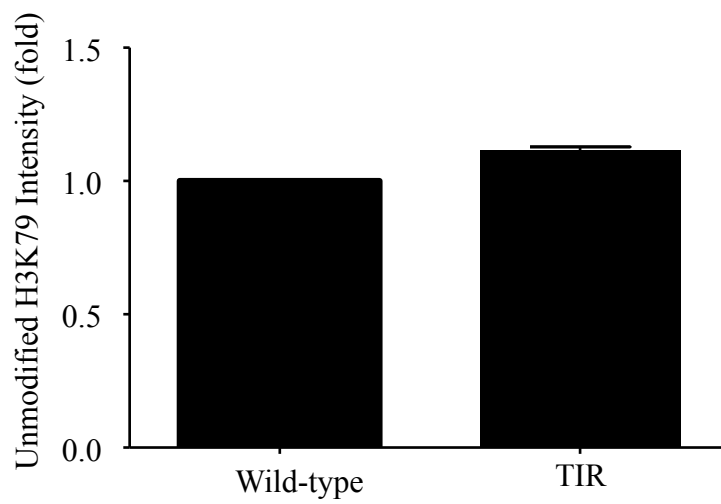
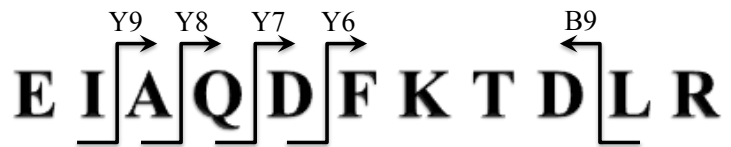
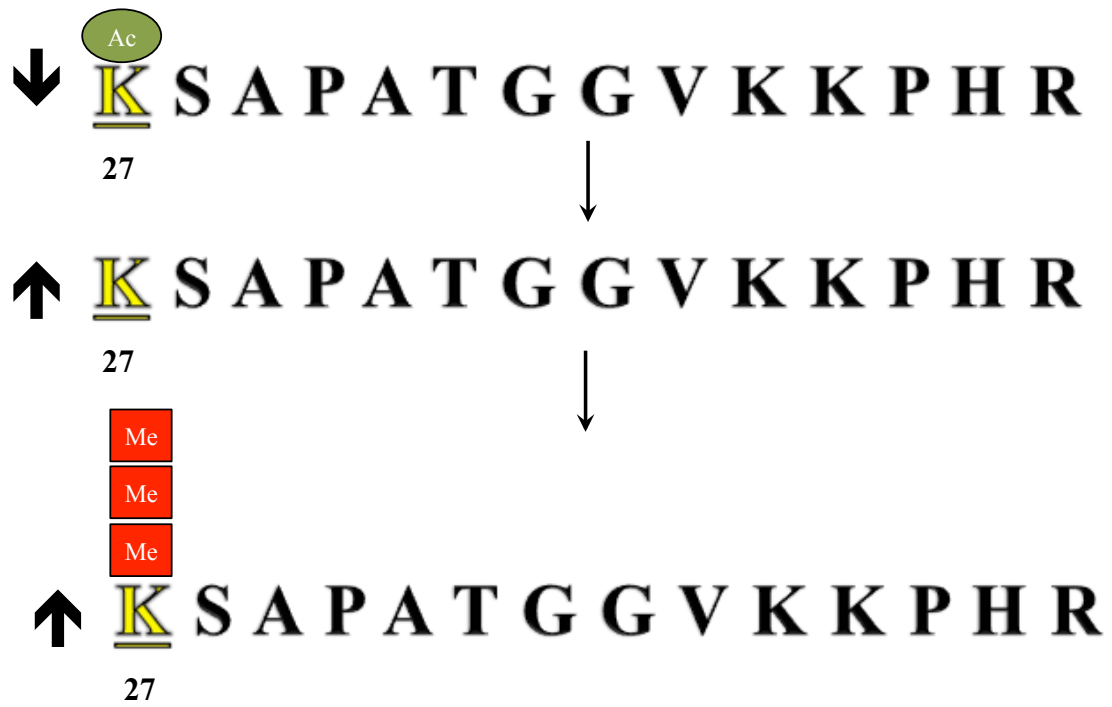


**Figure 3.11 Working model of H3K27Ac levels in RAW 264.7 short-term TIR macrophages.**

H3K27 is a mutually exclusive site that can be acetylated, methylated, or unmodified. Based on mutual the exclusiveness of H3K27 modifications and the involvement of mitochondrial death gene silencing in short-term TIR, when unmodified H3K27 levels increase, H3K27Ac levels should decrease, and H3K27Me3 levels should increase.





### 3.3.2 HDAC8-dependent H3K27 deacetylation is involved in RAW 264.7 TIR macrophages.

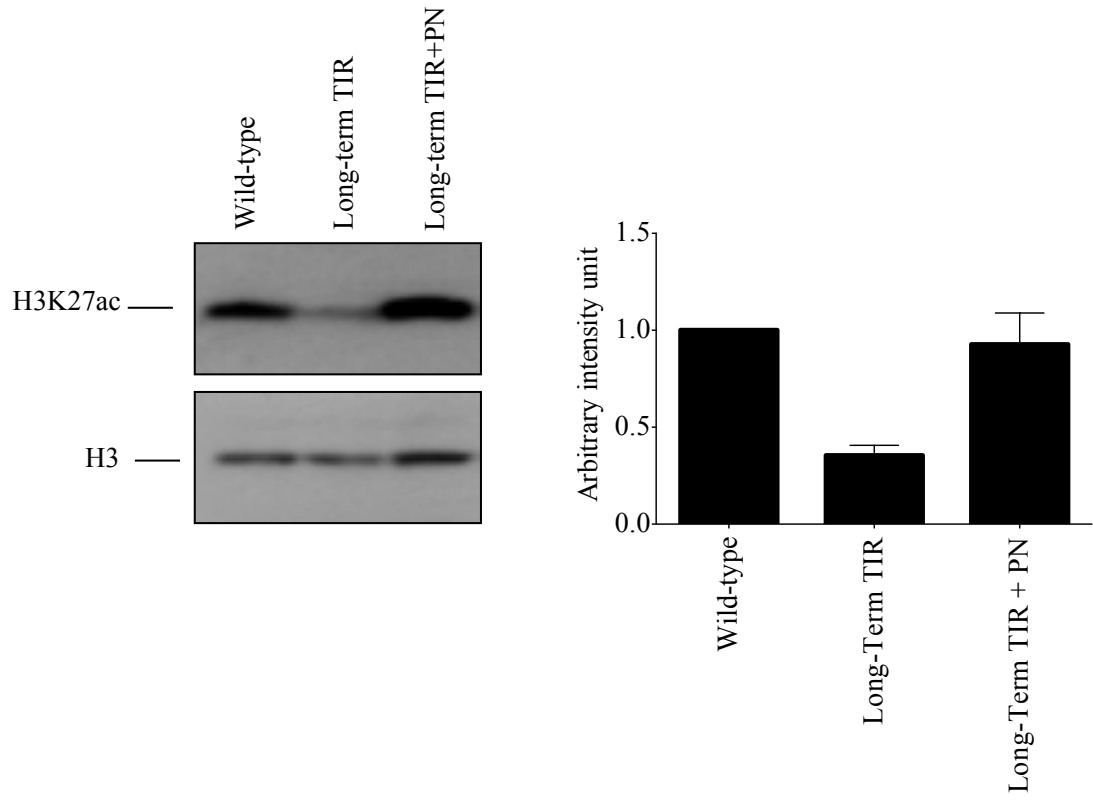
Since HDACs mediate the deacetylation of histones, I next sought to examine whether HDAC8 targets H3K27 for deacetylation in long-term TIR macrophages. Figure 3.12A shows that treatment of long-term TIR RAW 264.7 macrophages with the broad-spectrum HDAC inhibitor panobinostat (100 nM) restored H3K27Ac levels to those of wild-type macrophages, suggesting the involvement of HDACs in H3K27 deacetylation. To confirm if HDAC8 was one of the HDACs involved in H3K27 deacetylation, long-term TIR macrophages were transfected with scrambled siRNA or siRNA targeting HDAC8 and Western blots were conducted to examine H3K27Ac levels. Indeed, long-term TIR cells transfected with siRNAs against HDAC8 showed significantly increased levels of H3K27Ac (~3-fold) compared to the control (Fig. 3.12B). This data suggests that HDAC8 is involved in H3K27 deacetylation in long-term TIR macrophages.

To further examine H3K27Ac as a possible target for HDAC8, I utilized SILAC labeling in combination with SRM mass spectrometry analysis. Short-term TIR macrophages were labeled with heavy lysine, whereas short-term TIR macrophages treated with PCI-34051 (100 nM) were labeled with light lysine. Since long-term TIR macrophages showed a negative correlation between HDAC8 expression and H3K27Ac levels (Fig. 3.12), I expected that short-term TIR cells treated with PCI-34051 would show increased H3K27Ac levels relative to those of non-treated short-term TIR macrophages. Although further optimization is required to specifically quantify H3K27Ac, unmodified H3K27 showed about a 4-fold decrease in PCI-34051-treated macrophages relative to untreated short-term TIR macrophages (Fig. 3.13A). Given the mutual exclusiveness of H3K27 modifications, this data suggests that inhibiting HDAC8 with PCI-34051 increased H3K27Ac levels, leading to a decrease in unmodified H3K27, and vice versa for non-treated short-term TIR. Again, to ensure equal loadings of the samples, the E(73)IAQDFKTDLR(83) control peptide from histone H3 was used to quantify H3K79. As expected, both the light (TIR + PCI-34051) and heavy (TIR) samples were found in a 1:1 ratio (Fig. 3.13B). Collectively, this data suggests that TIR was mediated at least in part by HDAC8-mediated H3K27 deacetylation.

**Figure 3.12 HDAC8 targets H3K27Ac for deacetylation in long-term TIR macrophages.**

(A) RAW 264.7 wild-type macrophages, and long-term TIR macrophages treated in the presence or absence of panobinostat (100nM; PN) for 12 hours and (B) RAW 264.7 long-term TIR macrophages treated with either scrambled (si-scramble) or HDAC8 (si-HDAC8) siRNAs for 40 hours were harvested for total cell lysates and the levels of H3K27Ac were measured by Western blot. The NIH Image J program analyzed intensities of bands. (A) Intensities of bands in long-term TIR cells  $\pm$  PN were expressed as fold of change relative to those of wild-type cells and (B) intensities of bands in long-term TIR cells treated with si-HDAC8 were expressed as fold of change relative to long-term TIR cells treated with si-scramble. Histone H3 was used as a loading control and data are representative images of three independent experiments. Data are expressed as means  $\pm$  SE (n=3).

A)



B)

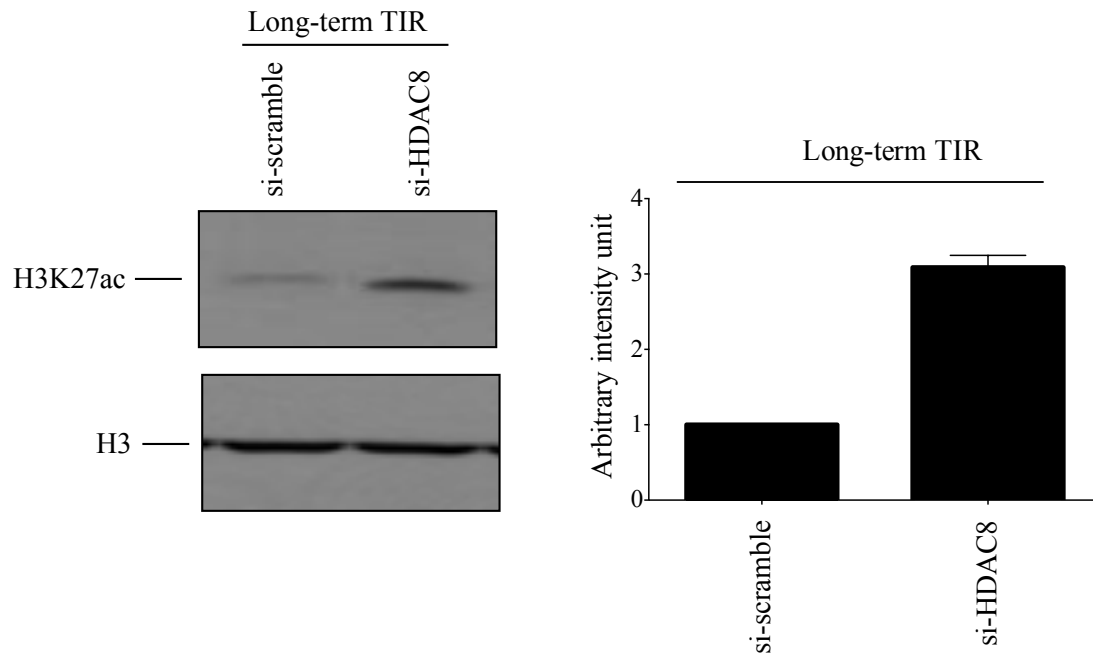
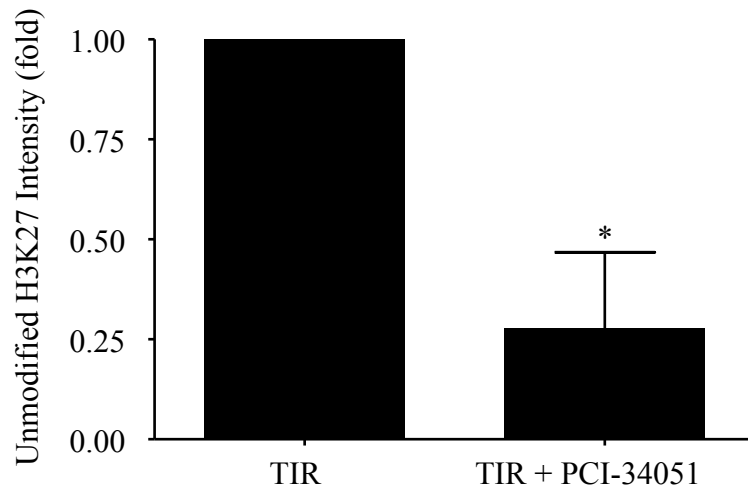
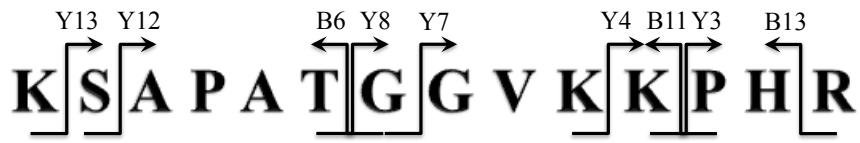


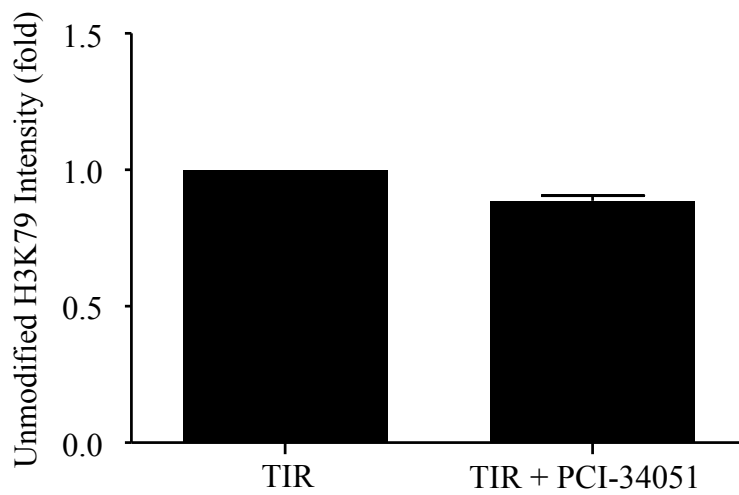
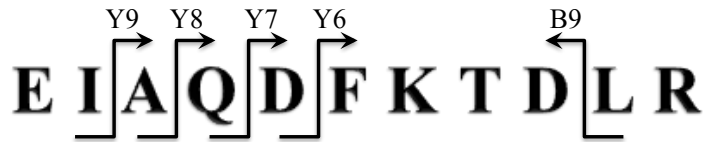
**Figure 3.13 Short-term TIR macrophages treated with the HDAC8-specific inhibitor PCI-34051 show decreased levels of unmodified H3K27 by SRM mass spectrometry.**

RAW 264.7 short-term TIR macrophages and short-term TIR macrophages treated with the HDAC8 inhibitor PCI-34051 (100 nM; 24 hours) were cultured in heavy 4,4,5,5-D4 and light L-Lysine-containing media respectively for 7 days and then pooled in a 1:1 ratio. Histone H3 was then in-gel digested using the Arg-C endoproteinase. The liquid chromatography-coupled triple quadrupole mass spectrometer with Q3 as a linear ion trap was used to quantify (A) H3K27 and (B) H3K79 by interrogating the K<sup>27</sup> SAPATGGVKKPHR<sup>40</sup> peptide and the E<sup>73</sup>IAQDFKTDLR<sup>83</sup> peptide, respectively, from digested histone H3. The Skyline software was used for the following data acquisition. (A) Transitions used for H3K27 (upper panel) and the intensity of H3K27 in TIR macrophages treated in the presence or absence of PCI-34051 (H3K27 peak heights were normalized to TIR). (B) Transitions used for H3K79 (upper panel) and the intensity of H3K79 in TIR macrophages treated in the presence or absence of PCI-34051 (H3K79 peak heights were normalized to the PCI-treated sample). Data are expressed as means  $\pm$  SE (n=2), \* P< 0.05; (Student's t-test).

A)



B)



### 3.3.3 HDAC8-dependent H3K27 deacetylation is involved in the down-regulation of the mitochondrial death genes in RAW 264.7 TIR macrophages.

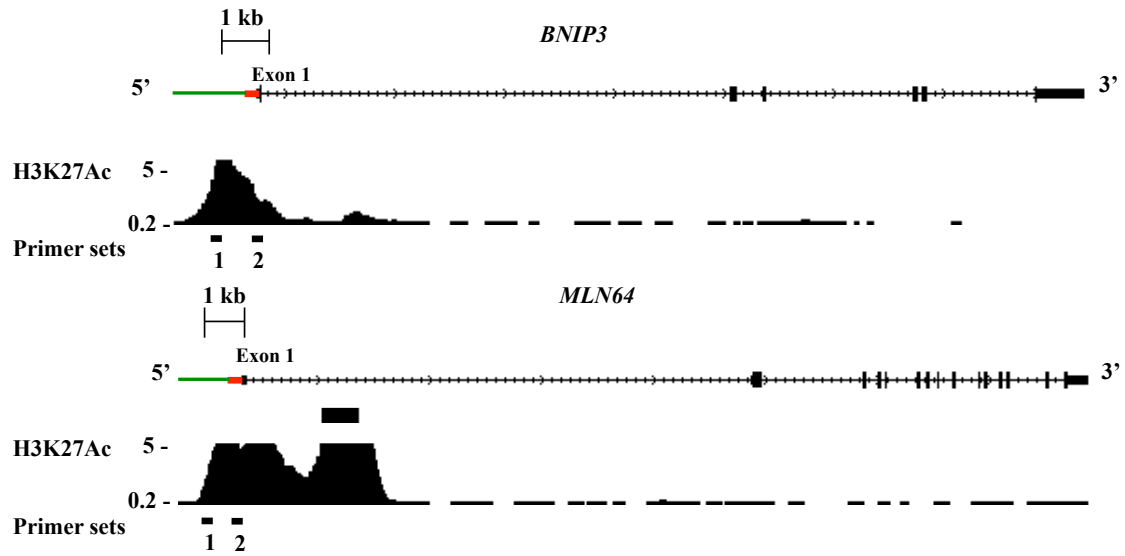
Previous work in our lab showed that H3K27Ac had decreased association with the regulatory regions of the mitochondrial death genes *BNIP3* (~1 kb upstream of exon 1) and *MLN64* (~1kb upstream of exon 1), but not *BNIP3L* in long-term TIR macrophages [177]. Since HDAC8 appears to target H3K27 for deacetylation, I examined whether HDAC8 was recruited to these regions of *BNIP3* and *MLN64* (Fig. 3.14A). Interestingly, HDAC8 was recruited to the H3K27Ac-associated regions (primer set 1) of *BNIP3* and *MLN64*, but not to the promoter regions (primer set 2) of either mitochondrial death genes (Fig. 3.14B). The control, HDAC3, was highly recruited to both the promoter and the H3K27Ac-associated regions of *BNIP3* and *MLN64*, but no significant differences were detected between wild-type and long-term TIR macrophages (Fig. 3.14B). Collectively, this data suggests that HDAC8 mediates deacetylation at the H3K27Ac regulatory regions of *BNIP3* and *MLN64*, thus inducing a “closed” chromatin conformation, which leads to the suppression of *BNIP3* and *MLN64* expression in long-term TIR macrophages.

**Figure 3.14 Long-term TIR macrophages show increased HDAC8 recruitment at the H3K27Ac-associated regulatory regions of *BNIP3* and *MLN64*.**

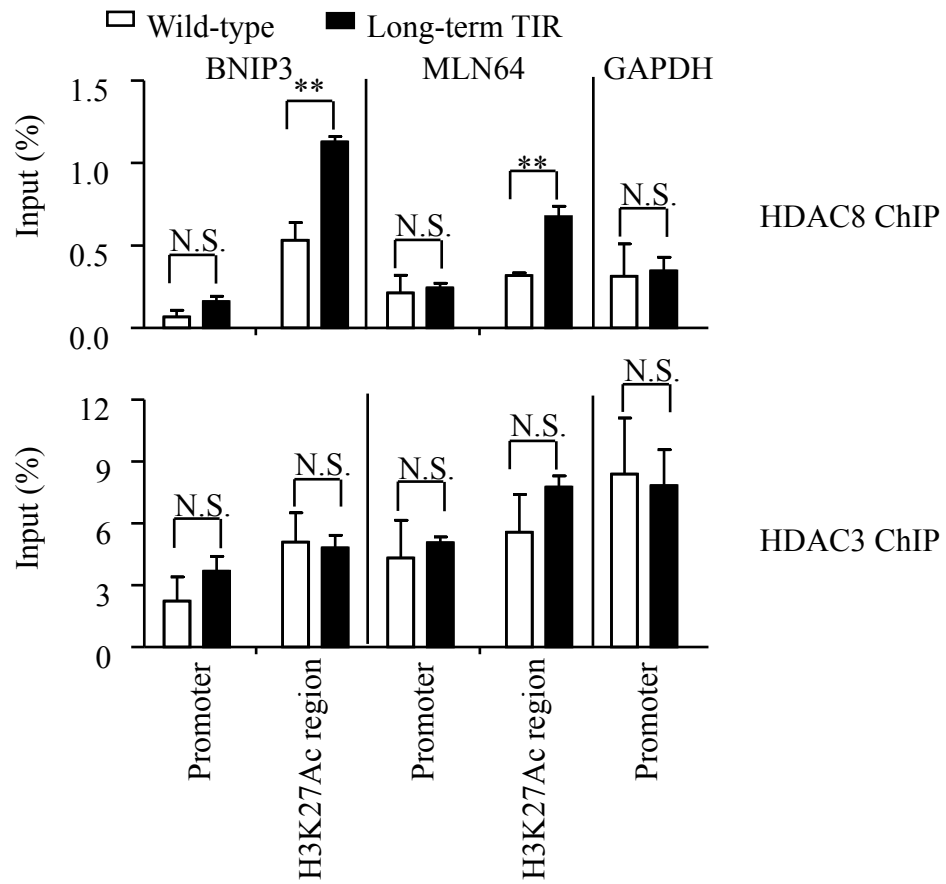
(A) Map of the primer sets targeting the H3K27Ac-associated regulatory regions (indicated by green line) amplifying ~1000 bps upstream and amplifying core promoter regions (indicated by red line) ~150 bps upstream of transcription start sites of *BNIP3* and *MLN64* in primary mouse BMDMs as indicated on ENCODE. Black boxes represent exons. (B) Levels of HDAC8 and HDAC3 recruitments to the promoter and H3K27Ac-associated regulatory regions of *BNIP3* and *MLN64* were analyzed by ChIP-qPCR. DNA from RAW 264.7 wild-type and long-term TIR macrophages were sonicated, and immunoprecipitated using antibodies against HDAC8 and HDAC3. Immunoprecipitated DNA was analyzed by qPCR using primers targeting the promoter and H3K27Ac-associated regulatory regions of *BNIP3* and *MLN64*. Recruitment of HDAC8 and HDAC3 to the promoter region of *GAPDH* was used as a control. For ChIP efficiency, the percentage of input DNA recovered by immunoprecipitation was determined by qPCR. Rabbit anti-IgG was used as a background control. Data are expressed as means  $\pm$  SE (n = 3); \*\*p < 0.01 (Student's T-test).



A)



B)



### 3.3.4 HDAC8 limits RNA polymerase II accessibility to the mitochondrial death gene promoters.

Due to HDAC8's role in down-regulating the expression of the three mitochondrial death genes, *BNIP3*, *BNIP3L*, and *MLN64* in long-term TIR, I sought to examine whether HDAC8 suppresses expression of these genes by limiting access of transcriptional machinery to their genomic regions. I first examined the accessibility of RNA polymerase II (Pol II) at the promoter regions of *BNIP3*, *BNIP3L*, and *MLN64* in long-term TIR macrophages using ChIP-qPCR analysis. Interestingly, the binding of RNA polymerase II to the promoter regions of these genes was significantly lower (at least 2-fold) in long-term TIR macrophages than wild-type macrophages (Fig 3.15). To further examine whether this decreased Pol II association in long-term TIR was HDAC8-dependent, RAW 264.7 macrophages were stably transfected with a plasmid over-expressing HDAC8 (pEGFP-HDAC8) and then harvested for Pol II ChIP-qPCR analysis. Interestingly, the over-expression of HDAC8 significantly reduced the access of Pol II to the promoter regions of *BNIP3*, *BNIP3L*, and *MLN64* (Fig 3.16). Surprisingly, Pol II accessibility at the promoter of the housekeeping gene *GAPDH* was also reduced in long-term TIR (Fig. 3.15) and in pEGFP-HDAC8 expressing wild-type macrophages (Fig. 3.16), suggesting that *GAPDH* expression is also down-regulated in long-term TIR. Since HDAC8 expression was increased in long-term TIR [177], *HDAC8* was used for Pol II ChIP-qPCR analysis as a positive control. As expected, Pol II recruitment to the promoter of *HDAC8* in long-term TIR (Fig 3.15) showed a significant increase (~2-fold) relative to the controls. Overall, this data suggests that HDAC8 limits the accessibility of Pol II to the promoter of the three mitochondrial death genes in long-term TIR.

**Figure 3.15 RNA polymerase II has limited accessibility to the promoter regions of *BNIP3*, *BNIP3L*, and *MLN64* in long-term TIR.**

Accessibility of Pol-II to the promoter regions of *BNIP3*, *BNIP3L*, *MLN64*, *GAPDH* and *HDAC8* was analyzed by ChIP-qPCR assays. DNA prepared from RAW 264.7 wild-type and long-term TIR macrophages was sonicated and immunoprecipitated using phospho-S5 Pol-II Abs. Power SYBR Green qPCR (for *MLN64*, *GAPDH* and *HDAC8*) and TaqMan qPCR analysis using the ZEN quencher system (for *BNIP3* and *BNIP3L*) was used to quantify the amounts of immunoprecipitated DNA using primers and an internal probe. ChIP efficiency is represented as the percentage of input DNA recovered by immunoprecipitation. Rabbit anti-IgG was used as a background control. Data are expressed as means  $\pm$  SE (n = 3); \*p < 0.05, \*\*p < 0.01 (Student's T-test).

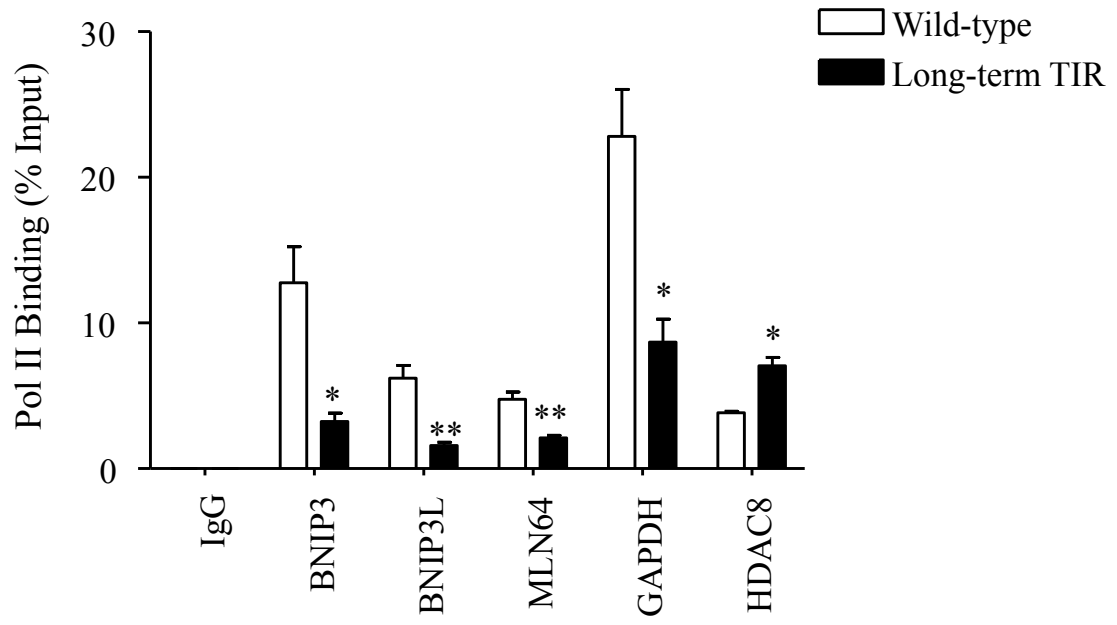
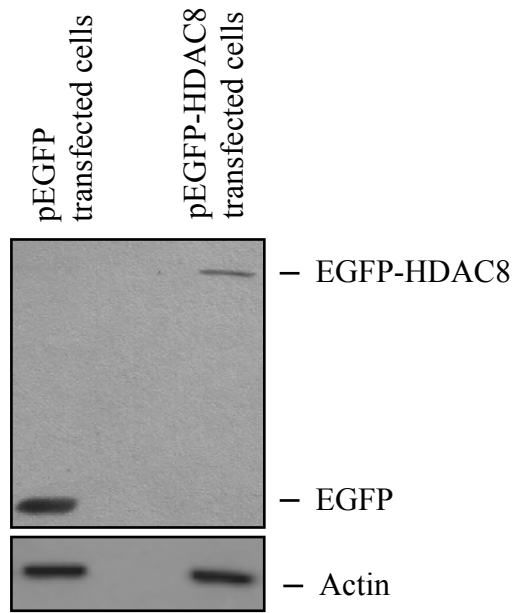
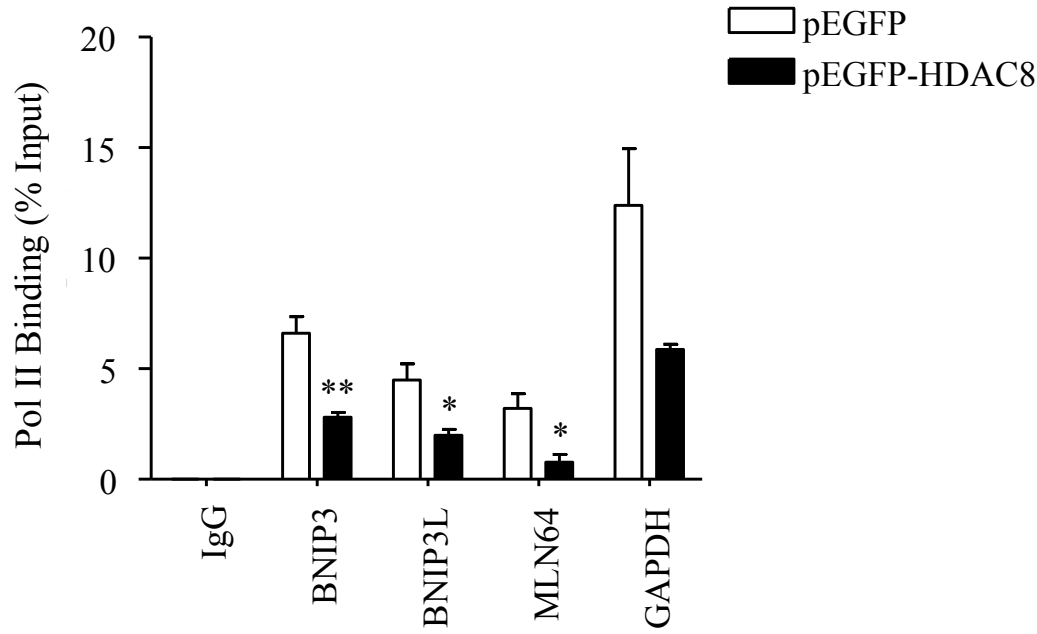


**Figure 3.16 RNA polymerase II has limited accessibility to the promoter regions of *BNIP3*, *BNIP3L*, and *MLN64* in RAW 264.7 macrophages over-expressing HDAC8.**

Accessibility of Pol-II to the promoter regions of *BNIP3*, *BNIP3L*, *MLN64* and *GAPDH* was analyzed by ChIP-qPCR assays (upper panel). Pol II immunoprecipitated DNA was analyzed by qPCR. ChIP efficiency is represented as the percentage of input DNA recovered by immunoprecipitation. Rabbit anti-IgG was used as a background control. Data are expressed as means  $\pm$  SE (n = 3), \*p  $\leq$  0.05, \*\*p  $\leq$  0.01 (Student's T-test). Total cell lysates from RAW 264.7 macrophages stably transfected with pEGFP or pEGFP-HDAC8 were used for EGFP western blots to confirm transfection efficacy (lower panel). Actin was used as a loading control.



### 3.4 LeTx suppresses cytokine production in an HDAC8-dependent manner.

In addition to inducing pyroptosis in certain subsets of murine macrophages [21], LeTx also causes immune suppression through inactivation of the MAPK signaling pathway. As epigenetic reprogramming is involved in macrophage activation [184], differentiation [185-187] and tolerance [188-190], and LeTx has been shown to alter histone modifications in a MAPK-dependent manner leading to IL-8 suppression [175], I suspected that histone modifications involved in the maintenance of TIR might also affect cytokine production.

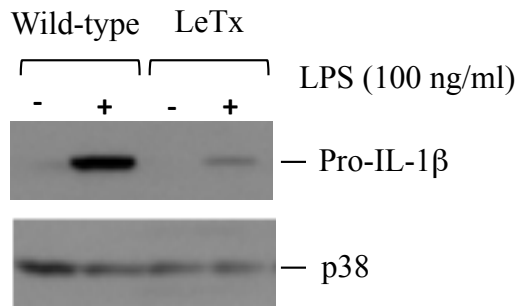
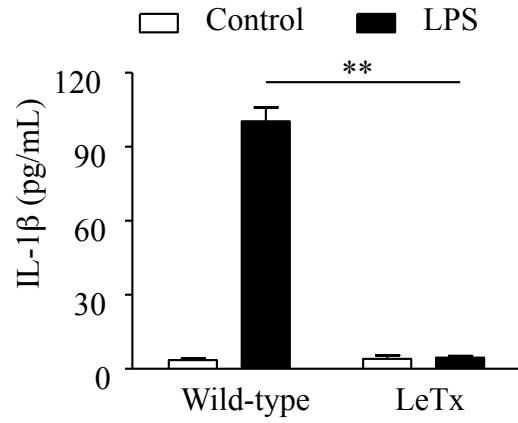
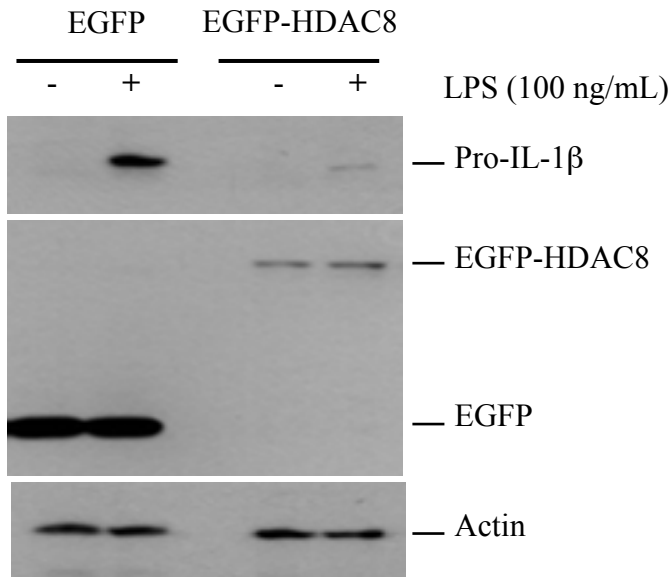
#### 3.4.1 LeTx-treated RAW 264.7 macrophages are defective in producing IL-1 $\beta$ in an HDAC8-dependent manner in response to LPS.

Various studies have shown that LeTx inhibits the production of pro-inflammatory cytokines including IL-1 $\beta$ , TNF $\alpha$ , and IL-6 in macrophages [63,191,192]. Consistent with these studies, I found that RAW 264.7 macrophages treated with a sub-lethal dose of LeTx are defective in the production and release of IL-1 $\beta$  in response to LPS when measured by Western blot (Fig. 3.17A) or ELISA (Fig. 3.17B), respectively. Since LeTx appears to up-regulate HDAC8 (Fig. 3.2), the next step examined whether LeTx-treated RAW 264.7 macrophages were defective in IL-1 $\beta$  production in an HDAC8-dependent manner. As such, RAW 264.7 macrophages were stably transfected with either a control plasmid (pEGFP) or a plasmid expressing HDAC8 (pEGFP-HDAC8) and then cells were harvested to measure pro-IL-1 $\beta$  production by western blot. Interestingly, RAW cells over-expressing HDAC8 were defective in pro-IL-1 $\beta$  production in response to LPS (Fig. 3.17C), thus suggesting the role of HDAC8 in the regulation of cytokine production.

**Figure 3.17 LeTx-treated and over-expressing HDAC8 RAW 264.7 macrophages are defective in IL-1 $\beta$  production in response to LPS.**

RAW 264.7 wild-type macrophages were treated with or without a sub-lethal dose of LeTx (PA: 100 ng/mL, LF: 100 ng/mL) for 5 hours and then fresh media was added for overnight incubation. The following day, samples were treated with LPS for 4 hours, and (A) production of pro-IL-1 $\beta$  and (B) release of IL-1 $\beta$  were analyzed by Western blots or ELISA, respectively. (C) RAW264.7 macrophages stably transfected with pEGFP or pEGFP-HDAC8 were analyzed for expression levels of pro-IL-1 $\beta$  by Western blots. Data are representative images of three independent experiments. Data are expressed as means  $\pm$ SE (n=3), \*\* p< 0.01 (Student's T-test). **Dr. Soon-Duck Ha solely performed parts A-C.**



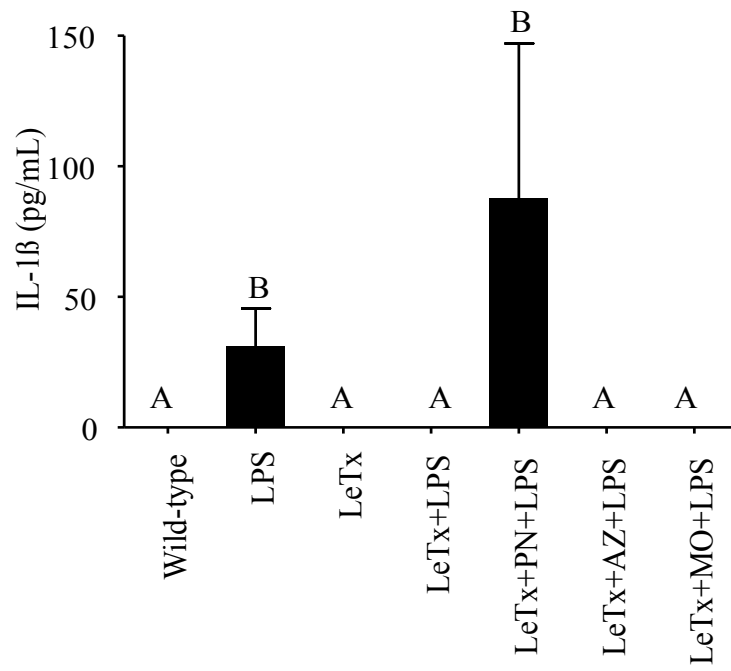
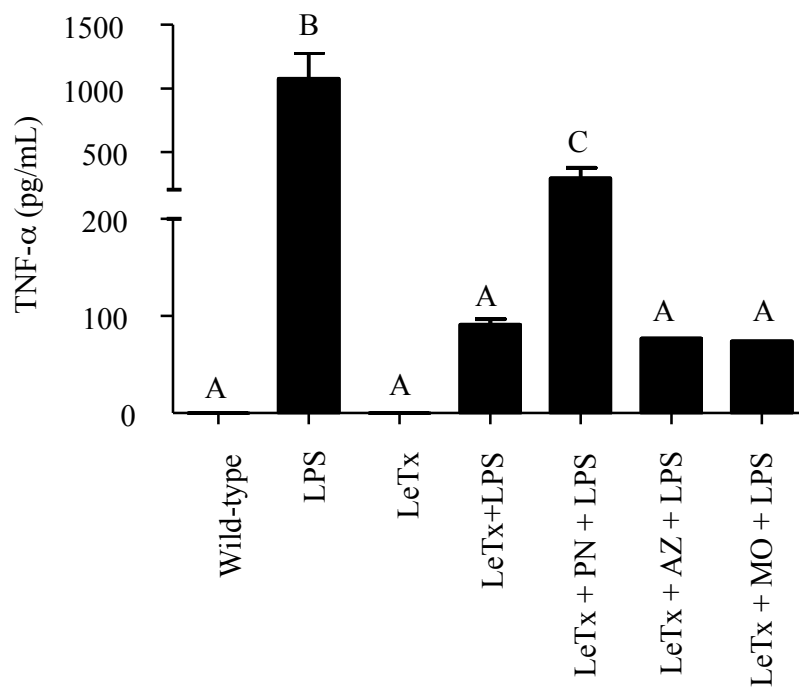
**A)****B)****C)**

### 3.4.2 Inhibiting HDAC8 restores the expression and production of IL-1 $\beta$ and TNF- $\alpha$ in LeTx-treated macrophages.

To further examine HDAC8's role in regulating cytokine production in response to LeTx, LeTx-treated RAW 264.7 macrophages were treated with various epigenetic inhibitors, including panobinostat (broad-spectrum HDAC inhibitor), azacitidine (DNMT inhibitor), and mocetinostat (HDAC 1, 2, 3, and 11 inhibitor) overnight, followed by LPS stimulation. Supernatants were then collected to measure the release of IL-1 $\beta$  and TNF- $\alpha$  by ELISA. Interestingly, LeTx-induced immune suppression was only reversed by panobinostat treatment, such that the levels of IL-1 $\beta$  (Fig. 3.18A) and TNF- $\alpha$  (Fig. 3.18B) were restored to that of wild-type levels in response to LPS. To specifically confirm the involvement of HDAC8 in regulating cytokine production, LeTx-treated RAW 264.7 macrophages were exposed to PCI-34051 overnight and then stimulated by LPS. As expected, PCI-34051 treatment increased the mRNA expression of IL-1 $\beta$  (Fig. 3.19A) and TNF- $\alpha$  (Fig. 3.19B) to nearly wild-type levels in response to LPS even in the presence of LeTx. PCI-34051 did not further induce TNF $\alpha$  release compared to wild-type in response to LPS (Fig. 3.20), however it slightly induced IL-1 $\beta$  mRNA in the presence of LPS (Fig 3.19A). Despite a slight induction of IL-1 $\beta$  by PCI-34051 alone, the data collectively suggests that inhibiting HDAC8 reversed the immunosuppressed state triggered by LeTx.

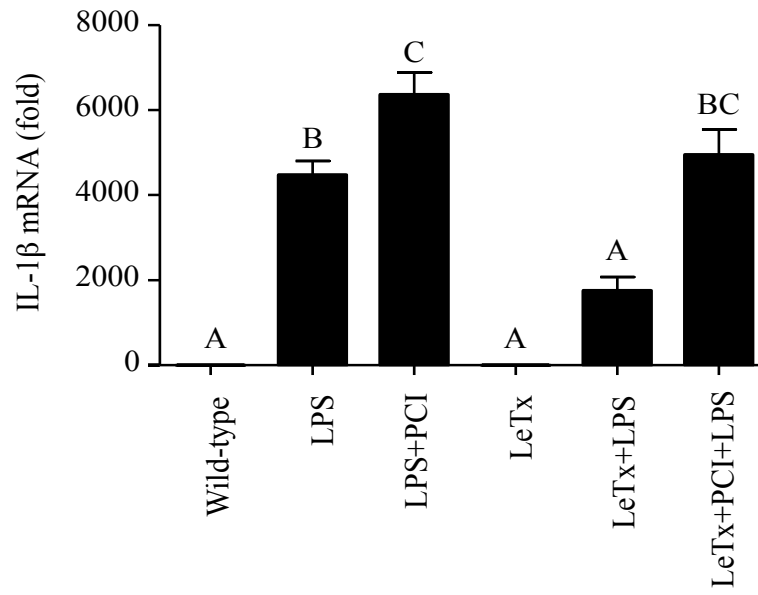
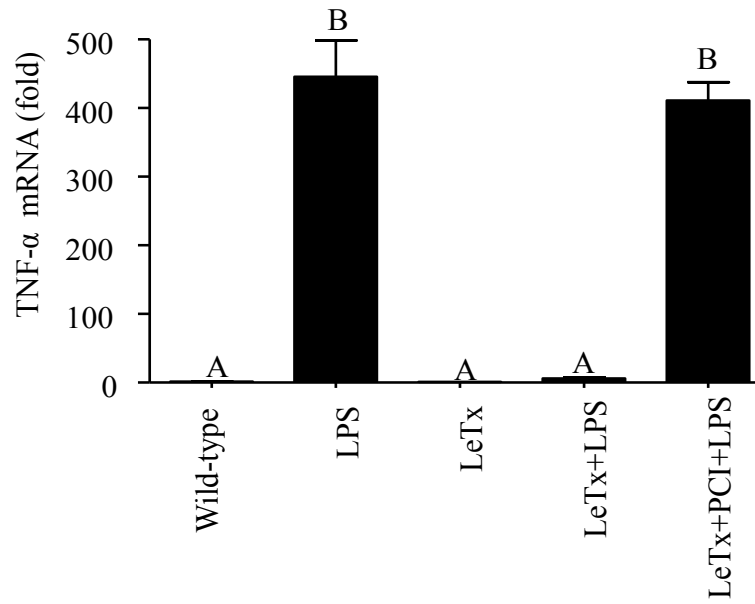
**Figure 3.18 The broad-spectrum HDAC inhibitor panobinostat (PN) restores production of IL-1 $\beta$  and TNF $\alpha$  in response to LPS in the presence of LeTx.**

RAW 264.7 wild-type macrophages were treated with or without a sub-lethal dose of LeTx (PA: 100 ng/mL, LF: 100 ng/mL) for 5 hours then left overnight. These LeTx-treated cells were then re-plated and exposed to various epigenetic inhibitors including, panobinostat (PN; broad-spectrum HDAC inhibitor; 1 nM), azacitidine (Az; DNMT inhibitor; 200 nM), and mocetinostat (MO; HDAC1-3/11 inhibitor; 150 nM) for 24 hours. Following 4 hours of LPS (100ng/mL) treatment, supernatants were collected and levels of (A) IL-1 $\beta$  and (B) TNF- $\alpha$  were measured by ELISA. Data are expressed as means  $\pm$  SE (n=3). Bars with same letter indicate no significant difference,  $p > 0.05$  (One-way Anova; Tukey's post-test). **Dr. Soon-Duck Ha prepared samples for part A and B.**

**A)****B)**

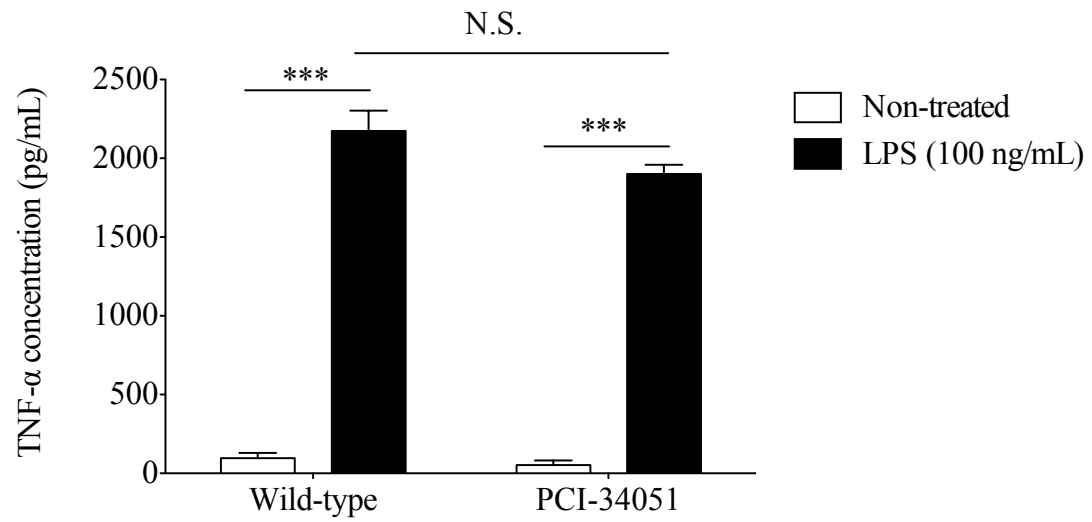
**Figure 3.19 The HDAC8 specific inhibitor PCI-34051 restores mRNA levels of IL-1 $\beta$  and TNF $\alpha$  in response to LPS in the presence of LeTx.**

RAW 264.7 wild-type macrophages were treated with or without a sub-lethal dose of LeTx (PA: 100 ng/mL, LF: 100 ng/mL) for 5 hours then left overnight. These LeTx-treated cells were then re-plated and exposed to the HDAC8-specific inhibitor PCI-34051 (20 nM) for 24. Following 3 hours of LPS (100ng/mL) stimulation, cells were harvested and mRNA levels of (A) IL-1 $\beta$  and (B) TNF $\alpha$  were measured relative to GAPDH using qPCR. All samples are normalized to the mRNA expression levels of the unstimulated wild-type macrophages. Data are expressed as means  $\pm$  SE (n=3). Bars with same letter indicate no significant difference,  $p > 0.05$  (One-way Anova; Tukey's post-test).

**A)****B)**

**Figure 3.20 The HDAC8 inhibitor PCI-34051 does not induce TNF- $\alpha$  production in RAW 264.7 macrophages in response to LPS.**

RAW 264.7 macrophages were treated in the presence or absence of the HDAC8-specific inhibitor PCI-34051 (20 nM) for 24 hours and then treated in the presence or absence of LPS (100 ng/mL) for 4 hours. Following LPS stimulation, supernatants were collected and TNF- $\alpha$  release was measured by ELISA. Data are expressed as means  $\pm$  SE (n=3), \*\*\*  $p < 0.001$  and N.S. (no significant difference); Two-way Anova (Bonferroni post-test).





### 3.4.3 Inhibiting HDAC8 in LeTx-treated macrophages increases H3K27Ac and Pol II association in the genomic regions of *IL-1 $\beta$* in response to LPS.

In long-term TIR macrophages, I showed an increased recruitment of HDAC8 to H3K27Ac-associated regions of *BNIP3* and *MLN64* (Fig. 3.14), suggesting that it targets H3K27 and silences mitochondrial death gene expression. In addition, H3K27Ac is largely associated with active enhancers [193]. Thus, a reduction in H3K27Ac may hinder the process of gene transcription. I suspected that HDAC8 similarly targets the H3K27Ac-associated regions of *IL-1 $\beta$* . Since HDAC8 was up-regulated in RAW 264.7 macrophages treated with LeTx (Fig. 3.2A), I hypothesized that LeTx decreases H3K27Ac-association of *IL-1 $\beta$*  in response to LPS and that inhibiting HDAC8 in this sample would restore H3K27Ac association to that of wild-type levels. To evaluate this hypothesis, a set of 8 primers (**Set 1**: ~1.4 kbp upstream of exon 1, **Set 2**: ~350 upstream of exon 1, **Set 3**: ~85 bp down stream of exon 1, **Set 4**: ~100 bp downstream of exon 2, **Set 5**: ~50 bp upstream of exon 3, **Set 6**: ~100 bp upstream of exon 4, **Set 7**: ~170 bp upstream of exon 6, and **Set 8**: ~10 bp downstream of exon 7) for H3K27Ac ChIP-qPCR analysis was randomly designed to encompass H3K27Ac-association regions of *IL-1 $\beta$* , based on the ENCODE database (Fig. 3.21A). Interestingly, LPS-stimulated LeTx-treated macrophages showed a significant decrease (~2-fold) in H3K27Ac association in the genomic regions of primer set 4 (~100 bp downstream of exon 2) and primer set 5 (~50 bp upstream of exon 3) compared to LPS-stimulated wild-type macrophages (Fig. 3.21B). Inhibition of HDAC8 by PCI-34051 in LPS-stimulated LeTx-treated macrophages restored H3K27Ac-association in the genomic regions to that of LPS-stimulated wild-type levels (Fig. 3.21B). Collectively, this data suggests that HDAC8 targets H3K27 for deacetylation in the intragenic region of *IL-1 $\beta$*  in LeTx-treated macrophages, rather than the promoter region (set 1 and set 2). In contrast, inhibiting HDAC8 restores H3K27Ac association and likely *IL-1 $\beta$*  expression.

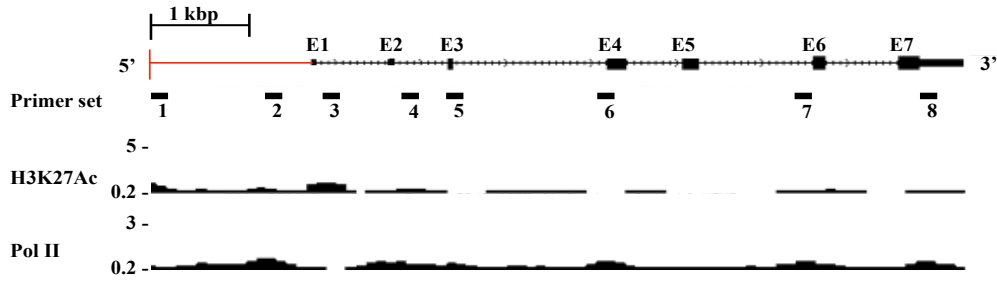
Since PCI-34051 increased H3K27Ac association in *IL-1 $\beta$*  in LeTx-treated macrophages (Fig. 3.21B), I also examined whether Pol II recruitment was increased to wild-type levels at the promoter or genomic regions of *IL-1 $\beta$*  in these macrophages using Pol-II ChIP-qPCR analysis. The same primer sets used to analyze H3K27Ac association were

used for Pol-II ChIP-qPCR (Fig. 3.21A). Interestingly, PCI-34051 significantly increased Pol II recruitment to the same genomic region that showed increased H3K27Ac association (primer set 4), but not to the promoter region (set 1 and set 2) in the LPS-stimulated LeTx-treated macrophages (Fig. 3.21C). Furthermore, recruitment of Pol II across to the entire genomic/promoter regions of *IL-1 $\beta$*  was increased by PCI-34051 in LeTx-treated macrophages, suggesting that HDAC8 inhibition restored *IL-1 $\beta$*  transcription.

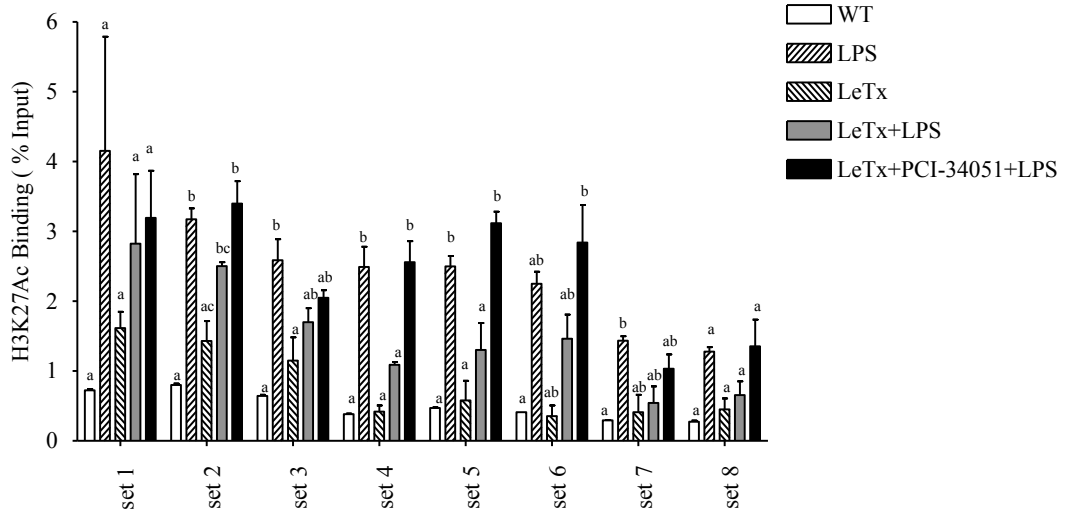
**Figure 3.21 Inhibiting HDAC8 by PCI-34051 in LeTx-treated macrophages increases H3K27Ac and Pol II association in the genomic regions of *IL-1 $\beta$*  in response to LPS.**

(A) Map of the primer sets expanding the H3K27Ac- and Pol II-associated regions of *IL-1 $\beta$*  in primary mouse BMDMs as indicated on ENCODE. The red line marks the primary promoter region and the black boxes represent exons (E). RAW 264.7 wild-type macrophages (WT) were treated in the presence or absence of LeTx (PA: 100 ng/mL, LF: 100 ng/mL) for 5 hours and then fresh media was added and cultures were left overnight. The following day, cultures were treated with or without the HDAC8 inhibitor PCI-34501 (20 nM) overnight and the next day were stimulated in the presence or absence of LPS (100 ng/mL) for 3 hours. These samples were then harvested to examine the levels of (B) H3K27Ac and (C) RNA polymerase II association to the (A) promoter and genomic regions of *IL-1 $\beta$*  by ChIP-qPCR analysis. DNA was sonicated and immunoprecipitated using antibodies against H3K27Ac and Pol II and analyzed by qPCR using primers targeting the promoter and genomic regions of *IL-1 $\beta$* . For ChIP efficiency, the percentage of input DNA recovered by immunoprecipitation was determined by qPCR. Rabbit anti-IgG was used as a background control. Data are expressed as means  $\pm$  SE (n = 3). Bars with same letter indicate no significant difference,  $p > 0.05$  (One-way Anova: Tukey's post-test).

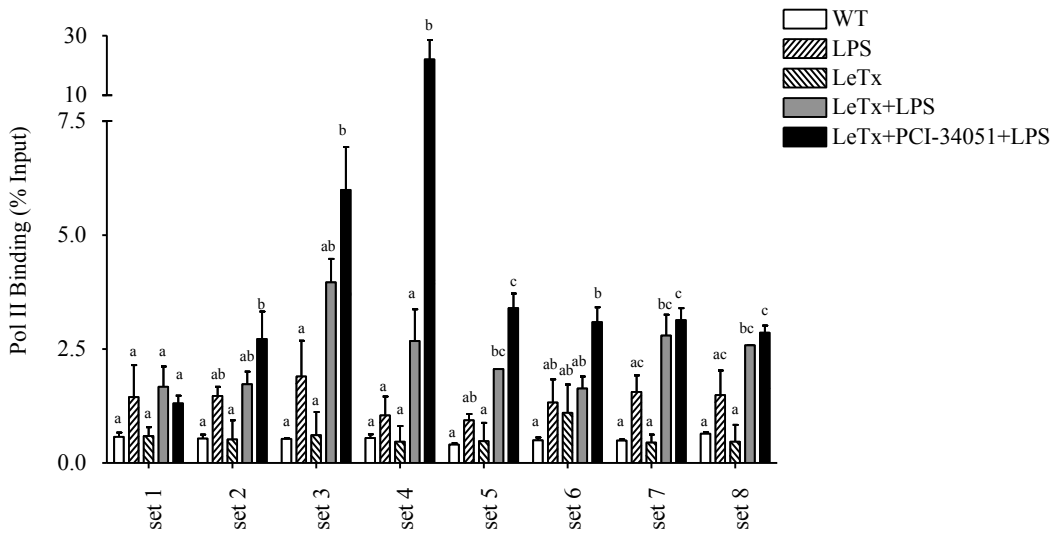
A)



B)



C)



## CHAPTER 4

### 4 DISCUSSION

#### 4.1 Resistance to LeTx-induced pyroptosis is HDAC8-mediated

Previous studies conducted by us [110,112] and others [139] found that RAW 264.7 macrophages exposed to sub-lethal doses of LeTx become temporarily (~ 4 days) refractory to subsequent cytotoxic doses, which we termed TIR. Interestingly, small subsets of these TIR macrophages are resistant to LeTx challenges for up to 6 weeks, known as long-term TIR [110]. Consistent with our previous studies in long-term TIR [110,112,177], RAW 264.7 short-term TIR macrophages are resistant to pyroptotic cell death, as RAW 264.7 wild-type macrophages become resistant in a caspase-1-dependent manner (Fig. 3.1C). Several mechanisms were suggested to be involved in TIR, such as the activation of ERK via a MEK-independent pathway, as well as an alteration in proteasome activity [139]. In LeTx-susceptible macrophages, Salles *et al.* detected a decrease in ubiquitin-conjugated proteins, which correlated with cell death. This may be due to increased proteasome activity, as inhibiting proteasome activity with lactacystin restored ubiquitination levels. Furthermore, TIR macrophages showed similar levels of protein ubiquitination compared to that of lactacystin treatment, suggesting that TIR may be a result of reduced proteasome activity [139]. Another study showed that TIR was linked to the up-regulation of a H3K27 demethylase, Jmjd3, in response to LPS [176]. Jmjd3 is known to play a vital role in the inflammatory response by contributing to macrophage differentiation, and therefore its expression may be crucial to the recovery of toxin exposed macrophages [176]. Nevertheless, this study failed to show the up-regulation of Jmjd3 in response to LeTx alone, suggesting the outcome was solely LPS-induced. In addition to these suggested mechanisms, we found that three mitochondrial death genes, *BNIP3*, *BNIP3L*, and *MLN64*, were down-regulated in long-term TIR macrophages, thus preventing caspase-1-dependent mitochondrial dysfunction and pyroptosis [110,112]. However, the mechanism leading to silencing of these three mitochondrial death genes remained unknown. This study showed that epigenetic reprogramming played a significant role in maintaining the TIR phenotype. Epigenetic

modifications known to play a role in gene silencing include DNA methylation and histone modifications (e.g. deacetylation). Although the role of DNA methylation in TIR still remains elusive, increased HDAC8 expression is highly correlated with long-term TIR [177]. Here, I showed that RAW 264.7 short-term TIR macrophages also had increased HDAC8 expression at both mRNA and protein levels (Fig. 3.2 and 3.3). Since HDAC8 expression was highly correlated with the TIR phenotype, I examined whether inhibiting HDAC8 with PCI-34051, which has greater than 200-fold selectivity over other HDACs [194], rendered RAW 264.7 short-term TIR macrophages sensitive to LeTx-induced pyroptosis. Indeed, Figure 3.4 confirmed that inhibiting HDAC8 in RAW 264.7 short-term TIR macrophages sensitized them to LeTx-induced cell death. Furthermore, the LeTx-induced cell death observed in these TIR macrophages was likely pyroptosis as sensitization occurred in a caspase-1-dependent manner (Fig. 3.4). The involvement of HDACs 1-3, 6, and 11 in mediating resistance to LeTx was dismissed, as treatment with mocetinostat, an HDAC 1, 2, 3, and 11-specific inhibitor, and CAY10603, an HDAC6-specific inhibitor, did not sensitize TIR macrophages to LeTx (Fig. 3.4B). Strikingly, HDAC8 was crucial for the suppression of *BNIP3*, *BNIP3L*, and *MLN64* expression in long-term TIR cells [177], as well as TIR-BMDMs (Fig. 3.5). Collectively, these studies suggest that sub-lethal doses of LeTx induced HDAC8, which plays a key role in resistance to subsequent LeTx challenges by contributing to the down-regulation of the three mitochondrial death genes. It would be interesting to examine how HDAC8 is up-regulated in response to LeTx, as this is currently unknown. While more extensive studies should be conducted to entirely reject the involvement of other HDACs in TIR, HDAC8 appears to be a key regulator in determining susceptibility to LeTx-induced pyroptosis.

## 4.2 TIR is mediated by an HDAC8-H3K27-dependent epigenetic mechanism

HDAC8 is a ubiquitously expressed class I HDAC, and is the most divergent member of this class as it can localize within both the cytoplasm and the nucleus [158,163-165]. HDAC8 has been implicated in the suppression of histocompatibility complex I genes by the adenoviral E1A-12 protein [195], as well as p53 in hepatocellular carcinoma cell lines

[172] and inv(16) fusion protein-positive leukemic stem cells [173]. To date, HDAC8 has been primarily studied with regards to cancer, whereas little is known about its role in infection and immunity. As such, the involvement of HDAC8 in regulating mitochondrial death gene expression is a novel finding [177]. *In vitro*, HDAC8 shows deacetylase activity towards all core histones [166-168]. Furthermore, HDAC activities are generally regulated by a variety of post-translational modifications, including acetylation, ubiquitination and SUMOylation. However, the only known modification regulating the activity of HDAC8 is phosphorylation by protein kinase A (PKA) at serine 39 (Ser39), which prevents its deacetylase function [167,196]. Although histone substrates for HDAC8-mediated deacetylation remain unclear *in vivo*, it likely targets histones H3 and H4, as activation of PKA increased their acetylation levels [167,196]. Consistent with these findings, our Western blots revealed an overall decrease in histone H3 acetylation in long-term RAW 264.7 TIR macrophages, which show increased HDAC8 expression [177]. Furthermore, among a wide range of acetylated histone H3 lysine residues, acetylation at H3K27 was most significantly reduced in long-term TIR [177]. Together, these observations suggested that HDAC8 might target H3K27. While Western blotting is a common technique used to examine the presence of a given protein in a sample, it is non-quantitative. More specifically, it is not possible to determine how much protein is present and the molecular weight of this protein can only be estimated based on a protein ladder. Furthermore, the H3K27Ac antibodies used in this Western blot experiment were polyclonal, meaning the blots may represent non-specific interactions. Due to these constraints in Western blotting, we employed a technique known as SRM mass spectrometry as a means to directly quantify H3K27Ac levels in TIR.

Currently, SRM mass spectrometry is the most definitive method for identifying and quantifying histone post-translational modifications, and is based on the detection of multiple product ions from one or more precursor ions [181,197,198]. Furthermore, in conjunction with stable isotope labeling of amino acids in cell culture (SILAC), SRM mass spectrometry can quantify differentially expressed histone modifications between two samples [197,198]. More specifically, measurements of differential H3K27Ac levels between wild-type and long-term TIR samples can be accomplished by isotopic labeling

of lysine residues (Fig. 3.6). In line with our previous findings [177], SILAC in combination with SRM mass spectrometry confirmed a significant reduction of acetylated H3K27 in long-term TIR macrophages (Fig. 3.9). Since short-term adaptation to stressors *in vivo* is more likely to occur, this methodology was also applied for comparing H3K27Ac levels between RAW 264.7 short-term TIR and wild-type macrophages. Despite the increased sensitivity of triple quadrupole (MS/MS) systems, our samples did not reach the lower detection limits for H3K27Ac, such that the background noise was high relative to the signal. This prevented absolute identification of the H3K27Ac peptide. Generally non-modified peptides are present at the highest abundance, making them easily identifiable by MS/MS analysis. However, when multiple combinations of modifications are possible at a single residue as for H3K9 [199], or H3K27 (Fig. 4.1), then analyses are much more complex. This is especially relevant when trying to distinguish acetylation (+42.01 Da) from tri-methylation (+42.04 Da) at a single site or two different sites, as well as acetylation at two or more different sites [197,199]. Unlike mass measurements, MS/MS can differentiate these post-translational modifications under ideal circumstances via the production of unique fragmentation ions at the N-terminal (b-ions) or C-terminal (y-ions). For example, acetylation at the N-terminus of the H3K9 peptide can be differentiated from tri-methylation at this site by the production of a  $b_2$  ion and a  $b_2-59$  ion, respectively [199]. Nonetheless, because our samples were not able to reach the lower detection limit, the MS/MS spectrum obtained was not conclusively able to differentiate acetylated H3K27 from tri-methylated H3K27. Collectively, with our previous findings [177] and SRM data from long-term TIR, the increase in the unmodified H3K27 peptide in short-term TIR (Fig. 3.10) suggests that H3K27Ac decreased, based on the exclusiveness of modifications at H3K27 (Fig 3.11). While H3K27 can also be tri-methylated, since mitochondrial death gene silencing is involved in TIR and H3K27 tri-methylation is a general marker for gene suppression [183], it seems most likely for H3K27Me3 levels to increase and H3K27Ac levels to decrease in short-term TIR.

Acetylated histones are thought to be key substrates for HDACs [164] and this study suggested acetylated H3K27 as one of HDAC8's downstream targets. Interestingly, there was a strong inverse correlation between HDAC8 and H3K27Ac expression.



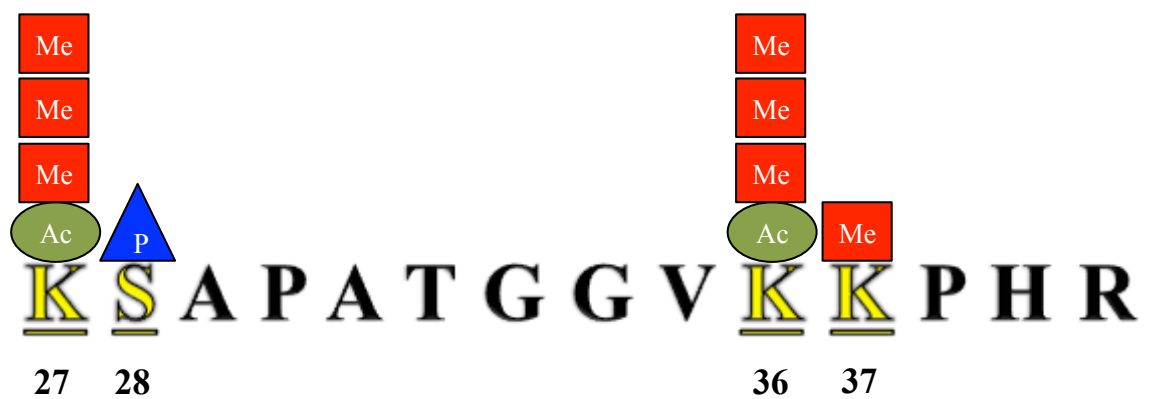
Specifically, treatment with the broad-spectrum HDAC inhibitor panobinostat or siRNAs targeting HDAC8 restored H3K27Ac levels in long-term TIR to that of wild-type macrophages (Fig. 3.12). Furthermore, reduced levels of the unmodified H3K27 peptide in TIR macrophages treated with the HDAC8 inhibitor PCI-34051 (Fig. 3.13) suggested an enhancement of H3K27Ac on the basis of exclusiveness at this site. H3K27Ac plays a prominent role in promoting gene expression [200,201], and a previous study conducted in our lab revealed that H3K27Ac was highly associated with the regulatory regions of *BNIP3* and *MLN64*, showing ~100- and ~40-fold increase above basal IgG levels, respectively, in RAW 264.7 macrophages [177]. Conversely, H3K27Ac association at these two mitochondrial death genes was significantly reduced in long-term TIR. Since H3K27Ac is a possible HDAC8 substrate, further ChIP-qPCR analysis was conducted to examine whether HDAC8 recruitment was increased at these sites. As expected, HDAC8 recruitment was increased at H3K27Ac-associated regions of *BNIP3* and *MLN64*, but not at the promoter in long-term TIR, compared to that of wild-type (Fig. 3.14). This is the second study to show HDAC8 interaction with a DNA target; a recent study demonstrated that HDAC8 suppresses the activity of pro-apoptotic gene Bcl-2-modifying factor (*BMF*) in colon cancer cells through interacting with the promoter regions [202]. Furthermore this study revealed activation markers H3K9Ac and H3K14Ac as potential HDAC8 targets. Consistent with these findings, we also noted a reduction in H3K9Ac and H3K14Ac in long-term TIR [177], suggesting that HDAC8 can deacetylate multiple lysine residues on histone H3. However, more extensive study is required to examine whether HDAC8 targets these sites in TIR and whether H3K9Ac and H3K14Ac play a role in mitochondrial death gene expression. In summary, increased HDAC8 recruitment plays a key role in silencing *BNIP3* and *MLN64* by deacetylating H3K27 in long-term TIR.

Histone acetylation plays a key role in gene expression through inducing an open chromatin confirmation, thus allowing for the binding of transcription machinery such as RNA polymerase II (Pol II). During transcription, Pol II becomes highly phosphorylated, such that it has different phosphorylation states based on its gene location. Specifically, within the promoter Pol II is primarily phosphorylated at serine 5 (Pol II-phospho S5), whereas within coding regions Pol II is generally phosphorylated at serine 2 [203]. Since

HDAC8 appears to play a key role in *BNIP3*, *BNIP3L* and *MLN64* suppression in long-term TIR. I indirectly measured the transcriptional activity of these mitochondrial death genes by examining Pol II-phospho S5 recruitment to the promoters. As expected, long-term TIR macrophages and RAW 264.7 macrophages over-expressing HDAC8 show a significant decrease in Pol II association at the mitochondrial death gene promoters compared to wild-type and vector controls, respectively (Fig. 3.15 and 3.16). Overall, this data suggests that HDAC8-mediated H3K27 deacetylation promoted a closed chromatin conformation, preventing the binding of Pol II transcriptional machinery, and silencing *BNIP3* and *MLN64* expression in long-term TIR. In support of this gene silencing mechanism, in colon cancer cells *BMF* expression was inhibited by promoter-HDAC8 interactions, which subsequently prevented Pol II binding [202]. Also, decreased levels of the gene activation markers H3K9Ac and H3K14Ac were correlated with decreased *BMF* expression in an HDAC8-dependent manner [202]. Collectively, this suggests that HDAC8-dependent deacetylation of H3K9Ac and H3K14Ac may play a role in silencing *BMF* expression through preventing access of Pol II to the promoter region. As such, it would be interesting to examine if HDAC8 plays a role in mediating *BNIP3L* silencing via targeting H3K9Ac or H3K14Ac.

**Figure 4.1 The H3K27 peptide histone modifications.**

The histone H3 lysine 27 (H3K27) peptide generated from Arg-C digestion can have a variety of post-translational modifications, including acetylation (Ac) or mono- di- or tri-methylation (Me) at lysine (K) 27, phosphorylation (P) at serine (S) 28, acetylation or mono- di- or tri-methylation at lysine 36, and mono-methylation at lysine 37.



### 4.3 LeTx-induced cytokine suppression is mediated by an HDAC8-H3K27-dependent epigenetic mechanism

In addition to inducing pyroptotic cell death in susceptible macrophages, LeTx, even at sub-lethal doses, disrupts inflammatory immune responses. This occurs by inhibiting the MAPK signaling cascade, which plays a vital role in several aspects of the immune defenses [67,204]. The inactivation of MAPK signaling impairs numerous innate immune responses, including the production of pro-inflammatory cytokines such as IL-1 $\beta$ , TNF- $\alpha$ , IL-6, and IL-8 [63,65,175,191]. LeTx-induced inhibition of IL-1 $\beta$  is particularly important, as it prevents early detection of germinating *B. anthracis* [104]. This immune suppressed state is the primary cause for uncontrolled proliferation of *B. anthracis* within the host [57,58,204,205]. In addition, IL-1 $\beta$  plays a key role in mounting immune responses against a number of other pathogenic bacteria, including *Francisella tularensis*, *S. typhimurium*, *Listeria monocytogenes*, *Shigella flexneri*, and *Legionella pneumophila* [72,97,98,104,206-208]. In line with previous studies, treatment with a sub-lethal dose of LeTx (100 ng/mL PA and 100 ng/mL LF) in RAW 264.7 macrophages inhibited the production of IL-1 $\beta$  in response to LPS (Fig. 3.17A and 3.17B). TLR signaling during infection, such as stimulation of TLR4 by LPS, is crucial for the activation of various transcription factors that behave in combination to regulate inflammatory gene expression [54,55]. Furthermore, TLRs are coupled to MAPK signaling cascades [60]. Therefore due to LeTx-induced MEK inactivation, it is not surprising that LPS stimulation failed to trigger IL-1 $\beta$  production in LeTx-exposed macrophages.

Since previous sections of this study revealed that HDAC8 could regulate mitochondrial death gene expression through altering H3K27Ac levels, I further examined whether HDAC8 played a role in LeTx-mediated cytokine gene silencing. Interestingly, RAW 264.7 macrophages over-expressing HDAC8 failed to express pro-IL-1 $\beta$  in response to LPS (Fig 3.17C). In contrast, when HDAC8 was inhibited in LeTx-exposed macrophages by the broad-spectrum HDAC inhibitor panobinostat or the HDAC8-specific inhibitor PCI-34051, IL-1 $\beta$ /TNF- $\alpha$  production and mRNA expression levels were restored to nearly the same levels as untreated macrophages in response to LPS (Fig. 3.18

and 3.19). Unlike HDAC8 inhibition, inhibiting HDACs 1, 2, 3, and 11 with mocetinostat or inhibition of DNMTs with azacitidine in LeTx-treated macrophages failed to restore IL-1 $\beta$  and TNF- $\alpha$  production in response to LPS (Fig. 3.18). Collectively, these results suggest that involvement of HDACs 1-3, and 11, and DNA methylation in LeTx-induced *IL-1 $\beta$*  and *TNF- $\alpha$*  suppression is minimal, whereas HDAC8 likely plays a key role in the silencing of these cytokine genes. In contrast to these findings, a recent study showed that selective inhibition of HDAC8 by ITF3056 actually suppressed the expression of these pro-inflammatory cytokines *in vitro* and *in vivo* [209]. Nevertheless, ITF3056's inhibitory effects were only seen at doses greater than 200 nM, whereas at lower doses this inhibitor showed little effect or even increased cytokine production. As presented in figure 3.20, PCI-34051 did not show any effects on TNF- $\alpha$  production in response to LPS at a 20 nM dose. Additionally, further studies in our lab showed no differences in LPS-induced TNF- $\alpha$  production up to doses of 1  $\mu$ M (unpublished) and over-expressing HDAC8 in RAW 264.7 macrophages showed significantly reduced pro-IL-1 $\beta$  expression in response to LPS (Fig. 3.17C), suggesting that HDAC8 functions as a negative regulator of cytokine expression, rather than a positive regulator as implied by Li *et al.* [209]. Regardless, it would be advantageous to examine whether ITF3056 has similar effects to PCI-34051 in LeTx-induced immune suppression.

As mentioned previously, H3K27Ac is an activation marker for gene expression [200,201] and HDAC8 was shown to regulate mitochondrial death gene expression in an H3K27Ac-dependent manner. Therefore, I also examined whether HDAC8-mediated H3K27Ac deacetylation was involved in LeTx-induced IL-1 $\beta$  suppression in response to LPS. Although no significant differences were noted within the promoter region, LeTx significantly decreased H3K27Ac association in response to LPS between exon 2 and exon 3 in a PCI-34051-sensitive manner (Fig. 3.21B). These results support the idea that HDAC8 suppresses IL-1 $\beta$  expression through deacetylating H3K27. Since deacetylation promotes a closed chromatin confirmation, I examined whether LeTx prevented Pol II recruitment to *IL-1 $\beta$* . Interestingly, relative to LeTx, inhibiting HDAC8 in LeTx-treated macrophages enhanced Pol II interactions in response to LPS across the entire *IL-1 $\beta$*

region, particularly between exon 2 and exon 3 (Fig. 3.21C) where increased H3K27Ac association occurred. Collectively, these findings suggest the role of enhancers in regulating *IL-1 $\beta$*  expression.

Enhancers are key regulatory elements that are capable of controlling gene expression at variable distances from their target genes [210], and studies have shown that stimulation of TLR4 by LPS triggers activation of numerous enhancers [211]. Although H3K4Me1 and HATs including CBP and P300 are general markers for enhancers [193,212-216], in a given cell type H3K27Ac positive regions within H3K4Me1 positive regions define active enhancers [193,215,217]. These enhancer elements possess binding sites for multiple transcription factors and are capable of recruiting Pol II, leading to the production of non-coding enhancer RNAs (eRNAs) [210]. Not surprisingly, the production of eRNAs is dynamically induced prior to the production of protein coding mRNAs [218], so that they can regulate mRNA production. eRNAs can promote gene transcription via chromatin looping, allowing access of the transcriptional complex to promoter regions of target genes [212]. Given these features of enhancer elements, as PCI-34051 increased H3K27Ac and Pol II association within the intragenic regions of *IL-1 $\beta$*  (between exon 2 and exon 3) in LeTx-treated macrophages in response to LPS (Fig. 3.21), this suggests that eRNAs may be involved in regulating its expression. However, further studies are required to determine whether this region does in fact encode for functioning eRNAs.

## 4.4 Future Studies

### 4.4.1 Examining the mechanism of LeTx-mediated HDAC8 up-regulation

This study revealed that HDAC8 expression was up-regulated in response to LeTx in RAW 264.7 macrophages and BMDMs in as little as 24 hours after treatment (Fig. 3.2). However, this study failed to address whether increased HDAC8 expression also lead to an increase in HDAC8 activity, as it is well known that protein expression does not always correlate to catalytic activity. As such, HDAC8 activity should be measured using a fluorometric HDAC8 activity assay kit (Abcam; product #ab156069), by

comparing deacetylation rates of the target substrate between wild-type and LeTx-treated (short-term TIR) samples. Since long-term TIR macrophages showed increased H3K27 deacetylation in an HDAC8-dependent manner (Fig. 3.12), this suggests that HDAC8 activity is in fact increased and specifically targets H3K27Ac. Regardless, the HDAC8 activity assay kit would validate an increase in HDAC8 activity in response to LeTx.

Next, this study also did not address how HDAC8 expression/activity was increased in response to LeTx. Despite preliminary data showing that MAPK inhibition correlates with the induction of HDAC8 (unpublished), LeTx also causes immune suppression via MEK inhibition-independent pathways [219]. This suggests that LeTx may regulate HDAC8 expression/activity independently of MAPKs. Interestingly, HDAC8 activity was found to be regulated by intracellular potassium concentration ( $[K^+]_i$ ), as *in vitro* concentrations around 130 mM or 10 mM inhibited or induced HDAC8 activity, respectively [220]. Since the  $[K^+]_i$  in most cells is greater than 100 mM [221], HDAC8 activity was thought to be minimal under normal conditions. However LeTx, as well as other bacterial toxins, have been shown to significantly reduce  $[K^+]_i$  through opening  $K^+$  channels [222-228], likely enhancing HDAC8 activity. As such, RAW 264.7 macrophages cultured in various  $[K^+]_i$  in the presence or absence of LeTx followed by measuring HDAC8 levels would determine whether HDAC8 acts as a  $[K^+]_i$  sensor. Furthermore, this study showed that HDAC8-mediated H3K27 deacetylation is at least in part responsible for *IL-1 $\beta$*  and mitochondrial death gene silencing in macrophages. Therefore, measuring H3K27Ac levels in the same samples used for measuring HDAC8 levels would determine whether HDAC8 acts as a  $[K^+]_i$  sensor that controls immune responses by H3K27 deacetylation.

#### 4.4.2 Examining LeTx-mediated H3K27 methylation

In addition to deacetylation at H3K27, tri-methylation at H3K27 (H3K27Me3) is also known to cause gene silencing through a polycomb complex [183,229]. Although this study clearly showed a role for HDAC8-mediated H3K27 deacetylation in gene silencing, it remains unknown whether H3K27Me3 levels are affected in an HDAC8-dependent manner. The Enhancer of Zeste Homolog 2 (EZH2), which is a vital component of the polycomb repressive complex 2 (PRC2), is responsible for mediating methylation of



H3K27 and promoting gene silencing [230,231]. Remarkably, a previous study showed that the PRC2 complex was depleted by broad-spectrum HDAC inhibition [231]. Since HDAC8 showed an inverse correlation with H3K27Ac (Fig. 3.14), it will be of interest to examine whether components of the PRC2 complex, as well as H3K27Me3 levels were reduced following inhibition of HDAC8 in macrophages. Furthermore, as LeTx appears to induce HDAC8 (Fig. 3.2), we should also examine expression levels of H3K27Me3 and PRC2 components in LeTx-treated macrophages to determine if they increase. Collectively, these experiments will provide insight as to whether LeTx/HDAC8 plays a role in silencing *IL-1 $\beta$*  and mitochondrial death genes through inducing H3K27Me3 as a result of H3K27 deacetylation.

Since western blot is a non-conclusive method for quantifying histone modifications, it would be advantageous to quantify levels of H3K27Me3 by SRM mass spectrometry. Quantifying differential H3K27Me3 levels in various macrophage samples can be accomplished by labeling with methionine isotopes as a methyl donor for histone methylation, followed by SRM mass spectrometry; a technique our collaborators successfully used to map protein lysine methylation events [181]. Isotopically labeling of the histone methyl groups within the H3K27 peptide, rather than the lysine, which was done in this study, eliminates the challenge of differentiating H3K27Me3 and H3K27Ac, since they will no longer be of similar mass. Furthermore, as this study failed to quantify H3K27Ac levels by lysine labeling and SRM mass spectrometry, levels of H3K27Me3 together with levels of unmodified H3K27 (Fig. 3.10 and 3.13) would definitively establish H3K27Ac levels in wild-type macrophages versus LeTx-treated macrophages and LeTx-treated macrophages versus HDAC8 inhibited LeTx-treated macrophages, based on exclusiveness at this site.

#### 4.4.3 Examining H3K9Ac and H3K14Ac in *IL-1 $\beta$* and mitochondrial death gene expression

This study revealed that HDAC8-mediated H3K27 deacetylation played a key role in the suppression of the mitochondrial death genes, *BNIP3* and *MLN64*, likely through preventing access of Pol II to the promoter regions. While *BNIP3L* also demonstrated decreased Pol II recruitment to its promoter region in an HDAC8-dependent manner (Fig.

3.15 and 3.16), we previously showed that it was likely not due to decreased H3K27Ac-association [177]. In addition to decreased levels of H3K27Ac in long-term TIR, there was also a significant reduction in H3K9Ac and H3K14Ac levels [177]. Furthermore, another study showed that *BMF* gene suppression partly occurred as a result of HDAC8-mediated H3K9Ac and H3K14Ac deacetylation [202]. Collectively, these findings suggest that *BNIP3L* suppression may be regulated by an H3K9Ac and/or H3K14Ac HDAC8-dependent deacetylation mechanism. Unlike, H3K27Ac, H3K9Ac and H3K14Ac associations are not available through the ENCODE database. Therefore ChIP-seq would be the most useful technique to examine whether *BNIP3L* suppression is correlated with decreased H3K9Ac and/or H3K14Ac associations in TIR. ChIP-seq data would further determine whether a decrease in these activation markers is also associated with *BNIP3* and *MLN64* suppression in TIR. Remarkably, H3K9Ac and H3K14Ac are vital for the recruitment of the Pol II-associated TFIID to the interferon (IFN)- $\gamma$  locus, thus playing a key role in promoting immune responses [232]. As such, it would be interesting to examine whether H3K9Ac and/or H3K14Ac show decreased association with *IL-1 $\beta$*  in response to LeTx. If positive results are obtained, recruitment of TFIID could be examined by ChIP-qPCR analysis at these *IL-1 $\beta$*  sites in LeTx-treated macrophages. Collectively, these studies would provide an alternate mechanism for *IL-1 $\beta$*  and mitochondrial death gene silencing.

#### 4.4.4 Examining eRNAs in regulating *IL-1 $\beta$* and mitochondrial death gene expression

This study found that LeTx-induced silencing of *BNIP3* and *MLN64*, as well as *IL-1 $\beta$* , occurred through the loss of H3K27Ac association in an HDAC8-dependent manner. While H3K27Ac is a marker for active enhancers [193,215,217], it would be interesting to examine whether these sites encode for active eRNAs. Additionally, active enhancers are capable of recruiting Pol II and other MAPK-dependent transcription factors, such as AP-1, NF- $\kappa$ B and ATF2 [212,233-236]. It appeared as though the intragenic region of *IL-1 $\beta$*  may possess an active enhancer negatively regulated by HDAC8, since Pol II was largely recruited to H3K27Ac-associated sites in a PCI-34051-sensitive manner (Fig. 3.21). To this end, ChIP-qPCR should be conducted to examine whether other

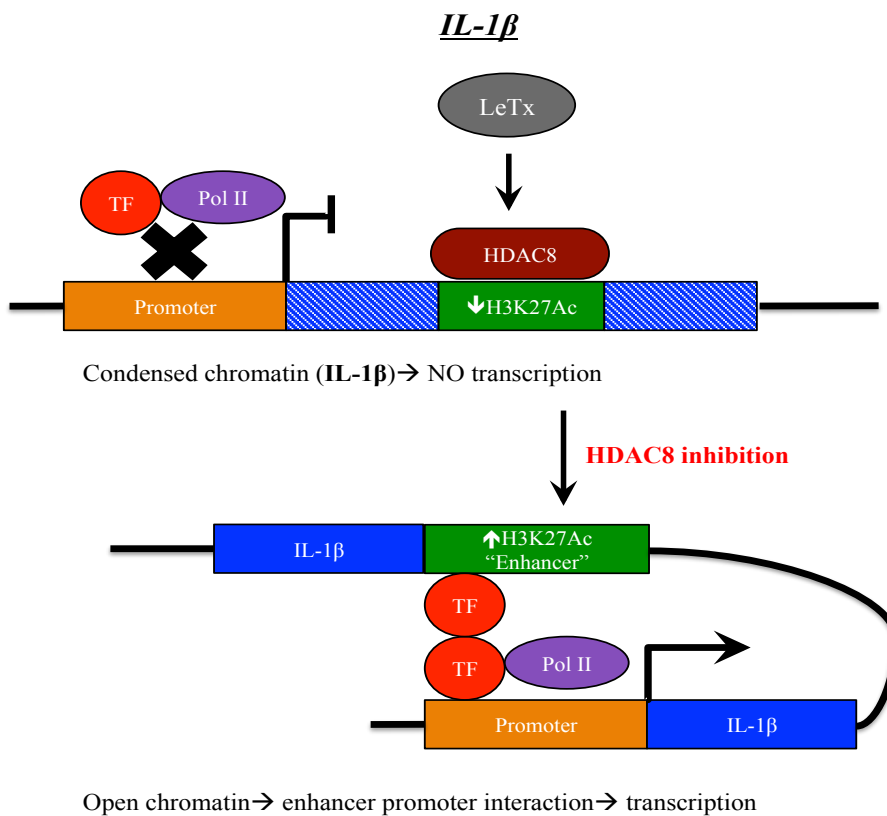
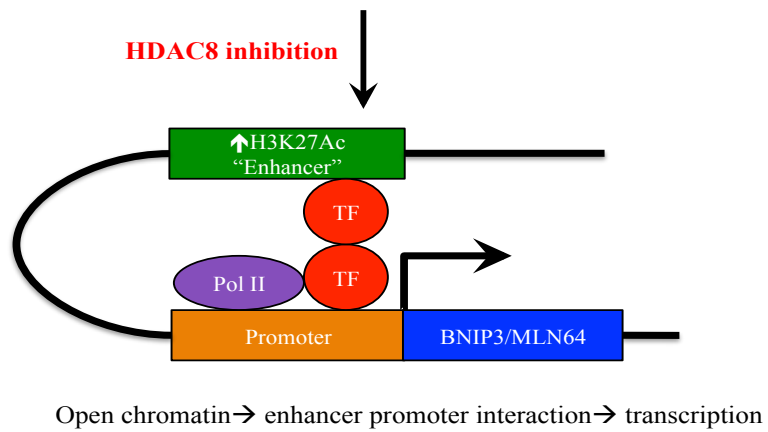
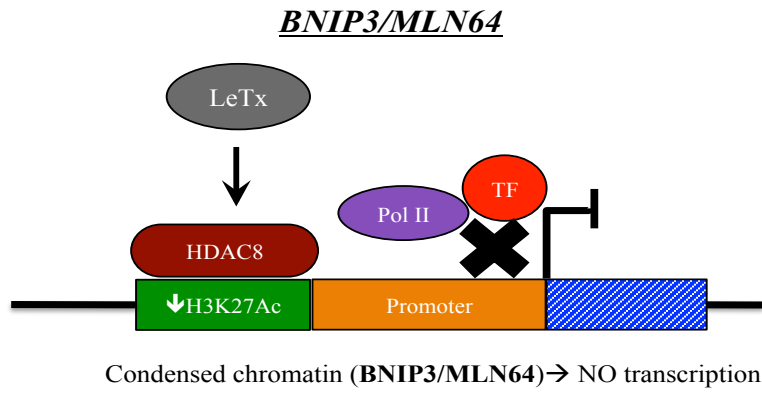
transcription factors including AP-1, NF- $\kappa$ B, and ATF2, are recruited to *BNIP3*, *MLN64*, and *IL-1 $\beta$*  H3K27Ac-associated regions in an HDAC8-inhibition dependent manner. Furthermore, a previous study revealed that extragenic enhancer regions are also capable of regulating gene expression [236]. Interestingly, the ENCODE database identified a highly enriched H3K27Ac area  $\sim 2.5$  kbps upstream of the *IL-1 $\beta$*  transcription start site. Therefore, similar experiments should be performed to examine whether this site encodes an enhancer element. To determine the functionality of such eRNAs in *BNIP3*, *MLN64*, and *IL-1 $\beta$* , eRNAs could be knocked down by siRNAs and expression levels of these genes could be measured. Collectively, these experiments will determine whether HDAC8-H3K27Ac histone modifications regulate *BNIP3*, *MLN64*, and *IL-1 $\beta$*  expression via enhancers.

## 4.5 Summary

In summary, this study addressed the role of HDAC8 mediated histone modifications in regulating the expression of pro-inflammatory cytokines, primarily *IL-1 $\beta$* , and the mitochondrial death genes during pyroptosis in macrophages. LeTx appears to induce HDAC8, which then deacetylates H3K27Ac “enhancer” gene regions of *BNIP3*, *MLN64*, and *IL-1 $\beta$* . While this promotes a gene-silenced state, HDAC8-inhibition restores expression of these genes (Fig. 4.2). As such, increased H3K27Ac levels mediated by HDAC8 inhibition may enable the recruitment of eRNA transcriptional components to these “enhancer” regions and compensate for LeTx-induced inactivation of MAPK signaling in macrophages.

**Figure 4.2 Working models for HDAC8-mediated silencing of *BNIP3*, *MLN64*, and *IL-1 $\beta$*  in response to LeTx.**

In response to LeTx, HDAC8 is up-regulated. HDAC8 associates with and subsequently deacetylates H3K27Ac-associated regions of *BNIP3*, *MLN64*, and *IL-1 $\beta$* , promoting a closed chromatin conformation and preventing the binding of Pol II and other transcription factors (TF) to mediate gene transcription. In contrast inhibiting HDAC8 restores H3K27Ac levels allowing the recruitment of transcriptional machinery and enhancer-promoter interactions, thus permitting the transcription of *BNIP3*, *MLN64*, and *IL-1 $\beta$* .



## 4.6 Significance

Overall, this study suggests that HDAC8 acts as key dual-function regulator of innate immune responses, such that it mediates susceptibility of macrophages to pyroptosis, as well as controlling macrophage-mediated immune signaling. NLR activation during infection appears to have double-edged effects, such that initially activation is protective. However, it can also lead to exacerbation of immune responses, resulting in septic shock. With regards to anthrax, mice that harbor NLRP1b, which upon activation initiates pyroptosis, are in fact much more susceptible to LeTx toxemia [20,103]. In addition, inactivation of MAPK signaling is another tactic used by LeTx as a means to evade detection by the host immune system and cause systemic infection [59]. Since LeTx-induced MEK inactivation is likely the primary virulence mechanism during anthrax infection in humans, antagonizing HDAC8 may act as a novel therapy for restoring host immune responses. While countless other bacteria produce virulence factors capable of inhibiting MAPK signaling and host immune responses [237-239], HDAC8 may also be involved in these infections, thus extending the potential of this therapeutic treatment beyond anthrax. In contrast, when pyroptosis is responsible for promoting overt inflammation, such as in autoinflammatory and autoimmune diseases [240-243], activating HDAC8 may be beneficial. Collectively, aside from anthrax, manipulating HDAC8 has therapeutic potential for treating a wide range of infectious and inflammatory diseases.

## CHAPTER 5

### 5 REFERENCES

- [1] Driks A. The *Bacillus anthracis* spore. Mol Aspects Med 2009 Dec;30(6):368-373.
- [2] Hanna P. Anthrax pathogenesis and host response. Bacterial Infection: Close Encounters at the Host Pathogen Interface: Springer; 1998. p. 13-35.
- [3] Guidi-Rontani C, Levy M, Ohayon H, Mock M. Fate of germinated *Bacillus anthracis* spores in primary murine macrophages. Mol Microbiol 2001;42(4):931-938.
- [4] Guidi-Rontani C, Weber-Levy M, Labruyère E, Mock M. Germination of *Bacillus anthracis* spores within alveolar macrophages. Mol Microbiol 1999;31(1):9-17.
- [5] Shadomy SV, Smith TL. Zoonosis update. Anthrax 2008;233:63-72.
- [6] Harris S. Japanese biological warfare experiments and other atrocities in Manchuria, 1932–1945, and the subsequent United States cover up: a preliminary assessment. Crime, Law and Social Change 1991;15(3):171-199.
- [7] Jernigan JA, Stephens DS, Ashford DA, Omenaca C, Topiel MS, Galbraith M, et al. Bioterrorism-related inhalational anthrax: the first 10 cases reported in the United States. Emerg Infect Dis 2001 Nov-Dec;7(6):933-944.
- [8] Grunow R, Verbeek L, Jacob D, Holzmann T, Birkenfeld G, Wiens D, et al. Injection anthrax—a new outbreak in heroin users. Deutsches Ärzteblatt International 2012;109(49):843.
- [9] Centers for Disease Control and Prevention (CDC). Types of Anthrax. 2013; Available at: <http://www.cdc.gov/anthrax/types/index.html>. Accessed 03/02, 2015.
- [10] Dixon TC, Meselson M, Guillemin J, Hanna PC. Anthrax. N Engl J Med 1999 Sep 9;341(11):815-826.

- [11] Beatty ME, Ashford DA, Griffin PM, Tauxe RV, Sobel J. Gastrointestinal anthrax: review of the literature. *Arch Intern Med* 2003;163(20):2527-2531.
- [12] Wright JG, Quinn CP, Shadomy SV, Messonnier N, Centers for Disease Control and Prevention (CDC). Use of anthrax vaccine in the United States: recommendations of the Advisory Committee on Immunization Practices (ACIP), 2009. : Department of Health and Human Services, Centers for Disease Control and Prevention; 2010.
- [13] Hendricks KA, Wright ME, Shadomy SV, Bradley JS, Morrow MG, Pavia AT, et al. Centers for disease control and prevention expert panel meetings on prevention and treatment of anthrax in adults. *Emerg Infect Dis* 2014 Feb;20(2):10.3201/eid2002.130687.
- [14] Mullard A. 2012 FDA drug approvals. *Nature Reviews Drug Discovery* 2013;12(2):87-90.
- [15] Albert H, Food U. US FDA approves raxibacumab for treating inhalational anthrax.
- [16] Okinaka R, Cloud K, Hampton O, Hoffmaster A, Hill K, Keim P, et al. Sequence and organization of pXO1, the large *Bacillus anthracis* plasmid harboring the anthrax toxin genes. *J Bacteriol* 1999;181(20):6509-6515.
- [17] Makino S, Uchida I, Terakado N, Sasakawa C, Yoshikawa M. Molecular characterization and protein analysis of the cap region, which is essential for encapsulation in *Bacillus anthracis*. *J Bacteriol* 1989 Feb;171(2):722-730.
- [18] Friedlander AM. Macrophages are sensitive to anthrax lethal toxin through an acid-dependent process. *J Biol Chem* 1986 Jun 5;261(16):7123-7126.
- [19] Hanna P. Anthrax pathogenesis and host response. *Bacterial Infection: Close Encounters at the Host Pathogen Interface*: Springer; 1998. p. 13-35.
- [20] Hanna PC, Acosta D, Collier RJ. On the role of macrophages in anthrax. *Proc Natl Acad Sci U S A* 1993 Nov 1;90(21):10198-10201.



- [21] Moayeri M, Leppla SH. Cellular and systemic effects of anthrax lethal toxin and edema toxin. *Mol Aspects Med* 2009 Dec;30(6):439-455.
- [22] Xu L, Frucht DM. *Bacillus anthracis*: a multi-faceted role for anthrax lethal toxin in thwarting host immune defenses. *Int J Biochem Cell Biol* 2007;39(1):20-24.
- [23] McAllister RD, Singh Y, du Bois WD, Potter M, Boehm T, Meeker ND, et al. Susceptibility to anthrax lethal toxin is controlled by three linked quantitative trait loci. *The American journal of pathology* 2003;163(5):1735-1741.
- [24] Welkos SL, Keener TJ, Gibbs PH. Differences in susceptibility of inbred mice to *Bacillus anthracis*. *Infect Immun* 1986 Mar;51(3):795-800.
- [25] Moayeri M, Haines D, Young HA, Leppla SH. *Bacillus anthracis* lethal toxin induces TNF-alpha-independent hypoxia-mediated toxicity in mice. *J Clin Invest* 2003 Sep;112(5):670-682.
- [26] Moayeri M, Martinez NW, Wiggins J, Young HA, Leppla SH. Mouse susceptibility to anthrax lethal toxin is influenced by genetic factors in addition to those controlling macrophage sensitivity. *Infect Immun* 2004 Aug;72(8):4439-4447.
- [27] Hanna P. Lethal toxin actions and their consequences. *J Appl Microbiol* 1999;87(2):285-287.
- [28] Bradley KA, Mogridge J, Mourez M, Collier RJ, Young JA. Identification of the cellular receptor for anthrax toxin. *Nature* 2001;414(6860):225-229.
- [29] Scobie HM, Rainey GJ, Bradley KA, Young JA. Human capillary morphogenesis protein 2 functions as an anthrax toxin receptor. *Proc Natl Acad Sci U S A* 2003 Apr 29;100(9):5170-5174.
- [30] Taft SC, Weiss AA. Toxicity of anthrax toxin is influenced by receptor expression. *Clin Vaccine Immunol* 2008 Sep;15(9):1330-1336.
- [31] Collier RJ, Young JA. Anthrax toxin. *Annu Rev Cell Dev Biol* 2003;19(1):45-70.

- [32] Bradley KA, Young JA. Anthrax toxin receptor proteins. *Biochem Pharmacol* 2003;65(3):309-314.
- [33] Abrami L, Liu S, Cosson P, Leppla SH, van der Goot, F Gisou. Anthrax toxin triggers endocytosis of its receptor via a lipid raft-mediated clathrin-dependent process. *J Cell Biol* 2003;160(3):321-328.
- [34] Klimpel KR, Arora N, Leppla SH. Anthrax toxin lethal factor contains a zinc metalloprotease consensus sequence which is required for lethal toxin activity. *Mol Microbiol* 1994;13(6):1093-1100.
- [35] Vitale G, Bernardi L, Napolitani G, Mock M, Montecucco C. Susceptibility of mitogen-activated protein kinase kinase family members to proteolysis by anthrax lethal factor. *Biochem J* 2000;352:739-745.
- [36] Vitale G, Pellizzari R, Recchi C, Napolitani G, Mock M, Montecucco C. Anthrax lethal factor cleaves the N-terminus of MAPKKs and induces tyrosine/threonine phosphorylation of MAPKs in cultured macrophages. *Biochem Biophys Res Commun* 1998;248(3):706-711.
- [37] Duesbery NS, Webb CP, Leppla SH, Gordon VM, Klimpel KR, Copeland TD, et al. Proteolytic inactivation of MAP-kinase-kinase by anthrax lethal factor. *Science* 1998 May 1;280(5364):734-737.
- [38] Ha SD, Ng D, Pelech SL, Kim SO. Critical role of the phosphatidylinositol 3-kinase/Akt/glycogen synthase kinase-3 signaling pathway in recovery from anthrax lethal toxin-induced cell cycle arrest and MEK cleavage in macrophages. *J Biol Chem* 2007 Dec 14;282(50):36230-36239.
- [39] Pannifer AD, Wong TY, Schwarzenbacher R, Renatus M, Petosa C, Bienkowska J, et al. Crystal structure of the anthrax lethal factor. *Nature* 2001;414(6860):229-233.
- [40] Morrison DK. MAP kinase pathways. *Cold Spring Harb Perspect Biol* 2012 Nov 1;4(11):10.1101/cshperspect.a011254.

- [41] Cuevas BD, Abell AN, Johnson GL. Role of mitogen-activated protein kinase kinases in signal integration. *Oncogene* 2007 May 14;26(22):3159-3171.
- [42] Kyriakis JM, Avruch J. Mammalian mitogen-activated protein kinase signal transduction pathways activated by stress and inflammation. *Physiol Rev* 2001 Apr;81(2):807-869.
- [43] Roskoski R. ERK1/2 MAP kinases: structure, function, and regulation. *Pharmacological research* 2012;66(2):105-143.
- [44] Dhanasekaran DN, Reddy EP. JNK signaling in apoptosis. *Oncogene* 2008;27(48):6245-6251.
- [45] Rincón M, Davis RJ. Regulation of the immune response by stress-activated protein kinases. *Immunol Rev* 2009;228(1):212-224.
- [46] Huang G, Shi LZ, Chi H. Regulation of JNK and p38 MAPK in the immune system: signal integration, propagation and termination. *Cytokine* 2009;48(3):161-169.
- [47] Johnson GL, Nakamura K. The c-jun kinase/stress-activated pathway: regulation, function and role in human disease. *Biochimica et Biophysica Acta (BBA)-Molecular Cell Research* 2007;1773(8):1341-1348.
- [48] Zarubin T, Jiahuai H. Activation and signaling of the p38 MAP kinase pathway. *Cell Res* 2005;15(1):11-18.
- [49] Cuadrado A, Nebreda A. Mechanisms and functions of p38 MAPK signalling. *Biochem J* 2010;429:403-417.
- [50] Schieven GL. The biology of p38 kinase: a central role in inflammation. *Current topics in medicinal chemistry* 2005;5(10):921-928.
- [51] Guan Z, Buckman SY, Pentland AP, Templeton DJ, Morrison AR. Induction of cyclooxygenase-2 by the activated MEKK1→SEK1/MKK4→p38 mitogen-activated protein kinase pathway. *J Biol Chem* 1998;273(21):12901-12908.

- [52] O'Neill LA, Golenbock D, Bowie AG. The history of Toll-like receptors [mdash] redefining innate immunity. *Nature Reviews Immunology* 2013;13(6):453-460.
- [53] Poltorak A, He X, Smirnova I, Liu MY, Van Huffel C, Du X, et al. Defective LPS signaling in C3H/HeJ and C57BL/10ScCr mice: mutations in Tlr4 gene. *Science* 1998 Dec 11;282(5396):2085-2088.
- [54] Medzhitov R, Horng T. Transcriptional control of the inflammatory response. *Nature Reviews Immunology* 2009;9(10):692-703.
- [55] Murray PJ, Smale ST. Restraint of inflammatory signaling by interdependent strata of negative regulatory pathways. *Nat Immunol* 2012;13(10):916-924.
- [56] Barton GM, Medzhitov R. Toll-like receptor signaling pathways. *Science* 2003 Jun 6;300(5625):1524-1525.
- [57] Baldari CT, Tonello F, Paccani SR, Montecucco C. Anthrax toxins: a paradigm of bacterial immune suppression. *Trends Immunol* 2006;27(9):434-440.
- [58] Coggeshall KM, Lupu F, Ballard J, Metcalf JP, James JA, Farris D, et al. The sepsis model: an emerging hypothesis for the lethality of inhalation anthrax. *J Cell Mol Med* 2013;17(7):914-920.
- [59] Fukao T. Immune system paralysis by anthrax lethal toxin: the roles of innate and adaptive immunity. *The Lancet infectious diseases* 2004;4(3):166-170.
- [60] Rao KM. MAP kinase activation in macrophages. *J Leukoc Biol* 2001 Jan;69(1):3-10.
- [61] Chang L, Karin M. Mammalian MAP kinase signalling cascades. *Nature* 2001;410(6824):37-40.
- [62] Karin M, Gallagher E. From JNK to pay dirt: jun kinases, their biochemistry, physiology and clinical importance. *IUBMB Life* 2005;57(4-5):283-295.

- [63] Erwin JL, DaSilva LM, Bavari S, Little SF, Friedlander AM, Chanh TC. Macrophage-derived cell lines do not express proinflammatory cytokines after exposure to *Bacillus anthracis* lethal toxin. *Infect Immun* 2001 Feb;69(2):1175-1177.
- [64] Cui X, Li Y, Li X, Haley M, Moayeri M, Fitz Y, et al. Sublethal doses of *Bacillus anthracis* lethal toxin inhibit inflammation with lipopolysaccharide and *Escherichia coli* challenge but have opposite effects on survival. *J Infect Dis* 2006 Mar 15;193(6):829-840.
- [65] Pellizzari R, Guidi-Rontani C, Vitale G, Mock M, Montecucco C. Anthrax lethal factor cleaves MKK3 in macrophages and inhibits the LPS/IFN $\gamma$ -induced release of NO and TNF $\alpha$ . *FEBS Lett* 1999;462(1):199-204.
- [66] Kang TJ, Basu S, Zhang L, Thomas KE, Vogel SN, Baillie L, et al. *Bacillus anthracis* spores and lethal toxin induce IL-1 $\beta$  via functionally distinct signaling pathways. *Eur J Immunol* 2008 Jun;38(6):1574-1584.
- [67] Agrawal A, Lingappa J, Leppla SH, Agrawal S, Jabbar A, Quinn C, et al. Impairment of dendritic cells and adaptive immunity by anthrax lethal toxin. *Nature* 2003;424(6946):329-334.
- [68] During RL, Li W, Hao B, Koenig JM, Stephens DS, Quinn CP, et al. Anthrax lethal toxin paralyzes neutrophil actin-based motility. *J Infect Dis* 2005 Sep 1;192(5):837-845.
- [69] Fang H, Xu L, Chen TY, Cyr JM, Frucht DM. Anthrax lethal toxin has direct and potent inhibitory effects on B cell proliferation and immunoglobulin production. *J Immunol* 2006 May 15;176(10):6155-6161.
- [70] Bergsbaken T, Fink SL, Cookson BT. Pyroptosis: host cell death and inflammation. *Nature Reviews Microbiology* 2009;7(2):99-109.
- [71] Fink SL, Cookson BT. Caspase-1-dependent pore formation during pyroptosis leads to osmotic lysis of infected host macrophages. *Cell Microbiol* 2006;8(11):1812-1825.

- [72] Mariathasan S, Weiss DS, Dixit VM, Monack DM. Innate immunity against *Francisella tularensis* is dependent on the ASC/caspase-1 axis. *J Exp Med* 2005 Oct 17;202(8):1043-1049.
- [73] Ceballos-Olvera I, Sahoo M, Miller MA, del Barrio L, Re F. Inflammasome-dependent pyroptosis and IL-18 protect against *Burkholderia pseudomallei* lung infection while IL-1 $\beta$  is deleterious. *PLoS pathogens* 2011;7(12):e1002452.
- [74] Aachoui Y, Leaf IA, Hagar JA, Fontana MF, Campos CG, Zak DE, et al. Caspase-11 protects against bacteria that escape the vacuole. *Science* 2013 Feb 22;339(6122):975-978.
- [75] Miao EA, Leaf IA, Treuting PM, Mao DP, Dors M, Sarkar A, et al. Caspase-1-induced pyroptosis is an innate immune effector mechanism against intracellular bacteria. *Nat Immunol* 2010;11(12):1136-1142.
- [76] Cohen TS, Prince AS. Activation of inflammasome signaling mediates pathology of acute *P. aeruginosa* pneumonia. *J Clin Invest* 2013 Apr;123(4):1630-1637.
- [77] The role of the inflammasome in cellular responses to toxins and bacterial effectors. *Seminars in immunopathology*: Springer; 2007.
- [78] Masters SL, Gerlic M, Metcalf D, Preston S, Pellegrini M, O'Donnell JA, et al. NLRP1 inflammasome activation induces pyroptosis of hematopoietic progenitor cells. *Immunity* 2012;37(6):1009-1023.
- [79] Soong G, Chun J, Parker D, Prince A. *Staphylococcus aureus* activation of caspase 1/calpain signaling mediates invasion through human keratinocytes. *J Infect Dis* 2012 May 15;205(10):1571-1579.
- [80] Takeuchi O, Akira S. Pattern recognition receptors and inflammation. *Cell* 2010;140(6):805-820.
- [81] Toll-like receptors (TLRs) and Nod-like receptors (NLRs) in inflammatory disorders. *Seminars in immunology*: Elsevier; 2009.

- [82] Martinon F, Tschopp J. NLRs join TLRs as innate sensors of pathogens. *Trends Immunol* 2005;26(8):447-454.
- [83] Ting JP, Willingham SB, Bergstralh DT. NLRs at the intersection of cell death and immunity. *Nature Reviews Immunology* 2008;8(5):372-379.
- [84] Gross O, Thomas CJ, Guarda G, Tschopp J. The inflammasome: an integrated view. *Immunol Rev* 2011;243(1):136-151.
- [85] Arlehamn CS, Petrilli V, Gross O, Tschopp J, Evans TJ. The role of potassium in inflammasome activation by bacteria. *J Biol Chem* 2010 Apr 2;285(14):10508-10518.
- [86] Franchi L, Kanneganti TD, Dubyak GR, Nunez G. Differential requirement of P2X7 receptor and intracellular K<sup>+</sup> for caspase-1 activation induced by intracellular and extracellular bacteria. *J Biol Chem* 2007 Jun 29;282(26):18810-18818.
- [87] Monie TP. NLR activation takes a direct route. *Trends Biochem Sci* 2013;38(3):131-139.
- [88] Fernandes-Alnemri T, Wu J, Yu J, Datta P, Miller B, Jankowski W, et al. The pyroptosome: a supramolecular assembly of ASC dimers mediating inflammatory cell death via caspase-1 activation. *Cell Death & Differentiation* 2007;14(9):1590-1604.
- [89] Moayeri M, Sastalla I, Leppla SH. Anthrax and the inflammasome. *Microbes Infect* 2012 May;14(5):392-400.
- [90] Lamkanfi M, Dixit VM. Inflammasomes and their roles in health and disease. *Annu Rev Cell Dev Biol* 2012;28:137-161.
- [91] Franchi L, Amer A, Body-Malapel M, Kanneganti T, Özören N, Jagirdar R, et al. Cytosolic flagellin requires Ipaf for activation of caspase-1 and interleukin 1 $\beta$  in *Salmonella*-infected macrophages. *Nat Immunol* 2006;7(6):576-582.

- [92] Miao EA, Alpuche-Aranda CM, Dors M, Clark AE, Bader MW, Miller SI, et al. Cytoplasmic flagellin activates caspase-1 and secretion of interleukin 1 $\beta$  via Ipaf. *Nat Immunol* 2006;7(6):569-575.
- [93] Amer A, Franchi L, Kanneganti TD, Body-Malapel M, Ozoren N, Brady G, et al. Regulation of *Legionella* phagosome maturation and infection through flagellin and host Ipaf. *J Biol Chem* 2006 Nov 17;281(46):35217-35223.
- [94] Miao EA, Mao DP, Yudkovsky N, Bonneau R, Lorang CG, Warren SE, et al. Innate immune detection of the type III secretion apparatus through the NLRC4 inflammasome. *Proceedings of the National Academy of Sciences* 2010;107(7):3076-3080.
- [95] Sun YH, Rolan HG, Tsolis RM. Injection of flagellin into the host cell cytosol by *Salmonella enterica* serotype Typhimurium. *J Biol Chem* 2007 Nov 23;282(47):33897-33901.
- [96] Broz P, Newton K, Lamkanfi M, Mariathasan S, Dixit VM, Monack DM. Redundant roles for inflammasome receptors NLRP3 and NLRC4 in host defense against *Salmonella*. *J Exp Med* 2010;207(8):1745-1755.
- [97] Raupach B, Peuschel S, Monack DM, Zychlinsky A. Caspase-1-mediated activation of interleukin-1 $\beta$  (IL-1 $\beta$ ) and IL-18 contributes to innate immune defenses against *Salmonella enterica* serovar Typhimurium infection. *Infect Immun* 2006;74(8):4922-4926.
- [98] Lara-Tejero M, Sutterwala FS, Ogura Y, Grant EP, Bertin J, Coyle AJ, et al. Role of the caspase-1 inflammasome in *Salmonella typhimurium* pathogenesis. *J Exp Med* 2006;203(6):1407-1412.
- [99] Mariathasan S, Weiss DS, Newton K, McBride J, O'Rourke K, Roose-Girma M, et al. Cryopyrin activates the inflammasome in response to toxins and ATP. *Nature* 2006;440(7081):228-232.
- [100] Boost KA, Hoegl S, Hofstetter C, Flondor M, Stegwerth K, Platadis I, et al. Targeting caspase-1 by inhalation-therapy: effects of Ac-YVAD-CHO on IL-1 $\beta$ , IL-18



and downstream proinflammatory parameters as detected in rat endotoxaemia. *Intensive Care Med* 2007;33(5):863-871.

[101] Mao K, Chen S, Chen M, Ma Y, Wang Y, Huang B, et al. Nitric oxide suppresses NLRP3 inflammasome activation and protects against LPS-induced septic shock. *Cell Res* 2013;23(2):201-212.

[102] Matsuda A, Jacob A, Wu R, Aziz M, Yang W, Matsutani T, et al. Novel therapeutic targets for sepsis: regulation of exaggerated inflammatory responses. *Journal of Nippon Medical School* 2012;79(1):4-18.

[103] Boyden ED, Dietrich WF. Nalp1b controls mouse macrophage susceptibility to anthrax lethal toxin. *Nat Genet* 2006 Feb;38(2):240-244.

[104] Terra JK, Cote CK, France B, Jenkins AL, Bozue JA, Welkos SL, et al. Cutting edge: resistance to *Bacillus anthracis* infection mediated by a lethal toxin sensitive allele of Nalp1b/Nlrp1b. *J Immunol* 2010 Jan 1;184(1):17-20.

[105] Boyden ED, Dietrich WF. Nalp1b controls mouse macrophage susceptibility to anthrax lethal toxin. *Nat Genet* 2006;38(2):240-244.

[106] Moayeri M, Crown D, Newman ZL, Okugawa S, Eckhaus M, Cataisson C, et al. Inflammasome sensor Nlrp1b-dependent resistance to anthrax is mediated by caspase-1, IL-1 signaling and neutrophil recruitment. *PLoS pathogens* 2010;6(12):e1001222.

[107] Frew BC, Joag VR, Mogridge J. Proteolytic processing of Nlrp1b is required for inflammasome activity. *PLoS pathogens* 2012;8(4):e1002659.

[108] Bhatnagar R, Singh Y, Leppla SH, Friedlander AM. Calcium is required for the expression of anthrax lethal toxin activity in the macrophage-like cell line J774A.1. *Infect Immun* 1989 Jul;57(7):2107-2114.

[109] Alileche A, Squires RC, Muehlbauer SM, Lisanti MP, Brojatsch J. Mitochondrial impairment mediates cytolysis in anthrax lethal toxin-treated murine macrophages. *Cell Cycle* 2006;5(1):100-106.

[110] Ha SD, Ng D, Lamothe J, Valvano MA, Han J, Kim SO. Mitochondrial proteins Bnip3 and Bnip3L are involved in anthrax lethal toxin-induced macrophage cell death. *J Biol Chem* 2007 Sep 7;282(36):26275-26283.

[111] Hanna PC, Kruskal BA, Ezekowitz RA, Bloom BR, Collier RJ. Role of macrophage oxidative burst in the action of anthrax lethal toxin. *Mol Med* 1994 Nov;1(1):7-18.

[112] Ha SD, Park S, Han CY, Nguyen ML, Kim SO. Cellular adaptation to anthrax lethal toxin-induced mitochondrial cholesterol enrichment, hyperpolarization, and reactive oxygen species generation through downregulating MLN64 in macrophages. *Mol Cell Biol* 2012 Dec;32(23):4846-4860.

[113] Fink SL, Bergsbaken T, Cookson BT. Anthrax lethal toxin and Salmonella elicit the common cell death pathway of caspase-1-dependent pyroptosis via distinct mechanisms. *Proc Natl Acad Sci U S A* 2008 Mar 18;105(11):4312-4317.

[114] Muehlbauer SM, Evering TH, Bonuccelli G, Squires RC, Ashton AW, Porcelli SA, et al. Anthrax lethal toxin kills macrophages in a strain-specific manner by apoptosis or caspase-1-mediated necrosis. *Cell cycle* 2007;6(6):758-766.

[115] Chapelsky S, Batty S, Frost M, Mogridge J. Inhibition of anthrax lethal toxin-induced cytolysis of RAW264.7 cells by celastrol. *PLoS One* 2008;3(1):e1421.

[116] Wickliffe KE, Leppla SH, Moayeri M. Anthrax lethal toxin-induced inflammasome formation and caspase-1 activation are late events dependent on ion fluxes and the proteasome. *Cell Microbiol* 2008;10(2):332-343.

[117] Chinnadurai G, Vijayalingam S, Gibson SB. BNIP3 subfamily BH3-only proteins: mitochondrial stress sensors in normal and pathological functions. *Oncogene* 2008;27:S114-S127.

- [118] Boyd JM, Malstrom S, Subramanian T, Venkatesh L, Schaeper U, Elangovan B, et al. Adenovirus E1B 19 kDa and Bcl-2 proteins interact with a common set of cellular proteins. *Cell* 1994;79(2):341-351.
- [119] Chittenden T. BH3 domains: intracellular death-ligands critical for initiating apoptosis. *Cancer Cell* 2002;2(3):165-166.
- [120] Yasuda M, Theodorakis P, Subramanian T, Chinnadurai G. Adenovirus E1B-19K/BCL-2 interacting protein BNIP3 contains a BH3 domain and a mitochondrial targeting sequence. *J Biol Chem* 1998;273(20):12415-12421.
- [121] Ray R, Chen G, Vande Velde C, Cizeau J, Park JH, Reed JC, et al. BNIP3 heterodimerizes with Bcl-2/Bcl-X(L) and induces cell death independent of a Bcl-2 homology 3 (BH3) domain at both mitochondrial and non-mitochondrial sites. *J Biol Chem* 2000 Jan 14;275(2):1439-1448.
- [122] Kim J, Cho J, Ha J, Park J. The carboxy terminal C-tail of BNIP3 is crucial in induction of mitochondrial permeability transition in isolated mitochondria. *Arch Biochem Biophys* 2002;398(2):147-152.
- [123] Vande Velde C, Cizeau J, Dubik D, Alimonti J, Brown T, Israels S, et al. BNIP3 and genetic control of necrosis-like cell death through the mitochondrial permeability transition pore. *Mol Cell Biol* 2000 Aug;20(15):5454-5468.
- [124] Kubli DA, Quinsay MN, Huang C, Lee Y, Gustafsson AB. BNIP3 functions as a mitochondrial sensor of oxidative stress during myocardial ischemia and reperfusion. *Am J Physiol Heart Circ Physiol* 2008 Nov;295(5):H2025-31.
- [125] Gustafsson AB. BNIP3 as a dual regulator of mitochondrial turnover and cell death in the myocardium. *Pediatr Cardiol* 2011;32(3):267-274.
- [126] Watari H, Arakane F, Moog-Lutz C, Kallen CB, Tomasetto C, Gerton GL, et al. MLN64 contains a domain with homology to the steroidogenic acute regulatory protein (StAR) that stimulates steroidogenesis. *Proc Natl Acad Sci U S A* 1997 Aug 5;94(16):8462-8467.

- [127] Soccio RE, Breslow JL. StAR-related lipid transfer (START) proteins: mediators of intracellular lipid metabolism. *J Biol Chem* 2003 Jun 20;278(25):22183-22186.
- [128] Rigotti A, Cohen DE, Zanolungo S. STARTing to understand MLN64 function in cholesterol transport. *J Lipid Res* 2010 Aug;51(8):2015-2017.
- [129] Charman M, Kennedy BE, Osborne N, Karten B. MLN64 mediates egress of cholesterol from endosomes to mitochondria in the absence of functional Niemann-Pick Type C1 protein. *J Lipid Res* 2010 May;51(5):1023-1034.
- [130] Zhang M, Liu P, Dwyer NK, Christenson LK, Fujimoto T, Martinez F, et al. MLN64 mediates mobilization of lysosomal cholesterol to steroidogenic mitochondria. *J Biol Chem* 2002 Sep 6;277(36):33300-33310.
- [131] Alpy F, Tomasetto C. MLN64 and MENTHO, two mediators of endosomal cholesterol transport. *Biochem Soc Trans* 2006;34(3):343-345.
- [132] Lavigne P, Najmanivich R, LeHoux J. Mammalian StAR-related lipid transfer (START) domains with specificity for cholesterol: structural conservation and mechanism of reversible binding. *Cholesterol Binding and Cholesterol Transport Proteins*: Springer; 2010. p. 425-437.
- [133] Rone MB, Fan J, Papadopoulos V. Cholesterol transport in steroid biosynthesis: role of protein–protein interactions and implications in disease states. *Biochimica et Biophysica Acta (BBA)-Molecular and Cell Biology of Lipids* 2009;1791(7):646-658.
- [134] Tichauer JE, Morales MG, Amigo L, Galdames L, Klein A, Quinones V, et al. Overexpression of the cholesterol-binding protein MLN64 induces liver damage in the mouse. *World J Gastroenterol* 2007 Jun 14;13(22):3071-3079.
- [135] Biswas KK, Sarker KP, Abeyama K, Kawahara K, Iino S, Otsubo Y, et al. Membrane cholesterol but not putative receptors mediates anandamide-induced hepatocyte apoptosis. *Hepatology* 2003;38(5):1167-1177.

- [136] Marí M, Caballero F, Colell A, Morales A, Caballeria J, Fernandez A, et al. Mitochondrial free cholesterol loading sensitizes to TNF-and Fas-mediated steatohepatitis. *Cell metabolism* 2006;4(3):185-198.
- [137] Lepe-Zuniga JL, Klostergaard J. Tolerance to endotoxin in vitro: independent regulation of interleukin-1, tumor necrosis factor and interferon alpha production during in vitro differentiation of human monocytes. *Lymphokine Res* 1990 Fall;9(3):309-319.
- [138] Zuckerman SH, Evans GF, Butler LD. Endotoxin tolerance: independent regulation of interleukin-1 and tumor necrosis factor expression. *Infect Immun* 1991 Aug;59(8):2774-2780.
- [139] Salles II, Tucker AE, Voth DE, Ballard JD. Toxin-induced resistance in *Bacillus anthracis* lethal toxin-treated macrophages. *Proceedings of the National Academy of Sciences* 2003;100(21):12426-12431.
- [140] Waddington CH. An introduction to modern genetics. *An Introduction to Modern Genetics*. 1939.
- [141] Bird A. DNA methylation patterns and epigenetic memory. *Genes Dev* 2002;16(1):6-21.
- [142] Portela A, Esteller M. Epigenetic modifications and human disease. *Nat Biotechnol* 2010;28(10):1057-1068.
- [143] Peterson CL, Laniel M. Histones and histone modifications. *Current Biology* 2004;14(14):R546-R551.
- [144] Luger K, Mäder AW, Richmond RK, Sargent DF, Richmond TJ. Crystal structure of the nucleosome core particle at 2.8 Å resolution. *Nature* 1997;389(6648):251-260.
- [145] Vaquero A, Loyola A, Reinberg D. The constantly changing face of chromatin. *Science's SAGE KE* 2003;2003(14):4.

- [146] Kouzarides T. Chromatin modifications and their function. *Cell* 2007;128(4):693-705.
- [147] Struhl K. Histone acetylation and transcriptional regulatory mechanisms. *Genes Dev* 1998;12(5):599-606.
- [148] Li B, Carey M, Workman JL. The role of chromatin during transcription. *Cell* 2007;128(4):707-719.
- [149] Martin C, Zhang Y. The diverse functions of histone lysine methylation. *Nat Rev Mol Cell Biol* 2005 Nov;6(11):838-849.
- [150] Grunstein M. Histone acetylation in chromatin structure and transcription. *Nature* 1997;389(6649):349-352.
- [151] Brownell JE, Allis CD. Special HATs for special occasions: linking histone acetylation to chromatin assembly and gene activation. *Curr Opin Genet Dev* 1996;6(2):176-184.
- [152] Wolffe AP, Pruss D. Targeting chromatin disruption: transcription regulators that acetylate histones. *Cell* 1996;84(6):817-819.
- [153] Yang X. Lysine acetylation and the bromodomain: a new partnership for signaling. *Bioessays* 2004;26(10):1076-1087.
- [154] Zeng L, Zhou MM. Bromodomain: an acetyl-lysine binding domain. *FEBS Lett* 2002 Feb 20;513(1):124-128.
- [155] Roth SY, Denu JM, Allis CD. Histone acetyltransferases. *Annu Rev Biochem* 2001;70(1):81-120.
- [156] Kuo M, Allis CD. Roles of histone acetyltransferases and deacetylases in gene regulation. *Bioessays* 1998;20(8):615-626.
- [157] Verdin E, Ott M. 50 years of protein acetylation: from gene regulation to epigenetics, metabolism and beyond. *Nature Reviews Molecular Cell Biology* 2014.

- [158] Bjerling P, Silverstein RA, Thon G, Caudy A, Grewal S, Ekwall K. Functional divergence between histone deacetylases in fission yeast by distinct cellular localization and in vivo specificity. *Mol Cell Biol* 2002;22(7):2170-2181.
- [159] Fischle W, Dequiedt F, Hendzel MJ, Guenther MG, Lazar MA, Voelter W, et al. Enzymatic activity associated with class II HDACs is dependent on a multiprotein complex containing HDAC3 and SMRT/N-CoR. *Mol Cell* 2002;9(1):45-57.
- [160] Perissi V, Jepsen K, Glass CK, Rosenfeld MG. Deconstructing repression: evolving models of co-repressor action. *Nature Reviews Genetics* 2010;11(2):109-123.
- [161] Jones PL, Veenstra GCJ, Wade PA, Vermaak D, Kass SU, Landsberger N, et al. Methylated DNA and MeCP2 recruit histone deacetylase to repress transcription. *Nat Genet* 1998;19(2):187-191.
- [162] Wade PA, Geggion A, Jones PL, Ballestar E, Aubry F, Wolffe AP. Mi-2 complex couples DNA methylation to chromatin remodelling and histone deacetylation. *Nat Genet* 1999;23(1):62-66.
- [163] Waltregny D, Glenisson W, Tran SL, North BJ, Verdin E, Colige A, et al. Histone deacetylase HDAC8 associates with smooth muscle alpha-actin and is essential for smooth muscle cell contractility. *FASEB J* 2005 Jun;19(8):966-968.
- [164] Wolfson NA, Pitcairn CA, Fierke CA. HDAC8 substrates: Histones and beyond. *Biopolymers* 2013 Feb;99(2):112-126.
- [165] Murko C, Lager S, Steiner M, Seiser C, Schoefer C, Pusch O. Expression of class I histone deacetylases during chick and mouse development. *Int J Dev Biol* 2010;54(10):1527-1537.
- [166] Buggy JJ, Sideris ML, Mak P, Lorimer DD, McIntosh B, Clark JM. Cloning and characterization of a novel human histone deacetylase, HDAC8. *Biochem J* 2000 Aug 15;350 Pt 1:199-205.

- [167] Hu E, Chen Z, Fredrickson T, Zhu Y, Kirkpatrick R, Zhang GF, et al. Cloning and characterization of a novel human class I histone deacetylase that functions as a transcription repressor. *J Biol Chem* 2000 May 19;275(20):15254-15264.
- [168] Gregoret IV, Lee YM, Goodson HV. Molecular evolution of the histone deacetylase family: functional implications of phylogenetic analysis. *J Mol Biol* 2004 Apr 16;338(1):17-31.
- [169] Lee H, Sengupta N, Villagra A, Rezai-Zadeh N, Seto E. Histone deacetylase 8 safeguards the human ever-shorter telomeres 1B (hEST1B) protein from ubiquitin-mediated degradation. *Mol Cell Biol* 2006 Jul;26(14):5259-5269.
- [170] Karolczak-Bayatti M, Sweeney M, Cheng J, Edey L, Robson SC, Ulrich SM, et al. Acetylation of heat shock protein 20 (Hsp20) regulates human myometrial activity. *J Biol Chem* 2011 Sep 30;286(39):34346-34355.
- [171] Canettieri G, Morante I, Guzmán E, Asahara H, Herzig S, Anderson SD, et al. Attenuation of a phosphorylation-dependent activator by an HDAC–PP1 complex. *Nature Structural & Molecular Biology* 2003;10(3):175-181.
- [172] Wu J, Du C, Lv Z, Ding C, Cheng J, Xie H, et al. The up-regulation of histone deacetylase 8 promotes proliferation and inhibits apoptosis in hepatocellular carcinoma. *Dig Dis Sci* 2013;58(12):3545-3553.
- [173] Qi J, Cai Q, Singh S, Li L, Liu H, McDonald T, et al. Inhibition of HDAC8 Reactivates p53 and Abrogates Leukemia Stem Cell Activity in CBF $\beta$ -SMMHC Associated Acute Myeloid Leukemia. *Blood* 2014;124(21):363-363.
- [174] Bierre H, Hamon M, Cossart P. Epigenetics and bacterial infections. *Cold Spring Harb Perspect Med* 2012 Dec 1;2(12):a010272.
- [175] Raymond B, Batsche E, Boutillon F, Wu Y, Leduc D, Balloy V, et al. Anthrax lethal toxin impairs IL-8 expression in epithelial cells through inhibition of histone H3 modification. *PLoS pathogens* 2009;5(4):e1000359.



- [176] Das ND, Jung KH, Chai YG. The role of NF- $\kappa$ B and H3K27me3 demethylase, Jmjd3, on the anthrax lethal toxin tolerance of RAW 264.7 cells. PloS one 2010;5(3):e9913.
- [177] Ha SD, Han CY, Reid C, Kim SO. HDAC8-mediated epigenetic reprogramming plays a key role in resistance to anthrax lethal toxin-induced pyroptosis in macrophages. J Immunol 2014 Aug 1;193(3):1333-1343.
- [178] DeKoter RP, Geadah M, Khoosal S, Xu LS, Thillainadesan G, Torchia J, et al. Regulation of follicular B cell differentiation by the related E26 transformation-specific transcription factors PU.1, Spi-B, and Spi-C. J Immunol 2010 Dec 15;185(12):7374-7384.
- [179] Deepe GS, Jr, Buesing WR. Deciphering the pathways of death of *Histoplasma capsulatum*-infected macrophages: implications for the immunopathogenesis of early infection. J Immunol 2012 Jan 1;188(1):334-344.
- [180] Grunstein M. Histone acetylation in chromatin structure and transcription. Nature 1997;389(6649):349-352.
- [181] Liu H, Galka M, Mori E, Liu X, Lin Y, Wei R, et al. A method for systematic mapping of protein lysine methylation identifies functions for HP1 $\beta$  in DNA damage response. Mol Cell 2013;50(5):723-735.
- [182] Tie F, Banerjee R, Stratton CA, Prasad-Sinha J, Stepanik V, Zlobin A, et al. CBP-mediated acetylation of histone H3 lysine 27 antagonizes Drosophila Polycomb silencing. Development 2009 Sep;136(18):3131-3141.
- [183] Lan F, Shi Y. Epigenetic regulation: methylation of histone and non-histone proteins. Science in China Series C: Life Sciences 2009;52(4):311-322.
- [184] De Santa F, Totaro MG, Prosperini E, Notarbartolo S, Testa G, Natoli G. The histone H3 lysine-27 demethylase Jmjd3 links inflammation to inhibition of polycomb-mediated gene silencing. Cell 2007;130(6):1083-1094.

- [185] Ishii M, Wen H, Corsa CA, Liu T, Coelho AL, Allen RM, et al. Epigenetic regulation of the alternatively activated macrophage phenotype. *Blood* 2009 Oct 8;114(15):3244-3254.
- [186] Satoh T, Takeuchi O, Vandenbon A, Yasuda K, Tanaka Y, Kumagai Y, et al. The Jmjd3-Irf4 axis regulates M2 macrophage polarization and host responses against helminth infection. *Nat Immunol* 2010;11(10):936-944.
- [187] Yasui T, Hirose J, Tsutsumi S, Nakamura K, Aburatani H, Tanaka S. Epigenetic regulation of osteoclast differentiation: possible involvement of Jmjd3 in the histone demethylation of Nfatc1. *Journal of Bone and Mineral Research* 2011;26(11):2665-2671.
- [188] Takahashi H, McCaffery JM, Irizarry RA, Boeke JD. Nucleocytosolic acetyl-coenzyme a synthetase is required for histone acetylation and global transcription. *Mol Cell* 2006;23(2):207-217.
- [189] Foster SL, Hargreaves DC, Medzhitov R. Gene-specific control of inflammation by TLR-induced chromatin modifications. *Nature* 2007;447(7147):972-978.
- [190] Chen X, El Gazzar M, Yoza BK, McCall CE. The NF-kappaB factor RelB and histone H3 lysine methyltransferase G9a directly interact to generate epigenetic silencing in endotoxin tolerance. *J Biol Chem* 2009 Oct 9;284(41):27857-27865.
- [191] Alibek K. Anthrax Lethal Toxin Inhibits the Production of Proinflammatory Cytokines. *Journal of Toxins* 2013;2013.
- [192] Pellizzari R, Guidi-Rontani C, Vitale G, Mock M, Montecucco C. Anthrax lethal factor cleaves MKK3 in macrophages and inhibits the LPS/IFN $\gamma$ -induced release of NO and TNF $\alpha$ . *FEBS Lett* 1999;462(1):199-204.
- [193] Creighton MP, Cheng AW, Welstead GG, Kooistra T, Carey BW, Steine EJ, et al. Histone H3K27ac separates active from poised enhancers and predicts developmental state. *Proc Natl Acad Sci U S A* 2010 Dec 14;107(50):21931-21936.

- [194] Balasubramanian S, Ramos J, Luo W, Sirisawad M, Verner E, Buggy J. A novel histone deacetylase 8 (HDAC8)-specific inhibitor PCI-34051 induces apoptosis in T-cell lymphomas. *Leukemia* 2008;22(5):1026-1034.
- [195] Zhao B, Ricciardi RP. E1A is the component of the MHC class I enhancer complex that mediates HDAC chromatin repression in adenovirus-12 tumorigenic cells. *Virology* 2006;352(2):338-344.
- [196] Lee H, Rezai-Zadeh N, Seto E. Negative regulation of histone deacetylase 8 activity by cyclic AMP-dependent protein kinase A. *Mol Cell Biol* 2004 Jan;24(2):765-773.
- [197] Witze ES, Old WM, Resing KA, Ahn NG. Mapping protein post-translational modifications with mass spectrometry. *Nature methods* 2007;4(10):798-806.
- [198] Garcia BA, Shabanowitz J, Hunt DF. Characterization of histones and their post-translational modifications by mass spectrometry. *Curr Opin Chem Biol* 2007;11(1):66-73.
- [199] Zhang K, Yau PM, Chandrasekhar B, New R, Kondrat R, Imai BS, et al. Differentiation between peptides containing acetylated or tri-methylated lysines by mass spectrometry: An application for determining lysine 9 acetylation and methylation of histone H3. *Proteomics* 2004;4(1):1-10.
- [200] Shin JH, Li RW, Gao Y, VI RB, Li C. Genome-wide ChIP-seq mapping and analysis reveal butyrate-induced acetylation of H3K9 and H3K27 correlated with transcription activity in bovine cells. *Functional & integrative genomics* 2012;12(1):119-130.
- [201] Wang Z, Zang C, Rosenfeld JA, Schones DE, Barski A, Cuddapah S, et al. Combinatorial patterns of histone acetylations and methylations in the human genome. *Nat Genet* 2008;40(7):897-903.

- [202] Kang Y, Nian H, Rajendran P, Kim E, Dashwood W, Pinto J, et al. HDAC8 and STAT3 repress BMF gene activity in colon cancer cells. *Cell death & disease* 2014;5(10):e1476.
- [203] Komarnitsky P, Cho EJ, Buratowski S. Different phosphorylated forms of RNA polymerase II and associated mRNA processing factors during transcription. *Genes Dev* 2000 Oct 1;14(19):2452-2460.
- [204] Turk B. Manipulation of host signalling pathways by anthrax toxins. *Biochem J* 2007;402:405-417.
- [205] Fukao T. Immune system paralysis by anthrax lethal toxin: the roles of innate and adaptive immunity. *The Lancet infectious diseases* 2004;4(3):166-170.
- [206] Tsuji NM, Tsutsui H, Seki E, Kuida K, Okamura H, Nakanishi K, et al. Roles of caspase-1 in *Listeria* infection in mice. *Int Immunol* 2004 Feb;16(2):335-343.
- [207] Sansonetti PJ, Phalipon A, Arondel J, Thirumalai K, Banerjee S, Akira S, et al. Caspase-1 activation of IL-1 $\beta$  and IL-18 are essential for *Shigella flexneri*-induced inflammation. *Immunity* 2000 May;12(5):581-590.
- [208] Fortier A, Diez E, Gros P. Naip5/Birc1e and susceptibility to *Legionella pneumophila*. *Trends Microbiol* 2005;13(7):328-335.
- [209] Li S, Fossati G, Marchetti C, Modena D, Pozzi P, Reznikov LL, et al. Specific inhibition of histone deacetylase 8 reduces gene expression and production of proinflammatory cytokines in vitro and in vivo. *J Biol Chem* 2015 Jan 23;290(4):2368-2378.
- [210] Smith E, Shilatifard A. Enhancer biology and enhanceropathies. *Nat Struct Mol Biol* 2014 Mar;21(3):210-219.
- [211] Kaikkonen MU, Spann NJ, Heinz S, Romanoski CE, Allison KA, Stender JD, et al. Remodeling of the enhancer landscape during macrophage activation is coupled to enhancer transcription. *Mol Cell* 2013;51(3):310-325.

- [212] Lam MT, Li W, Rosenfeld MG, Glass CK. Enhancer RNAs and regulated transcriptional programs. *Trends Biochem Sci* 2014;39(4):170-182.
- [213] Heinz S, Benner C, Spann N, Bertolino E, Lin YC, Laslo P, et al. Simple combinations of lineage-determining transcription factors prime cis-regulatory elements required for macrophage and B cell identities. *Mol Cell* 2010;38(4):576-589.
- [214] Heintzman ND, Hon GC, Hawkins RD, Kheradpour P, Stark A, Harp LF, et al. Histone modifications at human enhancers reflect global cell-type-specific gene expression. *Nature* 2009;459(7243):108-112.
- [215] Rada-Iglesias A, Bajpai R, Swigut T, Brugmann SA, Flynn RA, Wysocka J. A unique chromatin signature uncovers early developmental enhancers in humans. *Nature* 2011;470(7333):279-283.
- [216] Ghisletti S, Barozzi I, Mietton F, Polletti S, De Santa F, Venturini E, et al. Identification and characterization of enhancers controlling the inflammatory gene expression program in macrophages. *Immunity* 2010;32(3):317-328.
- [217] Zentner GE, Tesar PJ, Scacheri PC. Epigenetic signatures distinguish multiple classes of enhancers with distinct cellular functions. *Genome Res* 2011 Aug;21(8):1273-1283.
- [218] Kim TK, Hemberg M, Gray JM. Enhancer RNAs: a class of long noncoding RNAs synthesized at enhancers. *Cold Spring Harb Perspect Biol* 2015 Jan 5;7(1):a018622.
- [219] Kau J, Sun D, Huang H, Lien T, Huang H, Lin H, et al. Sublethal doses of anthrax lethal toxin on the suppression of macrophage phagocytosis. *PLoS One* 2010;5(12):e14289.
- [220] Gantt SL, Joseph CG, Fierke CA. Activation and inhibition of histone deacetylase 8 by monovalent cations. *J Biol Chem* 2010 Feb 26;285(9):6036-6043.
- [221] Kasner SE, Ganz MB. Regulation of intracellular potassium in mesangial cells: a fluorescence analysis using the dye, PBFI. *Am J Physiol* 1992 Mar;262(3 Pt 2):F462-7.

- [222] Hanna PC, Kochi S, Collier RJ. Biochemical and physiological changes induced by anthrax lethal toxin in J774 macrophage-like cells. *Mol Biol Cell* 1992 Nov;3(11):1269-1277.
- [223] Thomas J, Epshtein Y, Chopra A, Ordog B, Ghassemi M, Christman JW, et al. Anthrax lethal factor activates K(+) channels to induce IL-1beta secretion in macrophages. *J Immunol* 2011 May 1;186(9):5236-5243.
- [224] Cheneval D, Ramage P, Kastelic T, Szelestenyi T, Niggli H, Hemmig R, et al. Increased mature interleukin-1beta (IL-1beta) secretion from THP-1 cells induced by nigericin is a result of activation of p45 IL-1beta-converting enzyme processing. *J Biol Chem* 1998 Jul 10;273(28):17846-17851.
- [225] Walev I, Reske K, Palmer M, Valeva A, Bhakdi S. Potassium-inhibited processing of IL-1 beta in human monocytes. *EMBO J* 1995 Apr 18;14(8):1607-1614.
- [226] Muñoz-Planillo R, Kuffa P, Martínez-Colón G, Smith BL, Rajendiran TM, Núñez G. K efflux is the common trigger of NLRP3 inflammasome activation by bacterial toxins and particulate matter. *Immunity* 2013;38(6):1142-1153.
- [227] Bischofberger M, Gonzalez MR, van der Goot, F Gisou. Membrane injury by pore-forming proteins. *Curr Opin Cell Biol* 2009;21(4):589-595.
- [228] Palmer M. The family of thiol-activated, cholesterol-binding cytolysins. *Toxicon* 2001;39(11):1681-1689.
- [229] Tie F, Banerjee R, Stratton CA, Prasad-Sinha J, Stepanik V, Zlobin A, et al. CBP-mediated acetylation of histone H3 lysine 27 antagonizes Drosophila Polycomb silencing. *Development* 2009 Sep;136(18):3131-3141.
- [230] Schuettengruber B, Chourrout D, Vervoort M, Leblanc B, Cavalli G. Genome regulation by polycomb and trithorax proteins. *Cell* 2007;128(4):735-745.
- [231] Fiskus W, Pranpat M, Balasis M, Herger B, Rao R, Chinnaiyan A, et al. Histone deacetylase inhibitors deplete enhancer of zeste 2 and associated polycomb repressive

complex 2 proteins in human acute leukemia cells. *Mol Cancer Ther* 2006 Dec;5(12):3096-3104.

[232] Agaloti T, Chen G, Thanos D. Deciphering the transcriptional histone acetylation code for a human gene. *Cell* 2002 Nov 1;111(3):381-392.

[233] Kim T, Hemberg M, Gray JM, Costa AM, Bear DM, Wu J, et al. Widespread transcription at neuronal activity-regulated enhancers. *Nature* 2010;465(7295):182-187.

[234] Natoli G, Andrau J. Noncoding transcription at enhancers: general principles and functional models. *Annu Rev Genet* 2012;46:1-19.

[235] Ørom UA, Shiekhattar R. Long noncoding RNAs usher in a new era in the biology of enhancers. *Cell* 2013;154(6):1190-1193.

[236] De Santa F, Barozzi I, Mietton F, Ghisletti S, Polletti S, Tusi BK, et al. A large fraction of extragenic RNA pol II transcription sites overlap enhancers. *PLoS biology* 2010;8(5):e1000384.

[237] Sacconi S, Pantano S, Natoli G. p38-Dependent marking of inflammatory genes for increased NF- $\kappa$ B recruitment. *Nat Immunol* 2002;3(1):69-75.

[238] Arbibe L, Kim DW, Batsche E, Pedron T, Mateescu B, Muchardt C, et al. An injected bacterial effector targets chromatin access for transcription factor NF-kappaB to alter transcription of host genes involved in immune responses. *Nat Immunol* 2007 Jan;8(1):47-56.

[239] Hamon MA, Batsche E, Regnault B, Tham TN, Seveau S, Muchardt C, et al. Histone modifications induced by a family of bacterial toxins. *Proc Natl Acad Sci U S A* 2007 Aug 14;104(33):13467-13472.

[240] Jin Y, Mailloux CM, Gowan K, Riccardi SL, LaBerge G, Bennett DC, et al. NALP1 in vitiligo-associated multiple autoimmune disease. *N Engl J Med* 2007;356(12):1216-1225.

- [241] Ming X, Li W, Maeda Y, Blumberg B, Raval S, Cook SD, et al. Caspase-1 expression in multiple sclerosis plaques and cultured glial cells. *J Neurol Sci* 2002 May 15;197(1-2):9-18.
- [242] Hugot JP, Chamaillard M, Zouali H, Lesage S, Cezard JP, Belaiche J, et al. Association of NOD2 leucine-rich repeat variants with susceptibility to Crohn's disease. *Nature* 2001 May 31;411(6837):599-603.
- [243] Ogura Y, Bonen DK, Inohara N, Nicolae DL, Chen FF, Ramos R, et al. A frameshift mutation in NOD2 associated with susceptibility to Crohn's disease. *Nature* 2001 May 31;411(6837):603-606.



## CURRICULUM VITAE

**Name:** Chantelle Marie Reid

**Post-secondary Education and Degrees:** The University of Ottawa  
Ottawa, Ontario, Canada  
2009-2011 B.Sc. Honours Biopharmaceutical Sciences

The University of Waterloo  
Waterloo, Ontario, Canada  
2011-2013 B.Sc. Honours Science (Dean's Honour List)

The University of Western Ontario  
London, Ontario, Canada  
2013-2015 M.Sc. Microbiology and Immunology

**Honours and Awards:** Schulich Graduate & Western Graduate Research Scholarships  
2013-2015

**Related Work Experience:** Teaching Assistant  
The University of Western Ontario  
MicroImm 2500A  
2014-2015

### Abstracts:

"HDAC8-mediated epigenetic reprogramming in macrophages plays a key role in resistance to anthrax lethal toxin-induced pyroptosis" Epigenetics, Eh! Canadian Conference on Epigenetics 2014, London, ON, June 24-27, 2014.

"Anthrax lethal toxin induces HDAC8 expression that targets histone H3 lysine 27 in murine macrophages" Infection and Immunity Research Forum, London, ON, November 6, 2014.

### Publications:

Ha SD, Han CY, Reid C, and Kim SO. 2014. HDAC8-Mediated Epigenetic Reprogramming Plays a Key Role in Resistance to Anthrax Lethal Toxin-Induced Pyroptosis in Macrophages. J. Immunol. 193:1333-43.